Chemical Engineering
Western Australia School of Mines (WASM)
Faculty of Science and Engineering

Mechanistic insights into acid-catalysed pyrolysis of cellulose and its model compounds

Yu LONG

0000-0002-6182-4201

This thesis is presented for the Degree of
Doctor of Philosophy
of
Curtin University

June 2022

Declaration

To the best of my knowledge and belief this thesis contains no material previously published by any other person except where due acknowledgment has been made.

This thesis contains no material which has been accepted for the award of any other degree or diploma in any university.

Signature .....

Date: 28/06/2022

Abstract

Climate change has become a key threat to the survival of human beings and must be soon mitigated. Developing a circular bioeconomy based on renewable biomass resources, instead of conventional fossil resources, has become widely accepted as a means to achieve our sustainable development goals. The production of biofuels from renewable biomass has been considered as one of the main approaches to produce carbon-neutral fuels as replacements for fossil fuels. Achieving cost-effective production of biofuels requires innovations and advances in technologies based on in-depth fundamental understandings.

Fast pyrolysis is widely accepted as a readily available approach to convert lignocellulosic biomass mainly into bio-oils with high yields. However, the obtained bio-oils are far from qualified as fossil fuel replacements. To further improve the fuel quality of bio-oils, efforts are required to enhance the performances of fast pyrolysis and optimize the properties of obtained bio-oils. Acid loading has been recently considered as a means to enhance the quality of bio-oil by suppressing the effect of naturally occurring alkali and alkaline metallic species (AAEMs), which have been identified as catalysts that can enhance some decomposition reactions to produce unexpected bio-products and reduce the quality of bio-oil. However, the effect of acid loading on the pyrolysis of key components in lignocellulosic biomass (e.g., cellulose, hemicellulose and lignin) is far from being well understood. For instance, under pyrolysis conditions, cellulose and its derivatives can undergo various reactions such as dehydration, isomerization, polymerization and fragmentation. Insights into these reaction pathways with detailed yields and selectivities are scarcely reported. This thesis is thus purposely conducted to provide understanding of the reaction mechanisms of acid-catalysed biomass pyrolysis using cellulose and its derived species as model compounds.

Firstly, the pyrolysis mechanisms of the acid-impregnated cellulose at low temperatures (i.e., 50-325 ºC) have been investigated. There is a significant change in cellulose pyrolysis behavior when acid is present. Pyrolysis of raw cellulose mainly occurs via depolymerisation reactions, while dehydration reactions are more common in the pyrolysis of acid-impregnated cellulose. Hydrogen bonding networks in cellulose are weakened in the process of acid impregnation, promoting the formation of glucose oligomers as reaction intermediates. The presence of acid in the reaction

intermediates catalyses the hydrolysis reaction to produce glucose during the pyrolysis process, especially at low temperatures (i.e., 100 ºC) where the evaporation of water produced (via dehydration) is slow. The results from the study show that glucose is subsequently dehydrated to low molecular weight compounds at increased pyrolysis temperatures. The highly dehydrated cellulose further suppressed depolymerisation reactions, resulting in a low levoglucosan yield during acid-catalysed pyrolysis of cellulose. The char formation is also enhanced, likely via furanic structures which are finally transformed into aromatic structures at temperatures > 300 ºC.

Secondly, the pyrolysis of the acid-impregnated glucose has been further studied, as glucose is found to be a major intermediate product generated during the acid-catalysed pyrolysis of cellulose. Polymerisation reactions have been found to play a key role in the pyrolysis of the acid-impregnated glucose at 60-150 ºC, producing oligosaccharides of various linkages and degrees of polymerisation (DP). Disaccharide products with various α and β linkages (including 1,6-, 1,4-, 1,3-, 1,2- and 1,1-glycosidic bond) are successfully identified, indicating that mutarotation reactions also play an important role in the acid-catalysed glucose pyrolysis. Due to the high reactivity of the C6 position of the hydroxyl group on glucose, disaccharides with 1,6-glycosidic bond (i.e., gentiobiose and iso-maltose) are more favorable with high initial selectivities, such as ~27% and ~20% for gentiobiose and maltose at the acid loading of 0.5mm/g, respectively. Moreover, the formation of α-linkage disaccharides follows an order of 1,6-glycosidic bond > 1,4-glycosidic bond > 1,3-glycosidic bond > 1,2-glycosidic bond > 1,1-glycosidic bond. The maximal DP of the oligosaccharide products formed is dependent on pyrolysis temperatures, from ~4 at 60 ºC to ~18 at 120 ºC. The effect of acid loading level on glucose pyrolysis has been also studied, and the formation of disaccharides are enhanced at increased acid loading levels, especially those with 1,6-glycosidic bond. These experimental results provide new insights into the acid-catalysed glucose pyrolysis mechanism.

Thirdly, the pyrolysis of the acid-impregnated levoglucosan at 80–140 °C has been systematically investigated. Glucose, anhydro-disaccharides and disaccharides of various linkages are successfully identified as major primary products during the acid-catalysed levoglucosan pyrolysis at such low temperatures. Among all identified primary products, glucose has the highest initial selectivity of ~20%, indicating hydrolysis reaction plays an important role during the acid-catalysed levoglucosan

pyrolysis. The formation of anhydro-disaccharides of various α and β linkages (including 1,4-, 1,3-, and 1,2-glycosidic bond) clearly demonstrates the importance of polymerisation reactions during the acid-catalysed levoglucosan pyrolysis. In addition, disaccharides of various α and β linkages (including 1,6-, 1,4-, 1,3-, 1,2-, 1,1-glycosidic bond) are also minor primary products from the acid-catalysed levoglucosan pyrolysis. Once those primary products are formed, they are easily polymerised into high-DP anhydro-sugar and sugar oligosaccharides, with a highest DP of up to ~10 at 120 °C. At 140 °C, the oligosaccharides are also easily condensed to form char, as evidenced by post-hydrolysis results. Increasing acid loading level enhances the formation of glucose and disaccharides, but has negligible effect on the formation of anhydro-disaccharides. These results provide new insights into the fundamental mechanism of the acid-catalysed levoglucosan pyrolysis for producing biofuels and biochemicals.

Finally, the effect of glycosidic linkage on the pyrolysis of disaccharide has been investigated via the acid-impregnated trehalose (with 1,1-α-glycosidic bond) and cellobiose (with 1,4-β-glycosidic bond). It can be seen that cellobiose is more stable than trehalose under the acid-catalysed pyrolysis conditions. Pyrolsis of trehalose can start a low temperature of 40 °C, mainly via mutarotation reactions to produce disaccharides of various linkages and hydrolysis reaction to produce glucose. Among various disaccharides produced, gentibiose has the highest selectivity. As the temperature increases, polymerisation reactions plays an important role to produce oligosaccharides, and the DP of oligosaccharides increases from 3 at 80 °C to 15 at 140 °C. In comparison, cellobiose pyrolysis starts a much higher temperature of 80 °C, via mutarotation and hydrolysis reactions as major primary reactions. As the temperature increases, glucose dehydration reactions play an important role to form some dehydrated products such as levoglucosan, AGF and mannosan. The results clearly demonstate different pyrolysis mechanisms of disaccharides of different glycosidic linkages, and provide new data for developing advance pyrolysis technologies for producing biofuels and bio-chemicals.

Overall, the acid-catalysed pyrolysis mechanisms of cellulose and its major model compounds have been systematically investigated by characterising their reaction intermediates during the pyrolysis of the acid-impregnated samples. This study provides new insights into some important reaction pathways during the acid-

catalysed pyrolysis of cellulose, a main component of lignocellulosic biomass. The obtained knowledge will be critical to develop more advanced pyrolysis technologies for producing hihg-quality bio-oil and value-added biochemicals from lignocellulosic biomass.

Acknowledgments

To my lovely family, my wife Mrs. Minxue Yang and my daughters, Vanessa Long and Veronica Long: because I owe it all to you. Many thanks!

I would like to express my gratitude to my parents and parents-in-law, providing continuous encouragement through moral and emotional support in my life. I am also grateful to my other family members and friends who have supported me along the way.

I would like to express my great appreciation to my supervisor Prof. Hongwei Wu for offering me this golden opportunity to study in his research group. He provided professional advice, assistance, and guidance during my study period. Without his opportunity and supervision, this would not have been possible.

I would also like to thank my co-supervisor Dr. Yun Yu who was continuously generous in guiding my research project with all his valuable experience. When I faced the difficulties in my study journey, he provided his enthusiastic encouragement and useful critique like a teacher and friend.

I am very grateful to the Australian government for funding my tuition fee to reduce my financial pressure during my study.

I am also grateful to the following team members who have provided much assistance in my research. They are Dr. Suiboon Liaw, Dr. Dawei Liu, Dr. Feng Chao, Dr. Bing Song, Dr. Yeewen Chua, and Dr. Jinxiu Cao.

Finally, I wish to thank my colleagues in Curtin University providing generous support in my work and study. They are Ms. Karen Haynes, Mr. Jason Wright, Mr. Araya Abera, Dr. Roshanak Doroushi, Mr. Xiao Hua, and Mr. Andrew Chan.

List of publications

Long Y, Yu, Y, Wu H. Mechanistic insights into the primary reactions during acid-catalysed pyrolysis of levoglucosan at 80–140 °C. Fuel, **2020**, 268, 117390.

Long Y, Yu Y, Song B, Wu H. Polymerization of glucose during acid-catalysed pyrolysis at low temperatures. *Fuel*, **2018**, 230, 83-88.

Long Y, Yu Y, Chua YW, Wu H. Acid-catalysed cellulose pyrolysis at low temperatures. *Fuel*, **2017**, 193, 460-466.

Yu Y, Song B, **Long Y**, Wu H. Mass Spectrometry Analysis of Sugar and Anhydrosugar Oligomers from Biomass Thermochemical Processing. *Energy & Fuels*, **2016**, *30* (10), 8787-8789.

Yu, Y., **Y. Long** and H. Wu. Near-Complete Recovery of Sugar Monomers from Cellulose and Lignocellulosic Biomass via a Two-Step Process Combining Mechanochemical Hydrolysis and Dilute Acid Hydrolysis. *Energy & Fuels*, **2016**, 30: 1571-1578.

Liu, D., Y. Yu, **Y. Long** and H. Wu. Effect of MgCl2 loading on the evolution of reaction intermediates during cellulose fast pyrolysis at 325 C. *Proceedings of the Combustion Institute* **2015,** 35: 2381-2388.

Contents

List of tables

List of figures

Chapter 1 Introduction

1.1 Background and Aim

Fossil fuels, including coal, oil, and natural gas, are currently dominative energy sources which are motivating powers driving economic growth and human civilization. However, being organic material formed over millions of years, they are a finite resource and cause irretrievable harm on the environment by emitting greenhouse gases (GHGs) into the atmosphere during the combustion process. According to the report of the Australian Business Roundtable on Climate Change, average air temperatures of the Earth's surface have increased by around 0.6 °C over the 20th century[1]. It was observed that the increased average air temperature in Australia was 0.7 °C from 1910, and that Western Australia had experienced a steady decline in precipitation [1]. Moreover, Australia is experiencing an increase in extreme rainfall events, especially in winter. The Climate Change 2001 report stated that GHGs concentrations in the atmosphere have dramatically increased due to human activities since the industrial revolution: carbon dioxide (CO_2) by 30% (from 280 to 380 parts per million), and Nitrous oxide (NO_x) and methane (CH_4) by 17% and 151% respectively [2]. These gases can change the balance between incoming solar radiation and outgoing heat, since the radiation heat from the Earth into space is trapped by GHGs in the atmosphere to increase global temperatures.

Global warming can have serious effects on the climate, such as tropical cyclones, heat waves, and extreme precipitation events, causing a slowing or collapse of either the ocean's thermohaline circulation or the ice sheets of the West Antarctic or Greenland. Therefore, an emerging consensus on greenhouse gas stabilisation was reached at the Rio Earth Summit in 1992 to address the global challenge of anthropogenic climate change. Achieving stabilization is to maintain a stable level of CO_2, which means the CO_2 produced from natural and human sources must be equally reduced. Renewable energies, such as bio-energy, wind power, hydropower, solar energy, geothermal energy, and energy storage, have been developing and attracting investment in most countries in an attempt to stabilize the emission of CO_2. In the REN21 2018 report, the usage of renewable energy contributed to 18.2% of the global total energy consumption in 2016 and was supported by new policies in several countries in 2017 [3].

Biomass can either be directly used as a solid biofuel for power and heat generation via combustion or indirectly used as a source for producing biofuels in other forms (gaseous and liquid) and biochemicals via various techniques. Pyrolysis has been widely considered as a feasible means for converting biomass into various products. The history of biomass utilization indicates that pyrolysis, as a crucial application, has been used for the production of charcoals as a heat resource for hundreds of years, but in recent decades the focus has shifted to an emphasis on fast pyrolysis performed at moderate temperatures within a short residue time. Fast pyrolysis can produce highly valuable bio-liquids (up to 75 wt.%) and by-products including biochar and fuel gas, which can directly be used in many applications and energy carriers [4]. Moreover, the most beneficial feature of bio-liquid is its potential as an alternative liquid energy source to address various issues such as the energy shortage crisis and environmental crisis of GHGs emissions.

Figure 1-1 demonstrates how biofuels are generated from an industrial plant accesses to a resource market via thermal pyrolysis [5]. As the below figure depicts, bio-oil from fast pyrolysis can easily be transformed into various applications such as electricity and heat (power) generation through engine or turbine conversion because of its advantage in storage and transportation, which is beneficial in various energy industries.

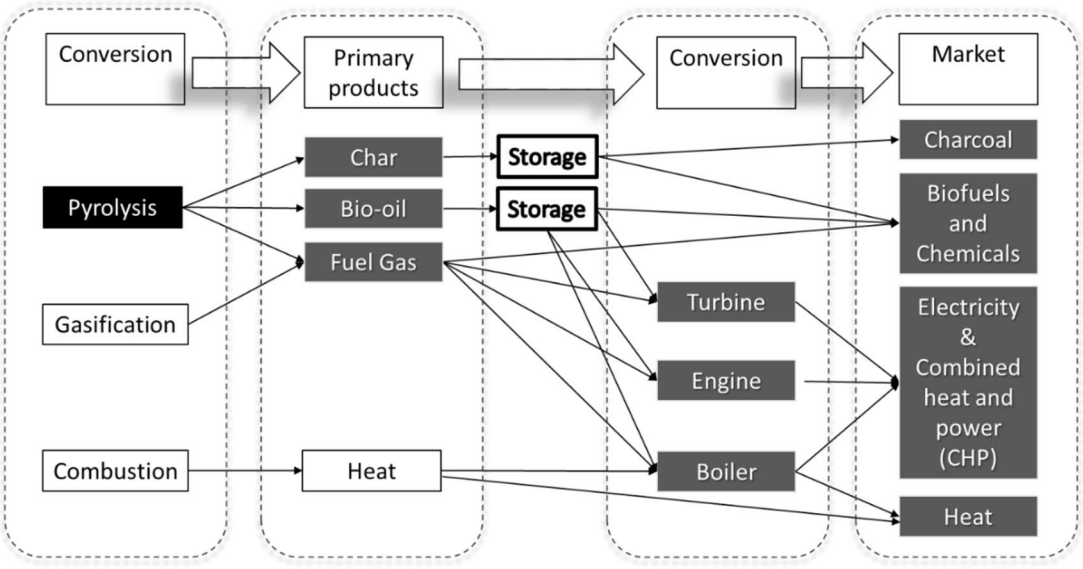

Figure 1-1 Bio-energy flow chart from industries to markets. [5]

Based on the application of products formed in pyrolysis, life cycle assessments, consisting of biomass collection, transportation, pyrolysis, and upgrading stages, have been studied by many researchers [6-11]. The results from life cycle assessments have concluded that CO_2 emissions could be effectively reduced during the utilization process, thus contributing a positive carbon credit in the carbon market as a profit. Therefore, the utilization of biofuels produced from sustainable biomass can be an essential alternative to fossil fuels to achieve the target of carbon reduction in the future world's energy strategy.

However, the undesired properties in bio-products (i.e., high water content, high acidity, high viscosity, low heating value, poor phase stability, incompatibility of bio-oil with conventional fuels and high cost) hinder its commercial promotion in the energy market.[4, 12-16] The natural portion of inherent inorganic species (i.e., alkali and alkaline metallic species, AAEM) can have a major effect on bio-oil quality, which significantly influences the pyrolysis behavior of biomass. Many researchers have identified that AAEM on biomass can catalyse the fragmentation and dehydration reactions to produce undesired products, such as formic acid and hydroxyacetaldehyde.[17-24] Although acid pre-treatment methods (acid leaching, acid impregnation, and combined methods) have been shown to improve the bio-oil quality by removing inherent AAEM in biomass,[25-29] it is critical to load an optimum amount of acid on the treatment process to achieve this benefit, since overloading the acid has a negative influence on the selectivity of bio-products. For example, the acid loading in cellulose could increase char yield and dehydrated products (levoglucosenone) during the pyrolysis process.[30-32] There has been less in-depth research conducted on a detailed pyrolysis mechanism focusing on the effects of acid pre-treatment in the formation of intermediates. Therefore, it is necessary to explore the fundamental mechanism of acid effects on biomass pyrolysis to optimise the application of biomass utilisation, especially in bio-oil quality improvement.

1.2 Scope and Objectives

The major purpose of the study is to fundamentally explore the acid-catalysed cellulose pyrolysis mechanism under a low-temperature profile by investigating interactions of reaction intermediates yielded from acid-catalysed cellulose pyrolysis and modelling compounds from the acid-catalysed cellulose pyrolysis. The details of the objectives of the study are outlined as follows:

- To characterise the formation of water-soluble intermediates via acid-catalysed cellulose pyrolysis in a low-temperature range including 50 °C to 320 °C
- To discover the evolution of acid-catalysed glucose pyrolysis at 60 to 150 °C, which is an important intermediate formed in acid-catalysed cellulose pyrolysis in the lower temperature.
- To investigate the evolution of a major intermediate levoglucosan under acid-catalysed pyrolysis at 60 to 140 °C so that a profile can be generated regarding the reaction mechanism of acid-catalysed levoglucosan pyrolysis.
- To identify the significant effect of disaccharides' linkages on the acid-catalysed pyrolysis, which can contribute to understanding the underlying mechanism of acid-catalysed cellulose pyrolysis.

1.3 Thesis Outline

There are eight chapters in this thesis which are highlighted in the thesis structure (*Figure 1-2*) and detailed as below:

- reviews the recent research of biomass and cellulose pyrolysis in the open literature to define the current research gaps corresponding to the objectives in the thesis.
- presents the applied methodology in this study to achieve the research objectives and explanations of the utilised experimental instruments.
- identifies the effects of acid on cellulose pyrolysis via characterisation of the water-soluble intermediates from the reaction.
- explores the reaction mechanism of glucose during acid-catalysed pyrolysis at low temperatures.
- investigates the reaction mechanism of levoglucosan during acid-catalysed pyrolysis at low temperatures.
- investigates the dimers' structures impact on at the acid-catalysed pyrolysis.
- concludes the present study, proposes a reaction mechanism on acid-catalysed cellulose pyrolysis and makes recommendations for future research.

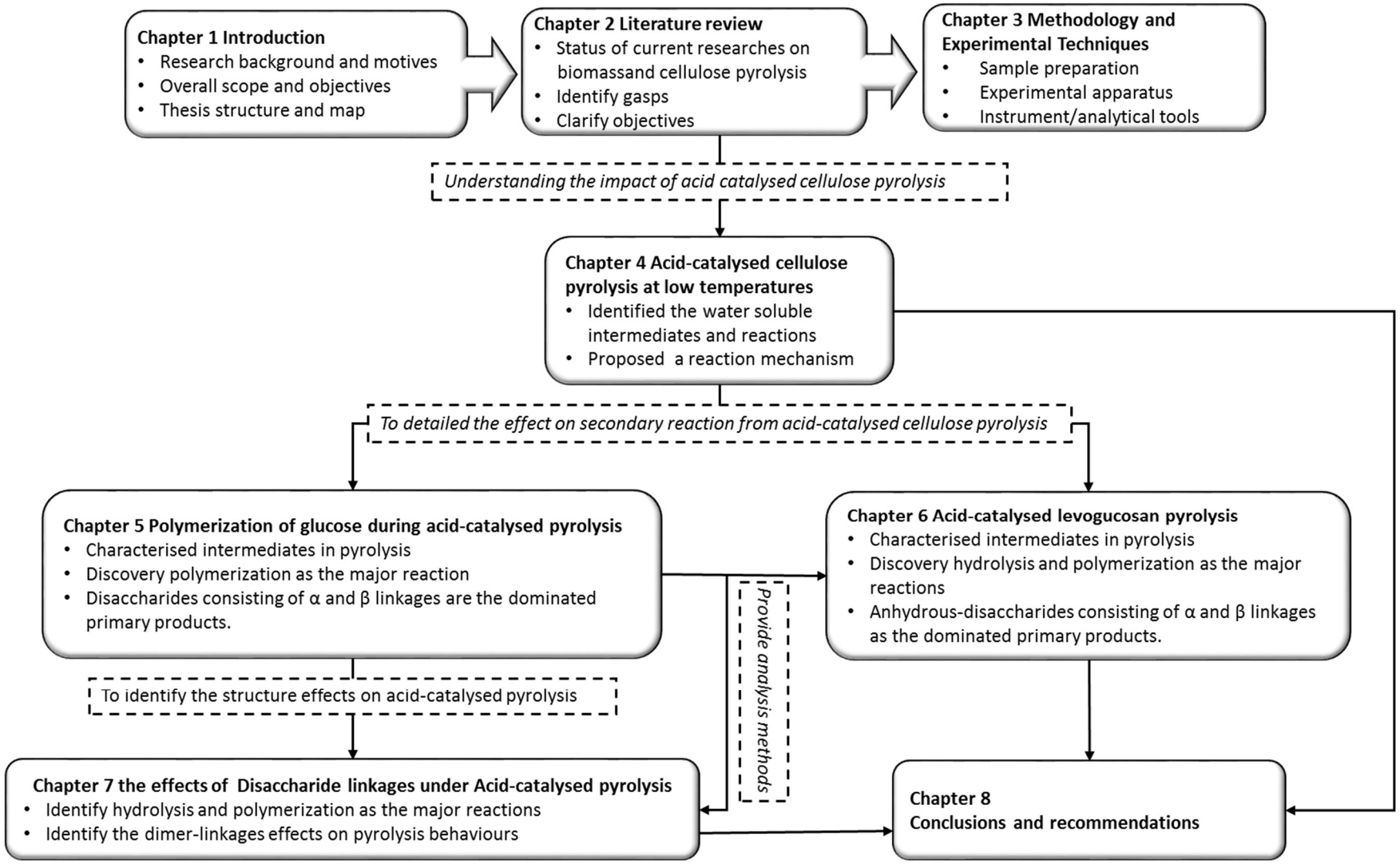

Figure 1-2 Thesis structure.

Chapter 2 Literature review

2.1 Introduction

Biomass utilisation can be traced back to thousands of years ago as shown in Figure 2-1. Referring to the history of utilisation, producing char and by-products (such as tars and pyroligneous acid) as fuels and chemicals from biomass by thermal treatments have been widely employed during the progress of civilization.[33] Currently, bio-products created by biomass pyrolysis are considered as renewable energy sources because they can neutralise greenhouse gas emissions (GHG) produced in the process of bio-energy utilisation, and meet the increasing energy demand of social and economic development. Depending on the form of bio-products such as solids, liquids, and gas, the application methodologies can be divided into pyrolysis, gasification, and combustion. Pyrolysis can be further subdivided into slow pyrolysis and fast pyrolysis, based on working temperatures and residence times. For example, low temperatures and longer vapor favour charcoal production; on the contrary, high temperatures and longer residence time favour gas and liquid formation.[5]

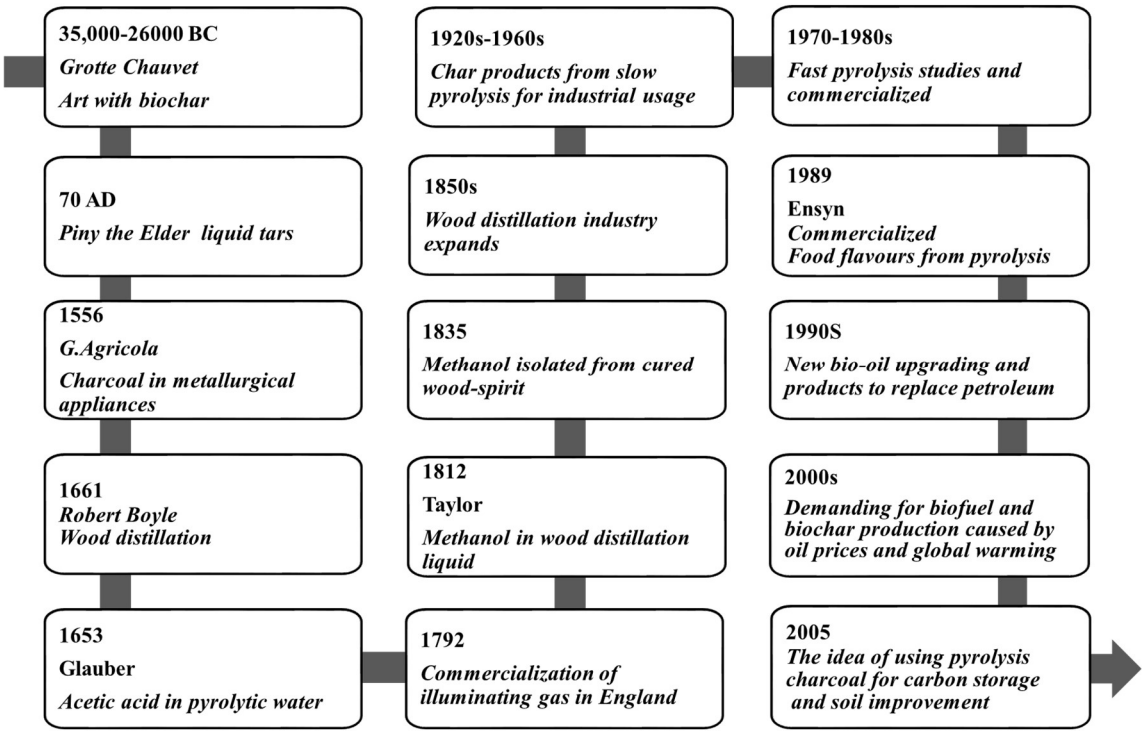

Figure 2-1 Milestone in biomass pyrolysis development.[34]

Bio-oil produced from fast pyrolysis of biomass is recognized as an essential energy resource and it is relatively easy to store and transport for further utilisation. Under an optimum pyrolysis condition, fast pyrolysis occurs at high temperatures around 500 ^{0}C within a short residence times between 30 to 1500 ms in an oxygen-free condition.[34] The performance of fast pyrolysis is decisively impacted by particle size, chemical reaction kinetics, pyrolysis temperatures, heating rate, and biomass pre-treatment methods. [35-38] Although impact factors have been studied in the past decades, the commercialization of bio-products, especially bio-oil, still needs to address issues such as low energy values and high density.[13, 15, 16] Therefore, understanding the reaction mechanisms plays an especially important role in developing advanced fast pyrolysis technologies resulting in product quality improvement. This research's targets intend to provide in-depth understandings of pyrolysis mechanisms, through studying the underlying reaction pathways of model compounds by characterising their reaction intermediates, which are also considered as the precursors of volatiles. Initially, the existing literature has been reviewed and summarized to identify the current research gaps related to the fundamental mechanism. Due to the complicated structures of biomass, the concentration on cellulose pyrolysis, which is a major component in biomass, is an effective start-up research to progress an understanding of biomass pyrolysis. The literature review structure is presented in Figure 2-2 and explained below.

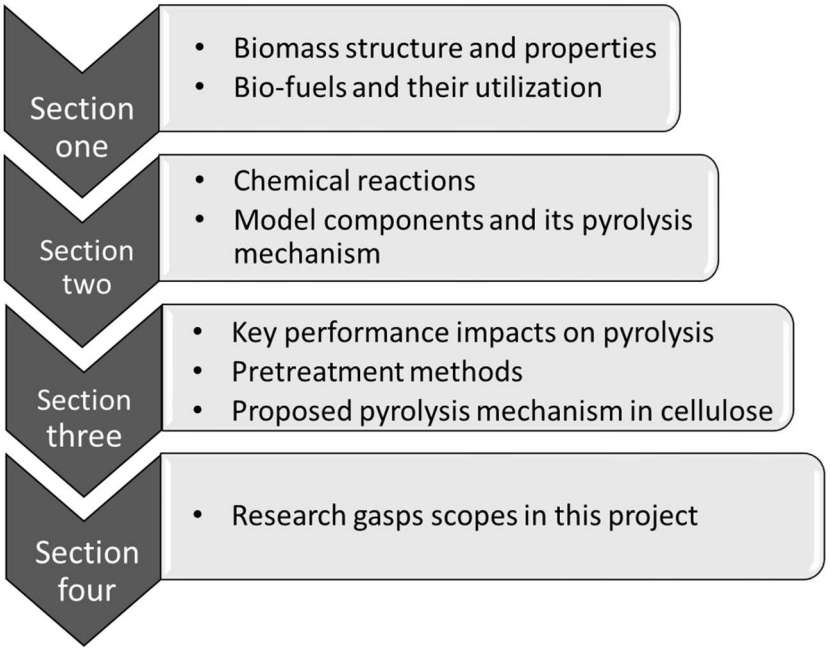

Figure 2-2 Structure of the literature review.

Firstly, the structure and compositions of lignocellulosic biomass have been briefly introduced, followed by introducing the utilisations of lignocellulosic biomass for producing biofuels via pyrolysis. Furthermore, current understandings on the reaction pathways of cellulose pyrolysis and its main products have been outlined. Secondly, key variables such as raw materials, temperature, heating rate, and alkali and alkaline earth metals [AAEM] and their effect on cellulose pyrolysis have been concluded. Thirdly, existing pyrolysis reaction models proposed by various researchers have been overviewed. Finally, based on previous studies, research gaps in the areas of acid-catalysed cellulose pyrolysis and the scope of the present study are established and outlined.

2.2 Lignocellulose Biomass

2.2.1 The structure and configuration of biomass

Lignocellulosic biomass is the most abundant biomass in the world. It includes various forestry and agricultural residues such as woodchips and rice straw. According to an FAO 2010 report[39], Asia including Asian Russia has the highest total forest area of 31% of Earth's, followed by 20% in South America >17% in North and Central America > 9% in Europe > 5% in Oceania. Forests cover 4.03 billion hectares globally, equivalent to 30% of Earth's total land area. 5% of forest is planted for commercial purposes.[40] The potential biomass energy are 100-400EJ/year, which means that 18% of the world's primary energy consumption can be satisfied in 2050 by producing bio-energy from woody biomass.[41] Basically, lignocellulosic contains cellulose, hemicellulose, lignin, pectin, and inorganic compounds. The organic compounds of lignocellulosic biomass mainly consist of carbon, hydrogen, oxygen, nitrogen, and sulphur, constituting more than 95% of total biomass content. The remaining inorganic compounds are comprised of AAEM which is mostly potassium and calcium.[42]

Figure 2-3 shows the distribution of the cell wall of plants as three zones, including the middle lamella, and the primary and secondary walls. The secondary walls consist of three layers from outside to inside, named as S1, S2, and S3. The middle lamella acts as a separating panel sharing two contiguous cells. Once it is formed in the cell during cytoplasmic division, carbohydrates start to be placed on both sides to produce the primary wall, which is the main skeleton of the plant and which controls cell growth. The secondary cell wall is formed and deposited on the primary wall, and has a similar structure as the primary wall.[43] The essential structure of the plant cell wall

is cellulose, hemicellulose, lignin, and pectin cross-linked by hydrogen and covalent bonds.[43] Cellulose is the main skeleton material in the cell wall presenting as tough microfibers, then hemicellulose and lignin are implanted into the internal spaces as shown in Figure 2-3 B and C.

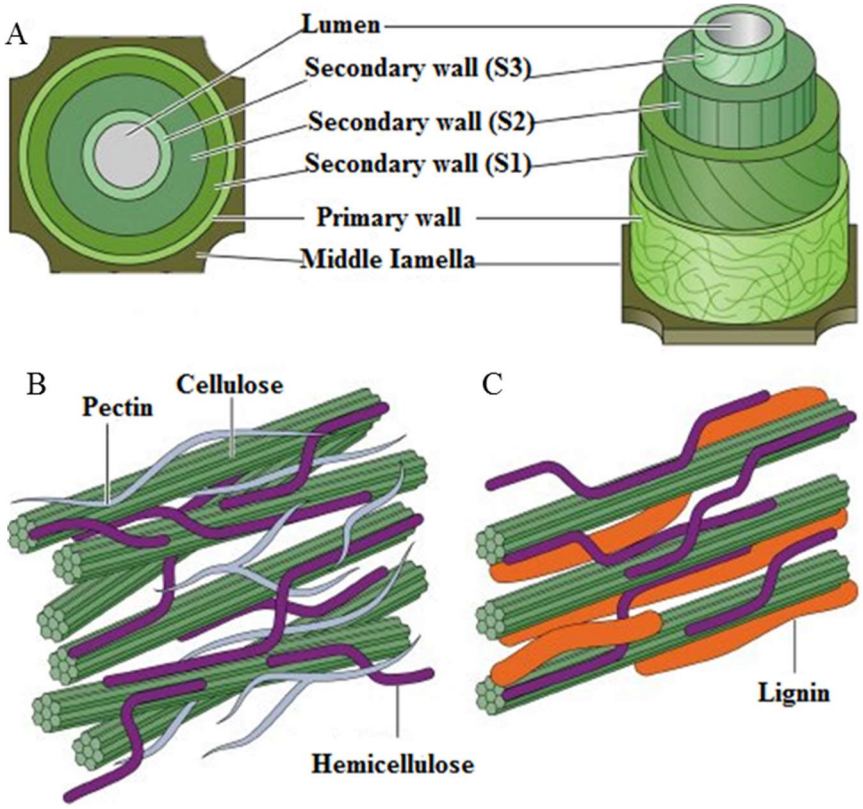

Figure 2-3 Schematic illustrations of the structure of lignocellulosic biomass. (A) main layers in biomass, (B) Primary wall structure (The lignin content is not present due to the various plant), (C) second wall structure.[44]

Comparing the structure and chemical composition in softwood (e.g., pine and spruce) and hardwood (e.g., birch, aspen, and oak), the major differences are caused by hemicelluloses and lignin. In the softwood, hemicellulose mainly contains galactoglucomanans, but glucuronoxylans is a major component in hemicellulose of the hardwood[45]. Moreover, softwood consists of a higher lignin content than hardwood.

Meanwhile, there is a difference in the structure and composition of flowering plants. For example, monocots mainly consist of cellulose and hemicellulose in the primary wall and have larger amounts of cellulose and lignin and variable compositions of hemicellulose. However, dicots have lower xylan and high xyloglucan and manna

contents. The major components of the second wall are cellulose, hemicelluloses, and lignin.[46] The major differences between the species are summarized in Table 2-1.

Table 2-1 Approximate compositions of plant cell walls in softwood, hardwood, monocot, and dicot.[46]

Chemical Composition (% dry wt.)							
Plant Material	**Cellulose**	**Hemicellulose**					
		Mannan	Xylan	B-Glucan	Xyloglucan	Pectin	Lignin
Softwood	33-42	10-15	5-11	~	~	~	27-32
Hardwood	38-47	2-5	15-30	~	~	~	21-31
Monocotyledons							
Primary cell	20-30	Minor	20-40	10-30	1-5	5	Minor
Secondary cell	35-45	Minor	40-50	Minor	Minor	Minor	20
Dicotyledons							
Primary cell	15-30	5-10	5	ND	20-25	20-30	Minor
Secondary cell	45-50	3-5	20-30	ND	Minor	Minor	7-10
Note: ~, not reported; ND, not detected							

A small amount of AAEM in biomass is obtained from natural water during the plant growth which contains Na, K, Ca and Mg. According to studies of characteristics of leaching organic and inorganic matters from biomass, Na, and K (~80%) can be found in water-soluble salts such as KCl, KOH and NaCl.[47, 48] On the contrary, Mg and Ca exist in the form of water-insoluble AAEM and strongly bond in the matrix structure of biomass.[23, 49] There are some rare inorganics found in the biomass such as Si, Al, P, S, and Fe.[50] Although there is a relatively lower content of AAEMs than other organics in biomass, they have a critical impact on biomass pyrolysis. Therefore, the AAEMs' effect on biomass is explained in the below section.

The major components have different structures and chemical characteristics, affecting the distribution of the product in biomass pyrolysis. Therefore, the following sections also explain their structures and characteristics.

2.2.2 Cellulose

Cellulose is an important skeleton in both the primary and secondary cell walls of biomass, forming linear microfibers in the formation of polysaccharides. They

polysaccharides consist of carbon, hydrogen, and oxygen and present as $(C_6H_{10}O_5)_n$ within the proportion of 44.2 wt.%, 6.3wt.%, and 49.5wt.% respectively[42].

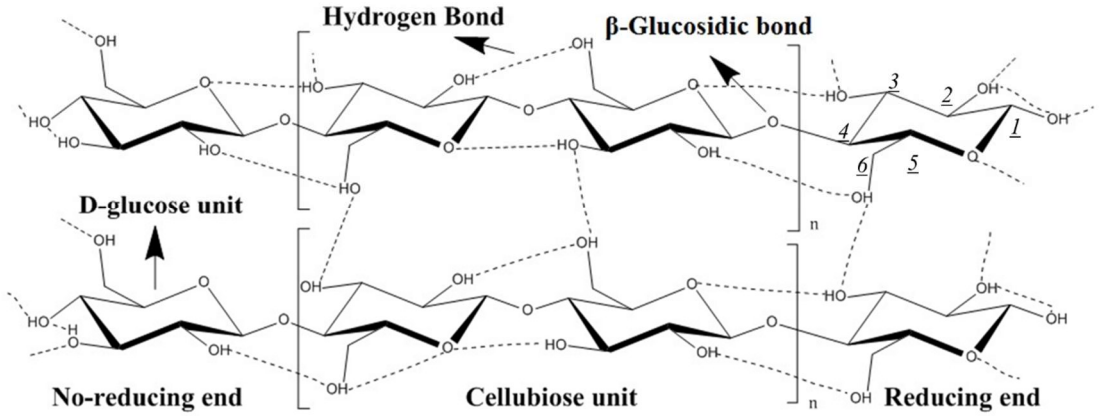

Figure 2-4 Cellulose structure.[51]

Figure 2-4 shows the linear polysaccharides contain mono-units of D-glucose linked by β-glycosidic bonds to form a layer of saccharides. In the termination of cellulose ends, there are two different structures of D-glucopyranose units, including a non-reducing end and a reducing end. The reducing end contains a free anomeric carbon atom in C1, but the anomeric carbon atom of C1 is contributed in the non-reducing β-glycosidic bonds and the hydroxyl group at C4 is free to contribute the non-reducing characteristics[52]. The various noncovalent interactions such as hydrogen bonds and van der Waals create an ultrastructure of cellulose between the different layers and glucose units.[53] For example, the intramolecular hydrogen bonds can stiffen two different polysaccharides chains to produce a certain degree polymer. Meanwhile, the intermolecular hydrogen bonds can form a supermolecular structure.[51] A relatively low density of bonding forms amorphous cellulose which can be partially dissolved in water and easily converted under thermochemical treatments.[54-57] In contrast, a high density of hydrogen bonding creates microcrystalline cellulose in the formation of a high degree of polymers which are insoluble in water and common organic solvents such as ethanol and acetone.

Four major crystalline cellulose are reported and interconverted by various conditions shown in Figure 2-5[58].

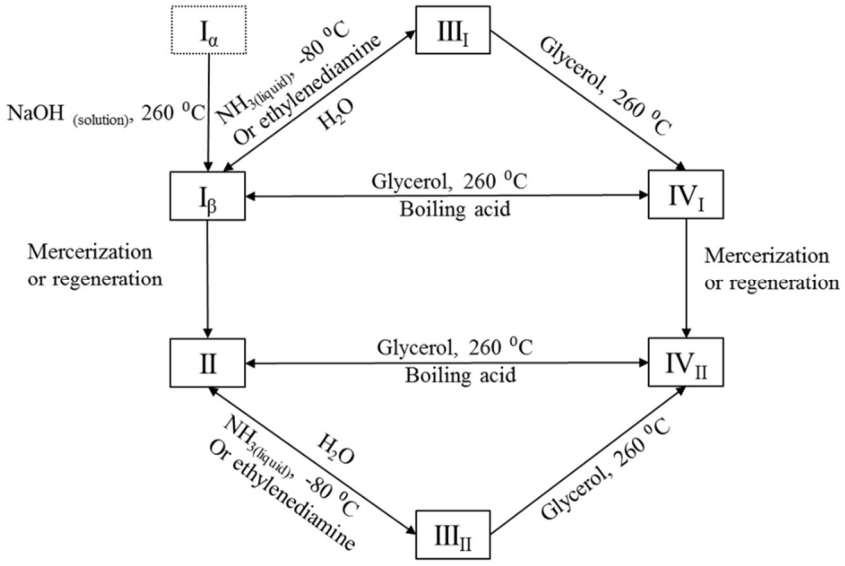

Figure 2-5 The cellulose allomorphs and their interconversion. [58]

Cellulose I can be found in two types of crystalline allomorphs including I_α (algal and bacterial celluloses) and I_β (higher plants and tunicates),[59, 60] but the structure of Iα is still under discussion because of the availability of pure cellulose I_α. The thermodynamic of cellulose II is higher than cellulose I, since cellulose II contains stronger hydrogen bonding than cellulose I.[61] Cellulose I can form cellulose II via either mercerisation or regeneration, but the process is irreversible. Using the method of swelling in liquid ammonia and amine, cellulose I and cellulose II can produce cellulose III_I and cellulose III_{II}, respectively. Moreover, cellulose IV_I and cellulose IV_{II} are formed from the annealing of cellulose III_I and cellulose III_{II} in a glycerol solution under 260 °C.

The amorphous cellulose is easier to be accessed than crystalline cellulose because of the density of hydrogen bonding in the structure. Furthermore, the accessibility of cellulose allomorphs follow the amorphous order of $III_I > IV_I > III_{II} > I > II$.[62]

2.2.3 Hemicellulose

Hemicellulose (20-30% plant dry weight) is the second major component in the plant cell providing support to the cellulose microfibrils in the primary and secondary walls of plant cells and it cross-links the cellulose and lignin via hydrogen bonds and van der Waals force.[42, 63] The majority of monosaccharides in hemicellulose include xylose, galactose, glucose, arabinose and mannose,[64] as shown in Figure 2-6.

Hemicellulose can be divided into three groups containing xylans, mannans, and Galatians forming the backbone structures.

Xylan is an important backbone polymer in hemicellulose and linked by a β-1,4-linked D-xylose. Meanwhile, other monosaccharides are linked to xylose as branches via C2 or C3 positions of xylan (e.g., D-glucose, D-mannose, D-galactose, D-fucose, and D-glucose) [65]. The molecular weight is much lower than cellulose because of the relatively lower degree of polymerization at 50~200[66].

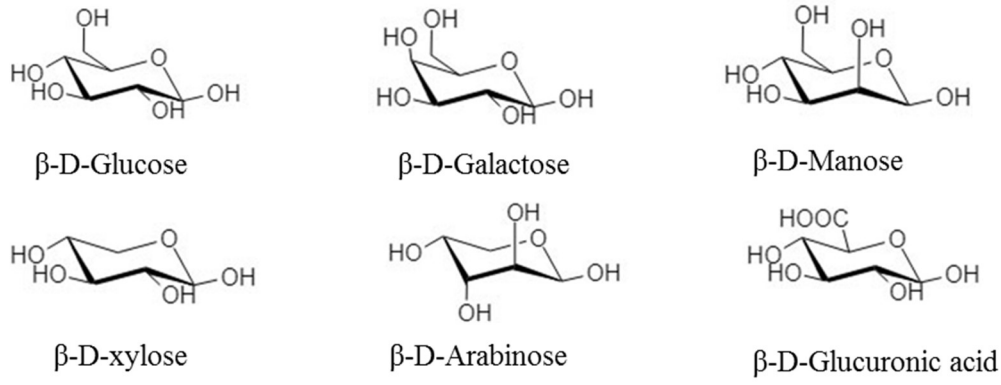

Figure 2-6 Major monosaccharides in hemicellulose. [64]

The main structures of xylan can be categorised by heterogeneously attached monosaccharides on the xylose backbone including glucuronoxylan, galactoglucomannan, arabinoglucuronoxylan, xyloglucan, and arabinoxylan. The most attached monosaccharide on xylan is arabinose, but sometimes it is observed that a single, or additional groups, are attached on xylans such as xylose, galactose, or 4-O-methyl-D-glucuronic acid. Due to the activity of the C2 and C3 position on xylose, it can be observed that glucuronic acid and its methylated form attach directly to xylose and the partially acetylated xylose backbone.[66] Moreover, different plants contain various side groups on the side of the xylose backbone. For example, monocotyledons have arabinose along with glucuronic acid (or its methylated form). Dicotyledons (including hardwoods) contain 4-O-methyl-glucuronic acid attached on every 10th xylose. By comparison, 4-O-methyl-glucuronic acid is occurred in every sixth xylose within fewer arabinose side groups in softwoods[66]. Hardwood xylan contains 4-O-methyl-glucuronic acid, 3.5-7 xylose acetylated at the C3 position, and some acetylation in the C2 postion[67].

Mannan, consisting of a high purity of mannose polymer (>95%), appears in some seeds. For example, vegetable ivory is a soruce rich in mannan and can be used for

producing mannose.[66] Other side groups attached on mannose include glucomannan in softwood (mannose to glucose rations of 3:1 to 4:1) and hardwood (mannose to glucose 2:1 to 1:1), galactomannan in the seeds, and galactoglucomannan[66].

Galactan is the third backbone type in hemicellulose families, containing galactose backbone via *β*-1,3-linkage. The common side group on galactan is arabinose named as arabinogalactan (arabinose to galactose ration from 1:4 to 1:8). Larchwood has a high galactan content of approximately 10-30%.[66]

2.2.4 Lignin

Lignin, consisting of complex phenolic polymers (non-saccharide), is the third major structure in biomass which contributes an implanting material at the secondary cell wall in the cellulosic polymers[68]. Moreover, it is the major component in the middle lamellae between adjacent cell walls which can assist in water transportation to heights up to 100m because of the hydrophobic surface[69, 70]. Lignin content occupies 20-35% in softwood and hardwood and 15-20% in graminaceous monocotyledon.[42] There are three monolignol precursors, including p-coumaryl alcohol, coniferyl alcohol, and sinapyl alcohol as shown in

Figure *2-7* [71].

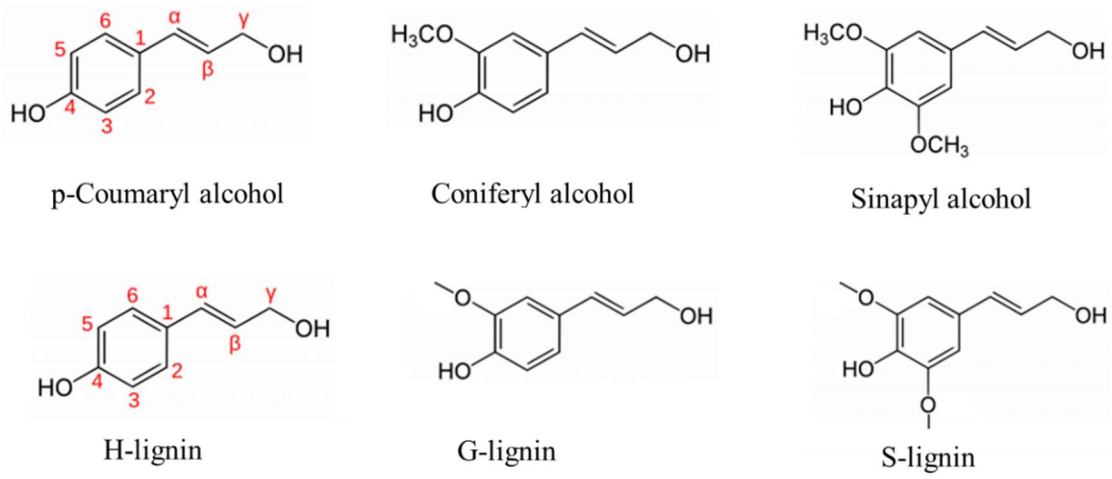

Figure 2-7 Three major monolignol monomers in lignin.[71, 72]

When the lignin polymers are formed, three basic structures are converted to hydroxyl-phenyl lignin (H-lignin, p-hydroxyl phenylpropanoid), guaiacyl lignin (G-lignin, guaiacyl phenylpropanoid) and syringyl lignin (S-lignin, syringyl phenylpropanoid).[72] Hardwood usually mainly contains S-lignin and G-lignin, but a small amount of H-lignin is also found. In contrast, G-lignin mostly exists in softwood and H-lignin in

herbaceous biomass.[72, 73] There are three different connections in lignin polymers, such as ether bonds (60-70%, β-O-4, α-O-4, γ-O-4, 5-O-4 and α -O-β', α -O- γ'), carbon-carbon bonds (30-40%, 5-5, β -1, β -5, β -6, α -6, and α – β), and ester bonds.[42] The most common linkage of lignin polymers is β-O-4 (β aryl ether) linkages which are easily cleaved by chemical processes such as pulping and biomass pre-treatments.[74] Other linkages (e.g., -5, β-β, 5-5, 4-O-5 and β-1) are mostly stable and resistant to chemical degradation.[69] Most of the structure of polymers is summarized in Figure 2-8.

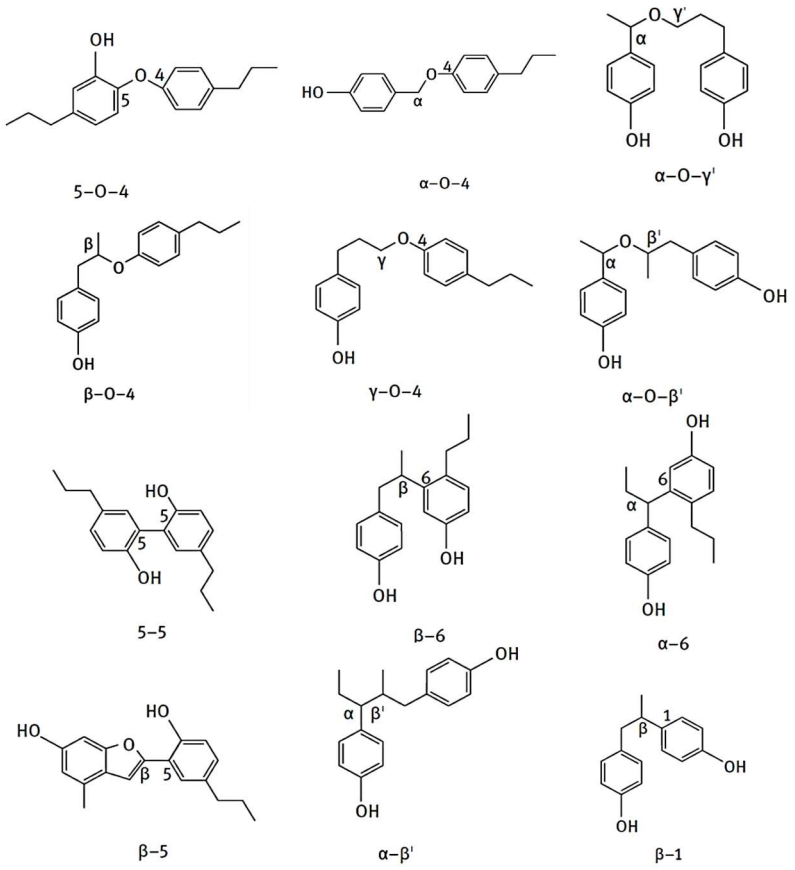

Figure 2-8 Various linkages of lignin polymers. [69]

2.3 Biomass pyrolysis

Lignocellulosic biomass is widely considered as a feedstock for producing fossil fuel replacements due to (1) the depletion of fossil fuels, (2) the use of biofuels produced from renewable biomass resources is carbon-neutral, thus reducing carbon emission and releasing the pressure caused by GHG emissions, and (3) lignocellulosic biomass is widely distributed and can be easily accessed in the world. Biomass pyrolysis considers decomposing biomass under thermal conditions with the absent of oxygen. It is an essential method to convert biomass into different valuable products such as

charcoal, gas, and biofuels. To fully understand this, it is necessary to review the pyrolysis processes and the application of products from biomass pyrolysis.

2.3.1 Pyrolysis of biomass

Pyrolysis is a widely used technique for converting biomass into various products. It normally considers treating dried biomass under thermal conditions with the absence of oxygen. Given different reaction temperatures, reaction times and vapor residence times, the products can be varied. The treatment conditions and their corresponding products distributions of different pyrolysis models for woody biomass are briefly summarized in Table 2-2.

Table 2-2 Product distribution from different thermal conditions. [5]

Type product weight yields from different modes of pyrolysis of wood				
Model	**Conditions**	**Liquid**	**Solid**	**Gas**
Fast	500 °C short hot vapour residence time~1 s	75%	12% char	13%
Intermediate	500 °C short hot vapour residence time~10-30 s	50% in 2 phases	25% char	25%
Carbonisation (slow)	~400 °C long vapour residence hours to days	30%	35% char	35%
Gasification	~750-900 °C	5%	10% char	85%
Torrefaction (slow)	~290 °C, solids residence time~10-60 min	0% unless condensed, then up to 5%	80% solid	20%

As shown, fast pyrolysis is the most appropriate for converting biomass to liquids, namely, bio-oils. An identical fast pyrolysis for generating high yield of bio-oils is conducted under following preferred conditions. They are:

- Biomass particle size of less than 3 mm due to low thermal conductivity of biomass,
- Optimum reaction temperature at around 500 °C, favoring the liquid yield,
- Residence time less than 2 seconds, minimizing secondary reactions,
- Rapid removal of produced char which reduces the cracking products into vapours, and
- Rapid cooling of the pyrolysis vapours to obtain bio-oil[5].

The type of reactors also has some effects on biomass pyrolysis by controlling reaction conditions such as temperatures and vapour residence times. According to the targeted major products, the reactors can be classified into traditional carbonization kilns (char-making), and retorts/converters (recovering char and liquid samples)[75, 76]. Moreover, according to the different treatment time, pyrolysis reactors can be also categorised into slow (kilns, retorts), intermediate (converters), and fast (microwave) reactors[76]. Currently, the most applicable reactors used for fast pyrolysis are fluid bed, spouted fluid bed, transported bed, rotating cone integral catalytic pyrolysis, vortex centrifuge reactor, augur (screw), radiative-convective entrained flow, microwave, moving bend and flexed bed, ceramic ball down-flow and vacuum [5, 76]. In general, fast pyrolysis of biomass under appropriate conditions is capable to convert lignocellulosic biomass into bio-oils containing various biochemicals, potential to be further upgraded to drop-in biofuels and valuable biochemicals as replacements for fossil fuels and its derived chemicals. Details of bio-oils and their applications are reviewed in the following section.

2.3.2 Bio-oil and its application

Bio-oil is a major valuable product produced from fast pyrolysis, which has great potential as an energy source alternative to fossil fuels in the future energy market. The advantages of utilisation of bio-oil can be summarised as:[77]

- It can be used in either a small-scale power generation system or large-scale power systems (co-firing), and in existing power plants to save large capital costs.
- It can easily be Stored and transported as liquid fuels.
- It has a high energy density in comparison with atmospheric biomass gasification fuel gases.
- It is feasible for intermittent operation.

The compositions of bio-oils are complex with various acids, aldehydes, alcohols, sugars, esters ketones, phenolics, oxygenates, hydrocarbons, and steroids. Some detectable biochemicals are shown in Table 2-3.

Table 2-3. Some biochemicals and their compositions in bio-oils obtained from fast pyrolysis of lignocellulosic biomass. [78]

Chemical	Minimum (wt.%)	Maximum (wt.%)
Levoglucosan	2.9	30.5
Hydroxyacetaldehyde	2.5	17.5
Acetic acid	6.5	17
Formic acid	1	9
Furfuryl alcohol	0.7	5.5
1-hydroxy-2-propanone	1.5	5.3
Catechol	0.5	5
Methanol	1.2	4.5
Methyl glyoxal	0.6	4
Cellobiosan	0.4	3.3
1,6-anhydroglucofuranose	0.7	3.2
Furfural	1.5	3
Glyoxal	0.6	2.8
Formaldehyde	0.4	2.4
4-methyl-2, 6dimetoxyphenol	0.5	2.3
Phenol	0.2	2.1
Propionic acid	0.3	2
Acetone	0.4	2
Methylcyclopentene-ol-one	0.3	1.9
Methyl formate	0.2	1.9
Hydroquinone	0.3	1.9
Acetol	0.2	1.7
2-cyclopenten-l-one	0.3	1.5
Syringaldehyde	0.1	1.5
1-hydroxy-2-butanone	0.3	1.3
3-ethylphenol	0.2	1.3
Guaiacol	0.2	1.1

Furthermore, the physical properties and elemental compositions of raw bio-oils are presented in Table 2-4 with comparison to heavy fuel oils. Compared with heavy fuel oils, bio-oils have high water content, low pH value, high oxygen content and high viscosity range (35-1000 cP at 40 °C). In addition, the characteristics of bio-oils and their corresponding effects and causes are listed in Table 2-5. The presence of water in the bio-oil can reduce the viscosity to increase the fluidity which is beneficial to the atomization and combustion of bio-oil in an engine[79]. Moreover, the water content has major effects on the oxygen content in bio-oil[79].

Table 2-4 Physical properties of crude bio-oil from fast pyrolysis. [4]

Physical property	**Bio-oil**	**Heavy fuel oil**
Moisture content	25%	0.1
pH	2.5	-
Specific gravity	1.2	0.94
Elemental analysis		
C	54-58%	85%
H	5.5-7%	11%
O	35-40%	1%
N	0-0.2%	0.3
Ash	0-0.2	0.1
HHV as produced	16-19 MJ/kg	40 MJ/kg
Viscosity (50 °C and 25% water)	40-100 mpa s	180
Solids (char)	0.2-1%	1
Vacuum distillation residue	up to 50%	1

Table 2-5 Characteristics of crude bio-oil. [5]

Characteristic	**Cause**	**Effects**
Acidity of low pH	Organic acids from biopolymer degradation	Corrosion of vessels and pipe work
Aging	Continuation of secondary reactions including polymerization	Slow increase in viscosity from secondary reactions such as condensation potential phase separation
Alkali metals	Nearly all alkali metals report to char so not a big problem High ash feed Incomplete solids separation	Catalyst poisoning Deposition of solids in combustion Erosion and corrosion Slag formation Damage to turbines
Char	In complete char separation in process	Aging of oil Sedimentation Filter blockage Catalyst blockage Engine injector blockage Alkali metal poisoning
Chlorine	Contaminants in biomass feed	Catalyst poisoning in upgrading
Color	Cracking of biopolymers and char	Discolouration of some products such as resins
Contamination of feed	Poor harvesting practice	Contaminants notably soil act as catalysts and can increase particulate carry over
Distillability is poor	Reactive mixture of degradation products	Bio-oil cannot be distilled – maximum 50% typically. Liquid begins to react at below 100 °C and substantially decomposes above 100 °C
High viscosity	---	Gives high pressure drop increasing equipment cost High pumping cost Poor atomization
Low H:C ratio	Biomass has low H:C ratio	Upgrading to hydrocarbons is more difficult
Materials incompatibility	Phenolics and aromatics	Destruction of seals and gaskets

Characteristic	Cause	Effects
Miscibility with hydrocarbons is very low	High oxygenated nature of bio-oil	Will not mix with any hydrocarbons so integration into a refinery is more difficult
Nitrogen	Contaminants in biomass feed High nitrogen feed such as proteins in wastes	Unpleasant smell Catalyst poisoning in upgrading NOx in combustion
Oxygen content is very high	Biomass composition	Poor stability Non-miscibility with hydrocarbons
Phase separation or inhomogeneity	High feed water High ash in feed Poor char separation	Phase separation Partial phase separation Layering Poor mixing
Smell or odour	Aldehydes and other volatile organics, many from hemicellulose	Inconsistency in handling, storage and processing White not toxic, the smell is often objectionable
Solids	See also Char Particulates from reactor such as sand	Sedimentation Erosion and corrosion
Structure	Particulates from feed contamination The unique structure is caused by the rapid de-polymerisatrion and rapid quenching of the vapours and aerosols	Blockage Susceptibility to aging such as viscosity increase and phase separation
Sulpur Temperature sensitivity	Contaminants in biomass feed Incomplete reactions	Catalyst poisoning in upgrading Irreversible decomposition of liquid into two phases above 100 °C
Toxicity	Biopolymer degradation products	Irreversible viscosity increases above 60 °C Potential phase separation above 60 °C Human toxicity is positive but small Eco-toxicity is negligible

Characteristic	Cause	Effects
Viscosity	Chemical composition of bio-oil	Fairly high and variable with time Greater temperature influence than hydrocarbons
Water content	Pyrolysis reactions Feed water	Complex effect on viscosity and stability: increased water lowers heating value, density, stability, and increase pH Affects catalysts

To improve the properties of bio-oils, efforts need to be taken either to upgrade bio-oils after catalyst-free pyrolysis or producing high-quality bio-oils via catalytic fast pyrolysis as illustrated in Figure 2-9.

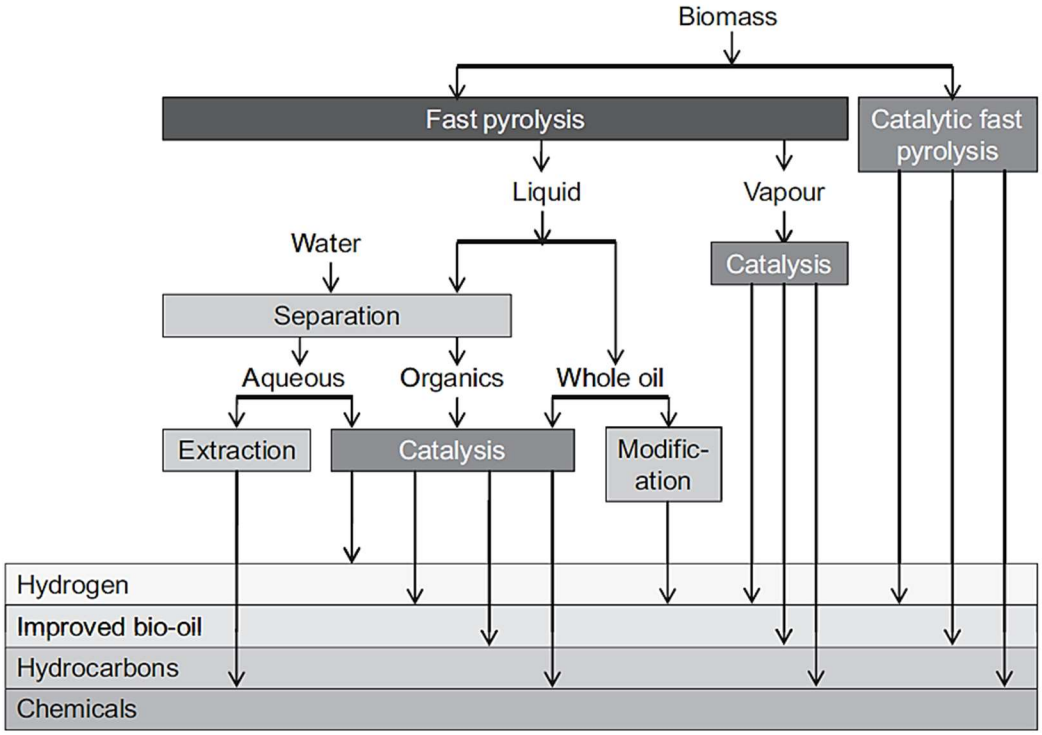

Figure 2-9 Upgrading methods and the main products from upgrading. [5]

The main physical methods for upgrading bio-oils include filtration, solvent addition, and emulsions. Furthermore, filtration can be divided into hot vapour filtration, (reducing viscosity, ash content and lower carbon content), and liquid filtration (removing large particles)[5]. Solvent addition reduces the viscosity of crude bio-oil by adding polar solvents, such as methanol. Adding surfactant is a favourite method of emulsifying bio-oil with diesel oil[5].

Achieving the application of conventional transport fuel requires full deoxygenation by two methods, namely, hydrotreating and catalyst vapour cracking, both need to use catalysts under different conditions to reduce oxygen content in bio-oil[4]. Hydrotreating treats bio-oil under high temperature in the presence of catalysts such us sulfided CoMo or NiMo supports on alumina with a source of hydrogen. In the process of vapour cracking, acidic zeolite catalysts are used under 450 °C and atmospheric pressure to achieve deoxygenation and dehydration-decarboxylation[4]. There are other chemical upgrading methods proposed by different research groups

including aqueous phase process, mild cracking, esterification, hydrogen gasification, and model compounds[4].

The major application of bio-oil is generating heat and electricity by combusting in burner/furnace and burner boiler systems. In terms of power generation, bio-oil can be combusted in different engines and turbines, such as diesel engines, Stirling engines, and gas turbines[4]. An important application of bio-oil is to produce commercial chemicals such as Biolime capturing SO_x emissions from coal combustors, low-molecular-weight aldehydes that are actual meat browning agents (especially glycolaldehyde), phenolic compounds that are providing smoky flavours, levoglucosan, and levoglucosenone[4]. All these applications of bio-oil are summarised in Figure 2-10.

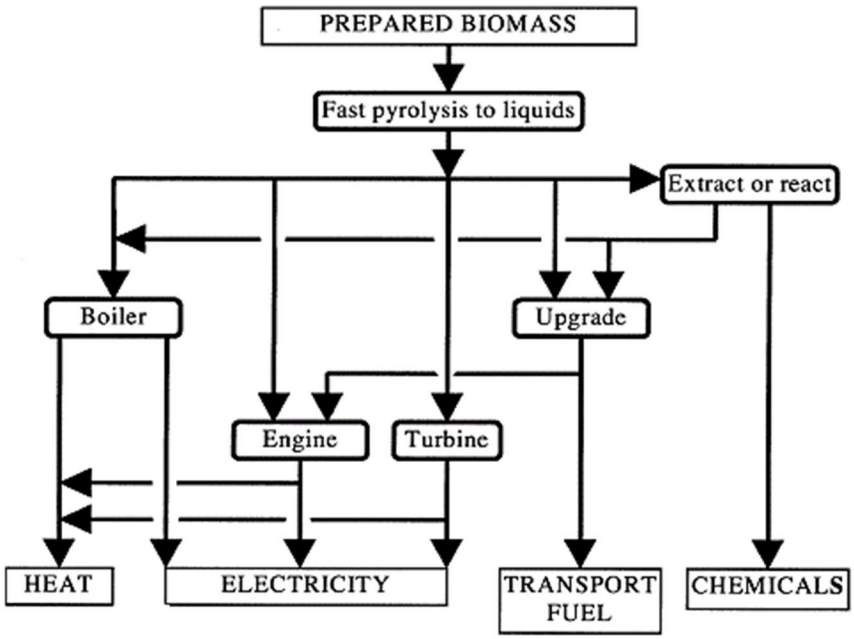

Figure 2-10 Application of pyrolysis liquids. [34]

2.3.3 Biochar and its application

Biochar produced from biomass pyrolysis has significant functions in soil quality improvement, treating wastewater, decreasing greenhouse gas emissions and sequestering atmospheric carbon into soil [80]. Figure 2-11 presents the major feedstocks and process methods to produce biochar. Biochar properties are significantly affected by the feedstocks and methods such as biochar yield, pH, cation

exchange capacity, specific surface area, ash content, volatile matter content and element compostion[81]. The critical effect on biochar quality is temperature and heating rates. Increasing pyrolysis temperature can increase surface area, ash content, and the pH of bio-chars, although the yield of biochar will be reduced. Moreover, the heating rate has an impact on bio-char yield. For example, lower pyrolysis and low heating rates produce more bio-char during the pyrolysis process. Therefore, optimising the pyrolysis condition is based on industrial applications.

Biochar can be produced by different thermal processes such as gasification, slow pyrolysis, fast pyrolysis, hydrothermal carbonisation and torrefaction as presented in Table 2-6. The major methods of producing bio-char are slow pyrolysis and fast pyrolysis. Slow pyrolysis, which is a traditional thermal process, can produce 85% homogeneity biochar, but it is a time consuming and energy intensive process[80]. Although the main product from fast pyrolysis is bio-oil, producing biochar as a by-product of fast pyrolysis is more economically feasible and environmentally-friendly than slow pyrolysis[83]. This has contributed to fast-pyrolysis attracting substantial attention from different researchers.

Table 2-6 Bio-char produced by different methods.[80]

Process	**Temperature (°C)**	**Residence time**	**Bio-char (Yields %)**	**Bio-oil (Yields %)**	**Syngas (Yields%)**
Slow pyrolysis	300-700	Hour-days	35	30	35
Intermediate pyrolysis	~500	10-20 s	20	50	30
Fast pyrolysis	500-1000	< 2 s	12	75	13
Gasification	~750-900	10-20 s	10	5	85
Hydrothermal carbonization (HTC)	180-300	1-16 h	50-80	5-20	2-5
Torrefactions	~290	~10-60 min	80	0	20

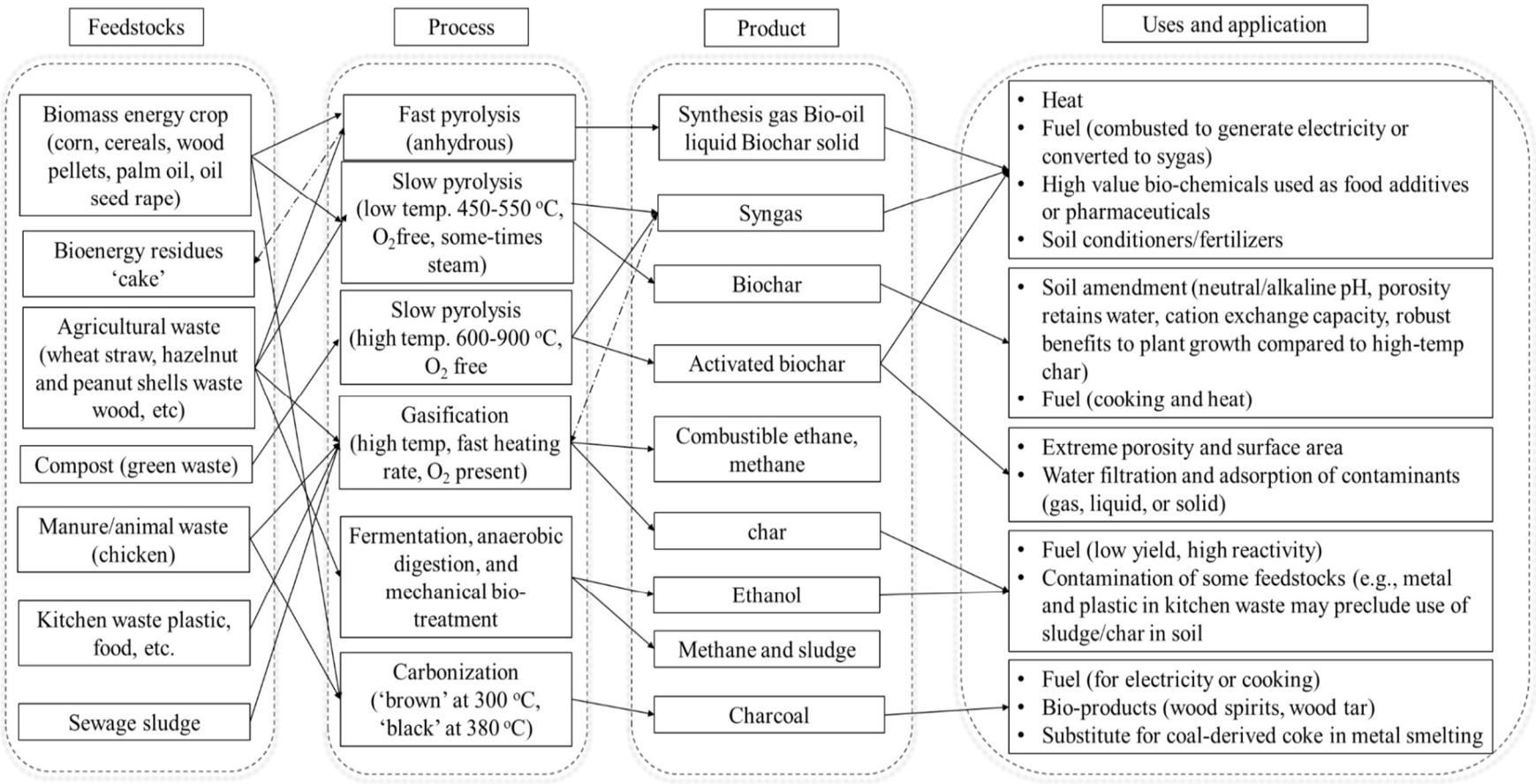

Figure 2-11Bio-char and other products from thermal conversion of biomass. [82]

Of the applications for biochar, the most important one is improving soil quality used in agriculture since it contains a naturally alkaline and high carbon content which can efficiently increase cation exchange capacity and enhance microbial growth[82]. Another significant application for biochar is to remove organic and heavy-metal contaminants from aqueous media during the process of wastewater treatment as it has a high degree of porosity, large surface area, and a strong affinity for non-polar substances (PAHs, dioxins, furans)[82]. Bio-char, especially as a by-product in fast pyrolysis, is, therefore, an environmentally and economically sustainable biomass pyrolysis product.

2.4 Cellulose pyrolysis fundamental and pyrolysis models

Cellulose has the highest content in lignocellulosic biomass. Studying its pyrolysis mechanisms is significant to understand the pyrolysis of biomass. In the past decades, the pyrolysis of cellulose has been widely studied to understand the distribution and properties of products, as well as analyzing the reaction mechanisms. The following sections are prepared to conclude recent advances in understanding the cellulose pyrolysis mechanism including cellulose pyrolysis chemical reactions and proposed pyrolysis models by different researchers.

2.4.1 Chemistry and reactions in cellulose pyrolysis

2.4.1.1 Depolymerisation and transglycosylation

During pyrolysis, a high degree of polymerisation (DP) initially experiences a reaction of depolymerisation. A cleavage of 1, the 4-glycosidic bond is generated by a homolytic or heterolytic process to produce relatively stable low DP or smaller molecule components in the process[84]. Moreover, the reaction rate is a second-order relationship with time of heating under a mild heat temperature. It was found that cellulose depolymerises, without loss in weight, could reach a DP of 300 average under mild temperatures of 180 to 300 °C[85].

Transglycosylation is a form of depolymerisation to produce anhydro-sugars, such as levoglucosan. A popular explanation of the formation of levoglucosan is that cellulose undergoes two transglycosylation steps in the LG chin-end as illustrated in Figure 2-12.

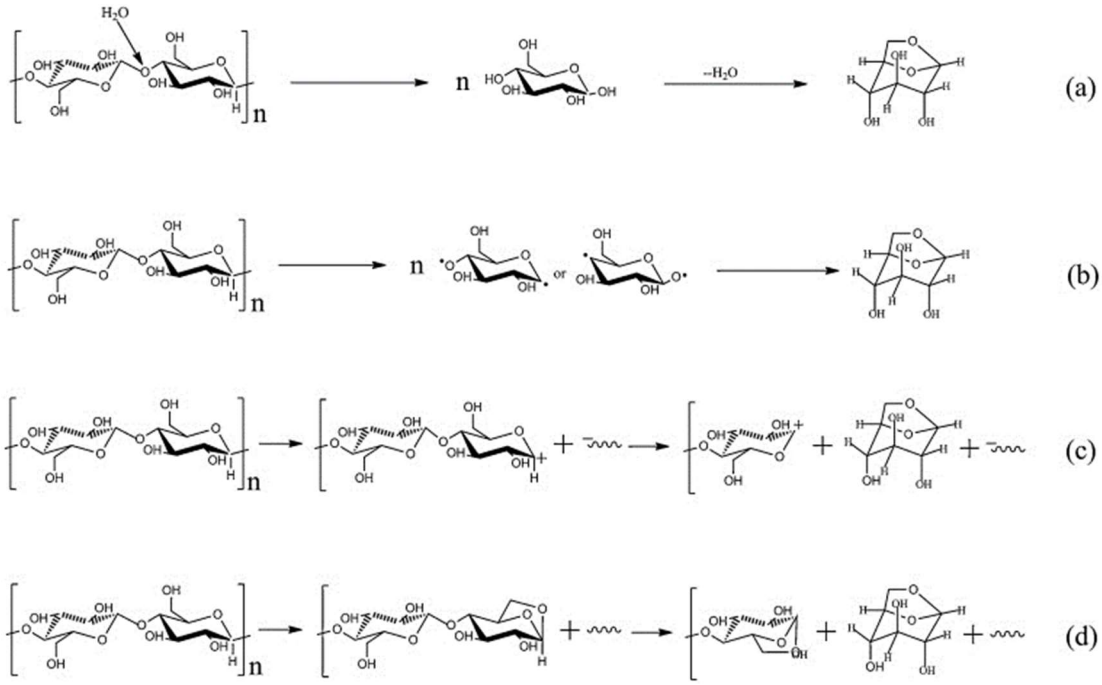

Figure 2-12 Main mechanisms for the formation of levoglucosan from cellulose pyrolysis. [86]

In the first step, a levoglucosan-end and a short cellulose chain are depolymerised from cellulose by 1,4-glycosidic bond cleavage. Then, levoglucosan is formed by unzipping the intermediate in the first step of transglycosylation.

2.4.1.2 Dehydration, cross-linking and isomerisation reaction

Once levoglucosan is formed from depolymerisation, it will undergo dehydration, isomerisation and cross-linking reactions. Dehydration can be a major contributor to weight loss during cellulose pyrolysis, especially at a low pyrolysis temperature (~250 ^{o}C)[87, 88]. The mechanisms of dehydration can be identified as intra-ring and inter-ring dehydration according to the dehydration position of the hydroxyl and hydrogen group. Intra-ring dehydration can produce mono-anhydrous-products by forming C=C at 250 ^{o}C[89, 90]. Inter-ring dehydration producing a cross-linked structure is constructed by two different bonds such as hydrogen and covalent bonds[91]. Comparing the two bonds, covalent bonds are a main form of chemical bonds in the cross-linkage structure since the hydrogen bonds are gradually broken during the pyrolysis process[92]. The covalent bonds are mainly formed in the ether between hydroxyl groups on adjacent chains and ester bridges between the carboxyl and hydroxyl group[92].

Isomerisation can occur before the cross-linking reactions to form mono-anhydrous products. For example, 6,8-dioxabicyclo[3.2.1]octane-2,3,4-triol (LGA) can undergo dehydration and isomerization reactions to generate other anhydrosugars including levoglucosenone (LGO; 6,8-dioxabicyclo[3.2.1]oct-2-en-4-one), 1,4:3,6-dianhydro-β-d-glucopyranose (DGP) and 1,6-anhydro-β-d-glucofuranose (AGF; 2,8-dioxabicyclo[3.2.1]octane-4,6,7-triol)[93]. Moreover, Levoglucosan and glucose can undergo isomerisation reactions to form the products including glyceraldehyde and aldehyde. The major isomerization reactions of glucose are shown in Figure 2-13.

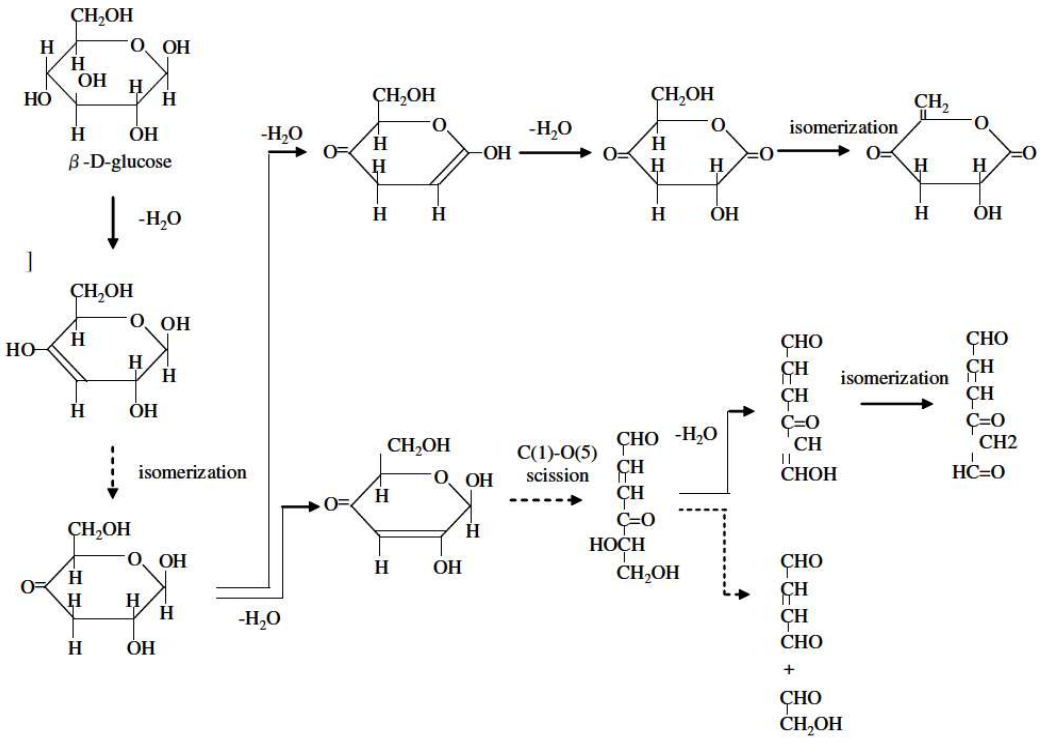

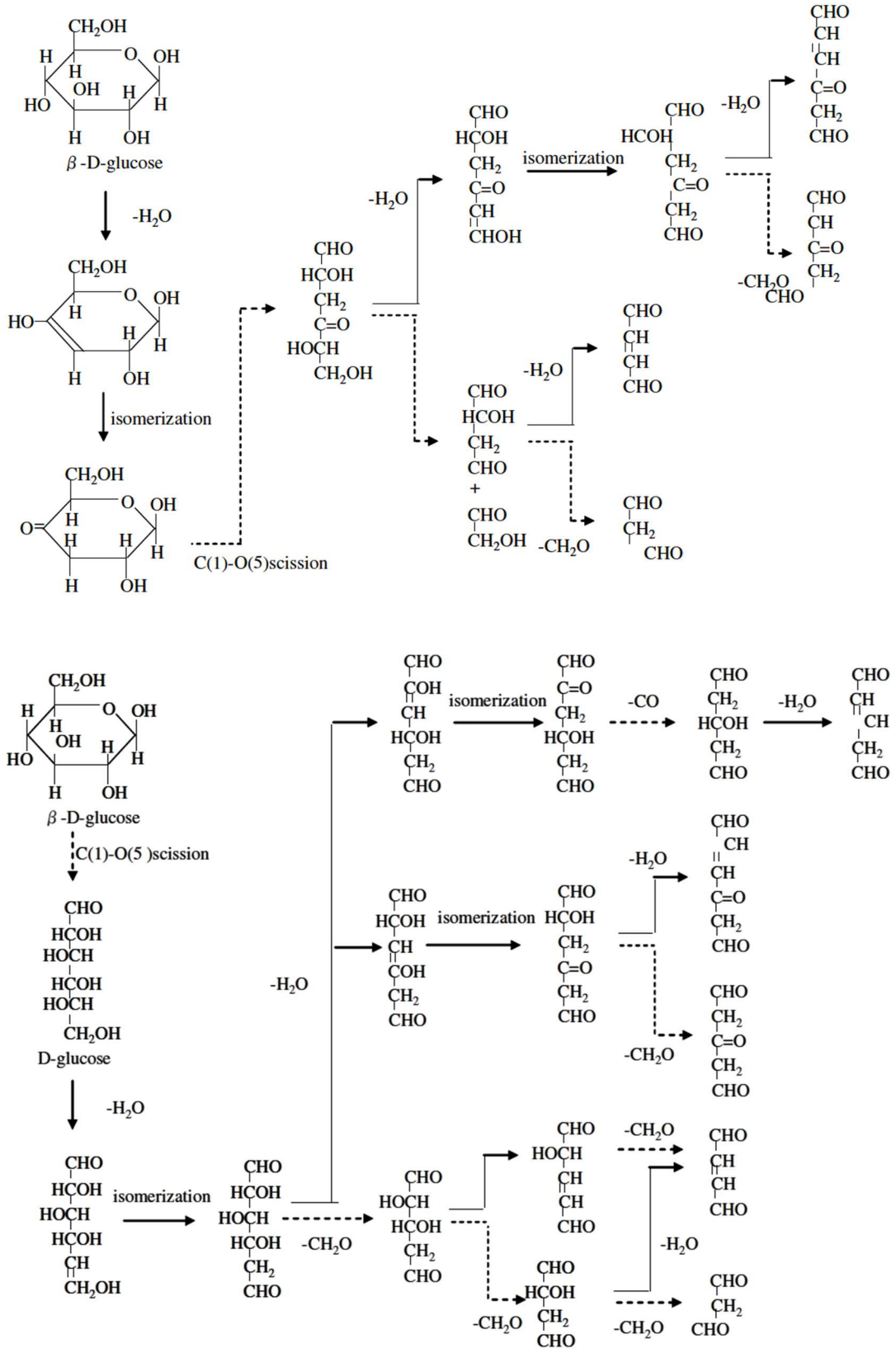

Figure 2-13 Isomerization in the glucose reaction pathways. [94]

2.4.1.3 Decarboxylation and decarbonylation

CO_2 and CO are generated in the pyrolysis process by the reaction of decarboxylation and decarbonylation respectively. A theoretical study on cellulose pyrolysis has found that CO and CO_2 are essentially affected by the decarbonization and decarboxylation respectively, and both reactions are processed via intramolecular hydrogen transfer, but decarbonylation is endothermic while decarboxylation is exothermic[95]. Moreover, oxygen influences the production rate of CO and CO_2 at low-temperature pyrolysis (less than 300 °C) because the autoxidation mechanism can assist on a β-scission in cleavage of the glycosidic bond and an alkoxy radical on the neighboring glucose unit. The mechanism is present in Figure 2-14.

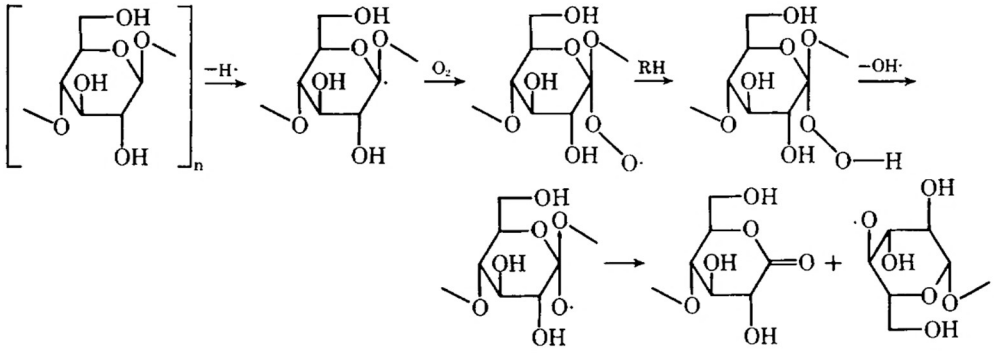

Figure 2-14 Proposed mechanism on cellulose hydroperoxide in air. [96]

However, there is less effect when the pyrolysis temperature is higher than 300 °C because of the independent of the oxidative reactions in thermal degradation process[96]. Meanwhile, the mechanisms of decarboxylation and decarbonylation are important on deoxygenation, which is a vital pathway of defunctionalisation to produce the desired chemicals and fuels[97].

2.4.1.4 Ring open reactions

Major volatiles formed by decomposition/ring scission from cellulose monomers pyrolysis are low molecule weight components, such as glycolaldehyde, hydroxyl acetaldehyde, and acetol[98]. According to the major chemical reaction pathway shown in

Figure 2-15, the routes of 3, 4, and 9 present the decomposed products via ring cleavage reactions.

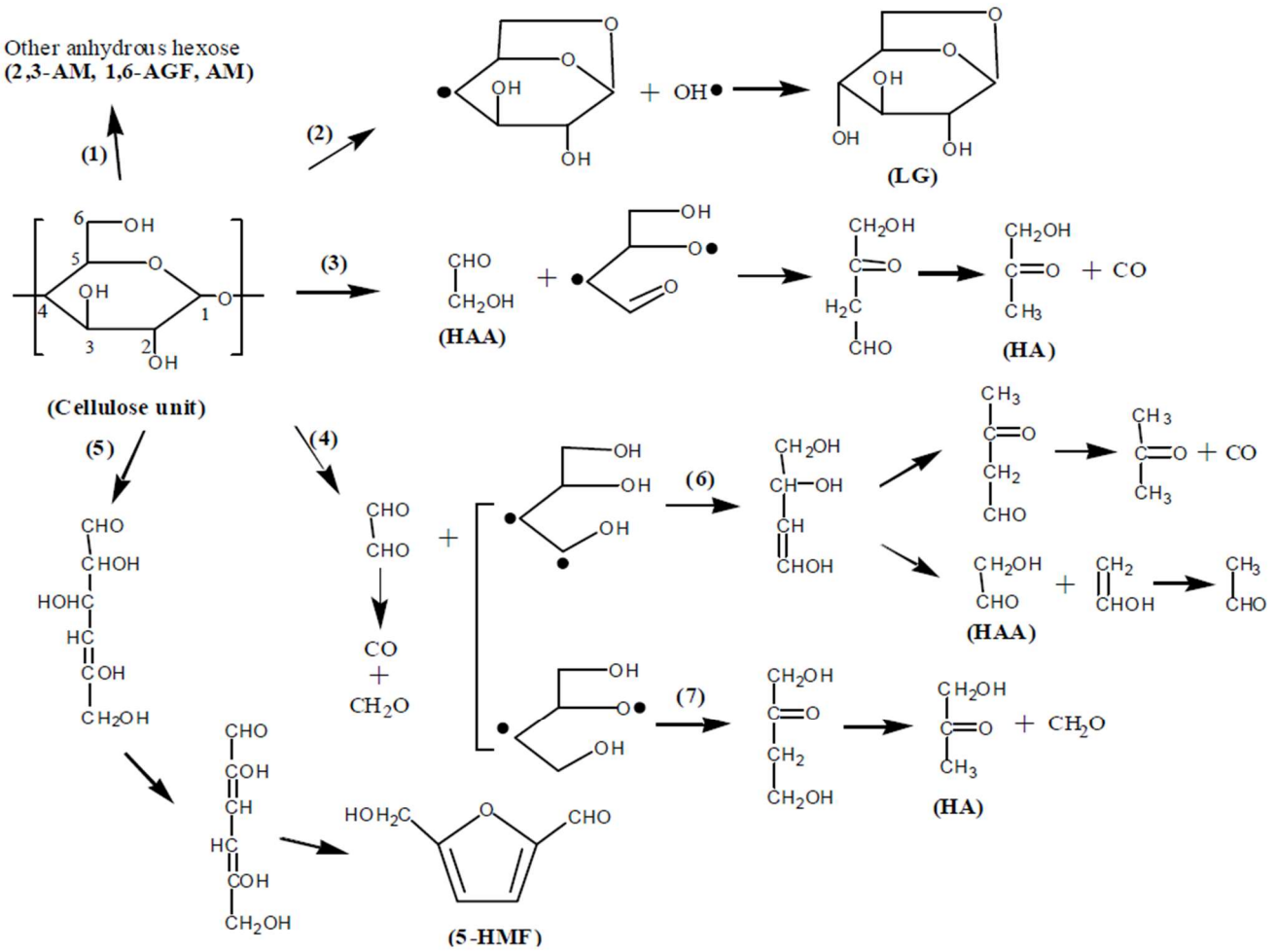
Other anhydrous hexose
(2,3-AM, 1,6-AGF, AM)
(1)
(2)
(LG)
(Cellulose unit)
(3)
(HAA)
(HA)
(4)
(5)
(6)
(7)
(HAA)
(HA)
(5-HMF)

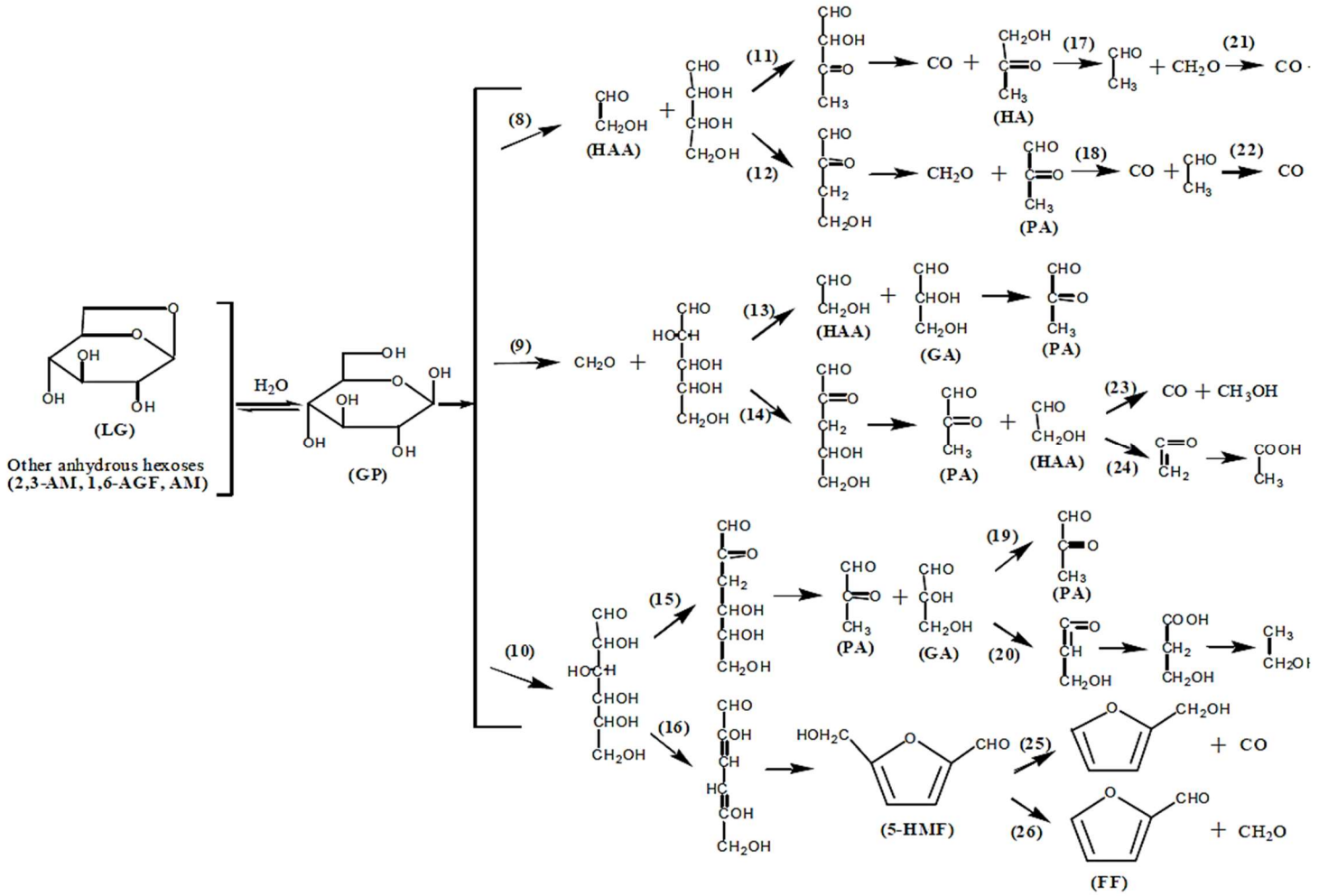

Figure 2-15 Chemical reaction pathways of cellulose and levoglucosan under pyrolysis conditions. [99]

Generally, ring open reactions contain (1) ring open reactions with subsequent decomposed products and (2) ring open reactions without fragment. The subsequent decomposed products can yield from four-carbon units (pathway 3, 4 and 8) or a five-carbon fragment (pathway 9). Pathways 5 and 10 demonstrate the ring open reactions without fragment. Pathway 5 can produce a double bond on C4 and C5 via the ring cleavage of a glycosidic bond, but pathway 10 can generate a hexose chain structure simply via a ring cleavage.

Meanwhile, the ring cleavage position can have a critical impact on the final products. For example, C1/C5 scission can produce a single carbon component such as CO_2 and formic acid; C2/C4 scission is likely to produce glycolaldehyde, while C3 scission may generate acetol formation.

2.4.2 Cellulose pyrolysis kinetics models

The kinetics of cellulose pyrolysis has been widely investigated for a long period via the thermogravimetric (TG) analysis method, TGA coupled with FTIR, GC, MS or other advanced analysis methods. Overall, there is some significant recognition of cellulose kinetic models proposed by Piskorz, Di Blasi, Banyaz, Agrawal, Wooten, Hosoya and so on. Broido's group could be the first proposed kinetic model on cellulose pyrolysis in the 1960s. Broido proposed cellulose pyrolysis kinetic under the temperature range 200-400 °C[100]. The results indicated pure cellulose decomposed by two competitive endothermic processes including the slight endothermic formation of anhydrous-cellulose below 280 °C and a competitive endothermic unzipping reaction above 280 °C, causing tar formation. Then, the anhydro-cellulose processes the exothermic decomposition reaction to form char and gas. The overall scheme is shown in Figure *2-16*.

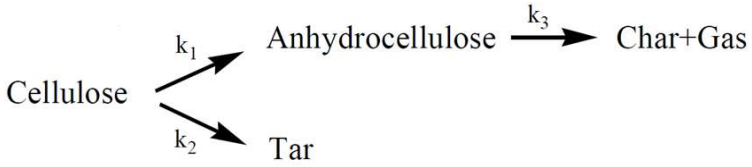

Figure 2-16 The kinetic model for cellulose pyrolysis proposed by Broido and Kilzer in 1965. [100]

Agrawal has provided a complete set of kinetic data to confirm that this kinetic only existed on the isothermal, fixed-bed conditions at the pyrolysis temperature ~270 °C[101]. However, there was no clear evidence proving the intermediate product of anhydrous

cellulose produced in the cellulose pyrolysis process in the above publication. In 1975, a kinetic model was proposed by Broido and Nelson when they studied the impact on the cellulose char yield during thermal pre-treatments at 230-275 °C.[102] The experiment method of applying a large sample of cellulose proved that the char was formed from solid-vapor interactions in the prolonged thermal pre-treatment without forming the intermediate of anhydrous-cellulose. The scheme is shown in Figure 2-17.

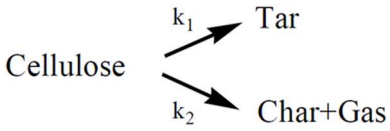

Figure 2-17 The kinetic model for cellulose pyrolysis proposed by Broido and Nelson in 1975.[102]

In 1979, Bradbury and Shafizadeh (BS model) proposed a kinetic model of cellulose pyrolysis at a low-temperature range of 259-341 ºC. BS model found an initial reaction of depolymerisation producing active cellulose at low temperatures (259-295 ºC), and then the active cellulose was decomposed via two competitive first-order reactions yielding either volatiles, or char and gases at the pyrolysis temperatures above 295 ºC [103]. The BS model is shown in Figure 2-18.

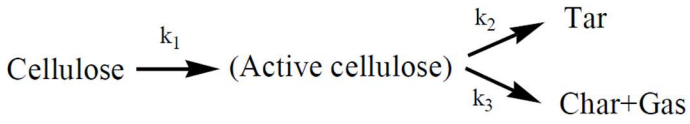

Figure 2-18 The kinetic model for cellulose pyrolysis proposed by Bradbury and Shafizadeh 1975. [103]

There is an argument from Antal-Varhegyi on the BS model, since Antal's group cannot prove the existence of active cellulose to support the BS model in the analysis of TGA and DSC. Consequently, Figure 2-19 is presented the proposed kinetic model on cellulose pyrolysis in the presence of water- catalysed decomposition reactions[104].

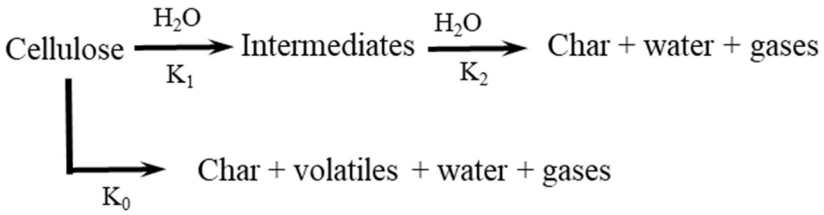

Figure 2-19 The cellulose pyrolysis kinetic model from Anta and Vahegyi proposed in 1993.[104]

According to their model, cellulose pyrolysis underwent two competitive reactions including the non-water catalysed decomposition, and the water catalysed decomposition. The non-water catalysed decomposition produced char, water and gas volatiles. However, the water-catalysed decomposition experienced intermediates and then further water catalysed decomposition reactions giving char and gases.

Recently, much research has observed intermediates of anhydro-oligosaccharides at low temperature pyrolysis such as levoglucosan, cellobiosan and cellotrosan[105-107]. Therefore, the kinetic model proposed by Diebold in 1994[108] (similar to that proposed by Wooden in 2004 [106]) is a systemic kinetic model.

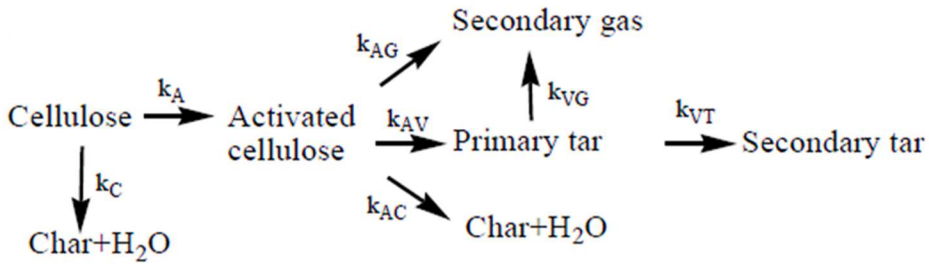

Figure 2-20 The kinetic model proposed by Diebold in 1994 (similar to that proposed by Wooden in 2004). [108]

The model (Figure 2-20) shows cellulose processes dehydration reactions giving char and water, and a chain-cleavage reaction to form a low DP (activated cellulose). Then, the activated cellulose decomposed to form secondary gases, primary tar, char, and water. The secondary tar was formed from re-polymerisation of primary vapours. Bradury[103] and Antal[104] advised the secondary tar was re-polymerised by anhydro-sugars which has been proven by Hosaya [109].

In 2009, Mamleev [110] highlighted a two-level model, shown in Figure 2-21, which indicated liquid intermediate (high boiling tar) formed by transglycosylation as an important electrode, then volatile acid from various heterolytic reactions dissolved in acid to catalyse β-elimination.

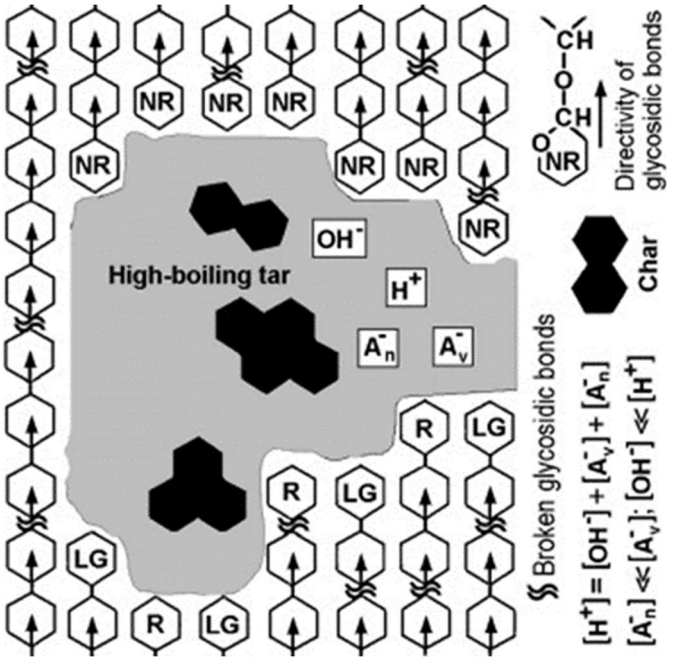

Figure 2-21 The two-level kinetic model proposed by Mamleev in 2009. [110]

Although these models have demonstrated the cellulose pyrolysis mechanism, there still exists ambiguity and controversy regarding the chemical reaction mechanisms, such as the structure changes of cellulose molecules to form specific products and the char formation process from re-polymerisation of anhydrous sugars.

2.5 Factors influencing pyrolysis

Cellulose pyrolysis behavior can be impacted by several variables, including raw material properties, heating rate, temperature, pressure, and inorganic metals (AAEM). The following sections summarize the major effects caused by these variables.

2.5.1 Raw material properties

Naturally existing material can directly affect the outcome of pyrolysis products because of crystallinity, degree of polymerisation (DP), and orientation. By comparison with high DP cellulose, low DP cellulose are less stable and DPs ≤ 200 are precursor to form levoglucosan during the pyrolysis process [111-113]. For example, the productivity of levoglucosan from different sources containing different DPs is following the order native cotton (60-63 wt.%) > mercerized cotton (36-37 wt.%) >Viscose rayon (4-5 wt.%[111]). The crystallinity has an important effect on the cellulose thermal stability during the pyrolysis. According to the results from Liu et al. and Wang et al., the amorphous cellulose yielded higher soluble intermediates (sugar oligomers) at the low pyrolysis temperature (<270 °C)[112] and the amorphous

cellulose produced more 5-HMF, 5-methylfurfural and furfural due to the dehydration reactions[113].

2.5.2 Heating rate

The heating rate can be a major factor in the yield of bio-oil and biochar. Various heating rates (from 5 to 800°C) have been studied by different groups to determine the effect on pyrolysis products in the fixed bed reactor. Most of the research reveals that increasing heating rate could enhance the bio-oil yield, but the growth in oil yield could be negligible if the heating rate is over the optimum heating rate[114-117]. For example, Onay et al found that the bio-oil yield from rapeseed pyrolysis was increased by 58 wt.% when the heating rate was increased from 100 to 300°C/min [115]. Tsai et al found that the bio-oil yield could reach a maximum yield at the heating rate of 200 °C/min[117].

It is worth mentioning that the optimum heat rate for achieving highest yields of bio-oils can be varied for different species of feedstock materials, especially in slow pyrolysis. For instance, maximum liquid yield of 37.7% was formed in olive residues slow pyrolysis at the temperature 550 °C with a heating rate 10 °C/min in comparison with the yield of 32% bio-oil at the same temperature with a heating rate of 50 °C/min [118]. However, some feedstock shows that increasing the heating rate could have an adverse effect on the yield of bio-oil. Hassen-Trabelsi et al. found that the bio-oil yield decreased from 80 wt.% to 5 wt.% when the heating rate was increased from 5 to 15 °C/min[119]. Although the yield of bio-oil from slow pyrolysis can be optimised by the heating rate, fast pyrolysis is still the best approach to obtain the highest yield of bio-oil. For example, the maximum bio-oil formed in slow pyrolysis of tobacco residues was 27% at the pyrolysis temperature 550°C with a heating rate of 7°C/min, but the yield of bio-oil still can be increased 10% in the fast pyrolysis (300 °C/min) [116].

Furthermore, the char yield is also affected by the heating rate. A low heating rate provides more residence time, allowing a more thermally stable cross-linking structure to form, stabilizing the solid residue when the pyrolysis is conducted at below 300 °C[120].

2.5.3 Temperature

In general, increasing pyrolysis temperature has a positive effect on the yield of liquid products; however, the high temperature can cause a negative effect on liquid product yield. Many researchers show that the optimum temperature of bio-oil yield is around 450-550 °C, depending on the feedstock and other variables[114, 117, 121-124]. For example, Tsai et al. observed the yield of bio-oil increased from 11.26 wt.% to 35.92 wt.% when temperature was increased from 400 °C to 500 °C[117]. Besides that, the optimum pyrolysis temperature for obtaining maximum bio-oil is slightly different for different feedstocks. For example, the highest yield for rick husk was 70 wt.% at 450 °C[125], that for palm waste was 72.4 wt.% at 500 °C[126], that for sugarcane bagasse was 46 wt.% at 475°C [127], while that for neem de-oiled cake was 40.2 wt.% at 400 °C [128]. Jung et al showed that an increased temperature reduced bio-oil yield of bamboo sawdust in the fluidized bed reactor during pyrolysis[129], where the highest bio-oil yield of 72 wt.% occurred at 405 °C, and the bio-oil yield was dropped to 61 wt.% when the temperature was increased to 487°C. Decreased bio-oil yield occurred because secondary cracking of volatiles was enhanced at higher temperatures and led to higher gas yields[130].

High pyrolysis temperature can affect the quality of bio-oil and enhance cracking reactions during the pyrolysis process. For instance, the low pyrolysis temperature mainly produces alkenes, alkanes, long-chain fatty acids and esters, whereas high temperature favorably produces aromatics, shorter aliphatic carbons and lower-molecular-weight compounds (alcohols and ketones), which are formed from the cracking of the aliphatic species[131, 132].

2.5.4 Inorganic metals' influence on cellulose pyrolysis

Theoretically, large amounts of sugar could be produced in the carbohydrate-rich biomass pyrolysis process via depolymerisation reactions. However, the natural presence of AAEMs can catalyse decomposition reactions to yield lower –molecular-weight components such as glycolaldehyde and organic acids. Various researchers studied the impacts of AAEMs on cellulose pyrolysis to understand the underlying mechanisms on biomass pyrolysis.

Mineral metals can act as Lewis acidity and basicity to form complexes and stabilize specific reaction intermediates in the pyrolysis process[133]. The analysis results from the research are summarised in Table 2-7. The influence of inorganic minerals (Ca, K,

Na, and Fe) on cellulose pyrolysis has been widely studied[17-24, 133-135]. From the research results, it can be concluded AAEMs catalyse depolymerisation and decomposition reactions to increase char and gas yields, and shift pyrolysis temperatures lower. Varhegyi suggested that the catalysed effective order of AAEMs was $ZnCl_2$>NaCl> $FeSO_4$ but with $MgCl_2$ having a limited effect on the overall reactions[136]. This order has been proven by a variety of research; however, it was also found that Mg has an effect on cellulose pyrolysis which is similar to other minerals[20, 21, 23, 135-137]. Shimada suggested that the influence of Mg and Ca depended on the loading ratio during pyrolysis[135]. Moreover, Liu found that Mg and Ca had a significant effect on cellulose pyrolysis during the heating process[20]. The anion effect on cellulose pyrolysis was also studied by Müller-Hagedorn in 2003. They found the anions could reduce the yield of levoglucosan with the order of $Cl^- > SO_4^{2-} > HCO_3^-$ [134]. Inorganic minerals have significant effects on cellulose pyrolysis via catalysed dehydration and decomposition reactions which implies a natural presence of AAEMs considerably affects biomass pyrolysis behaviors and product distributions.

Table 2-7 AAEM effects on cellulose pyrolysis.

Authors	Effects
Varhegyi et al. (1988) [136]	increasing the productivity of volatile species including Furan, 2-furaldehyde and other aldehydes; Increasing H_2O, CO and CO_2 produced at the earlier stage, reducing the decomposition temperature, and Increasing the Char yield; The catalyzation order: $ZnCl_2$>NaCl>$FeSO_4$ and $MgCl_2$ did not change the overall reactions.
Müller-Hagedorn et al. (2003) [134]	NaCl and KCl had remarkable effects on the pyrolysis temperature and the product distribution, but $CaCl_2$ only changed low-temperature degradation and had no effect on the product distribution; Based on studies of anions, they found the effect of the anion on the reduction of levoglucosan order of magnitude was Cl^->SO_4>HCO_3.
Shimada et al. (2007) [135]	NaCl and KCl had no change on the weight loss temperature but $MgCl_2$ and $CaCl_2$ had a substantial reduction in weight loss temperature at the pyrolysis temperature range from 150-400 ºC. The influence of $MgCl_2$ and $CaCl_2$ on the weight loss behavior were dependent on the loading ratio but NaCl and KCl are independent of the amount; All metal chlorides significantly changed the low molecular weight product composition even at a lower metal addition.
Khelfa et al. (2008) [137]	Inorganic salts ($MgCl_2$, $ZnCl_2$, and $NiCl_2$) have an influence on the primary degradation; $MgCl_2$ decreased the preliminary dehydration temperature and increased the char and gases yields and disfavored the depolymerisation mechanism; $ZnCl_2$ acted as a Lewis acid to catalysed the chemical reactions of C-O and C-C heterolytic scissions, dehydration, depolymerisation and ring-opening; $ZnCl_2$ largely shifted the degradation temperature to lower temperature (~ 60ºC); $NiCl_2$ had no contribution to catalyzing the cellulose degradation reaction and favored depolymerisation reactions.
Liu et al. (2014) [20]	Inorganic salts (NaCl, KCl, $MgCl_2$, and $CaCl_2$) had contributions on dehydration, and depolymerisation reactions to the decomposition of sugar structures; Alkaline earth metal ions (Mg^{2+} and Ca^{2+}) were more effective than the alkali metal ions (Na+ and K^+) to catalyse the dehydration reactions of sugars during heating-up; Na^+/K^+ were more effective than Mg^{2+} and Ca^{2+} to catalyse dehydration reactions during isothermal pyrolysis

2.6 Pre-treatment methods on biomass pyrolysis, and the effects on pyrolysis

Common methods of passivating AAEMs and enhancing the yield of bio-oil can include acid-leaching, acid-infusion and a combination of both.

Shafizadeh et al. have adapted the acid-leaching method to remove inorganic ash which enhanced the yield of hexoses in the pyrolysis of Douglas-fir pyrolysis because the acid-leaching removed AAEMs in biomass and trace amounts of acid can catalyse the lignocellulose pyrolysis [138]. The method of acid leaching has been applied to different materials (rick husk, straw, hay and bagasse, and herbaceous feedstocks [29, 139-142]) and different pyrolysis methods (flash pyrolysis, vacuum pyrolysis[143, 144]) over several decades. They have proven that acid leaching could effectively remove inorganic acid, improving levoglucosan yield and bio-oil quality.

Another method, acid-infusing, can also passivate AAEMs to enhance the yield of levoglucosan, because AAEMs are converted to stable salt and a pH buffer system favoring glycosidic bond breakage[26, 145, 146 147, 148]. The combined method has also been investigated and found to passivate AAEMs and increase the productivity of anhydrous sugars because acid wash removed AAEMs from the biomass and acid-infused catalyse glycosidic bond breakage during the pyrolysis to improve levoglucosan yield[149].

Overall, these methods aim to passivate or remove AAEMs in biomass pyrolysis, to increase anhydrous sugar yields and improve the quality of bio-oil. However, it is critical to control the amount of acid in the pre-treatment process.

The effect of acid loading has been studied by different researchers. For example, Wang et al. found that a small amount of sulphuric acid (0.04 wt.%) led to the decrease of levoglucosan and formation of 1,6 anhydro-glucofuranose because of accelerated dehydration reactions[147]. Zhou et al. found the presence of sulphuric acid decreased bio-oil yield and increased water and char yield since the high concentration of acid favoured dehydration reactions [141]. Moreover, other researchers have concluded that the presence of acid can catalyse decomposition reactions to yield 1,4:3,6-dihydro-α-D-glucopyranose and levoglucosan [30, 150]. Therefore, acid-pre-treatment methods either passivate AAEMs to increase the yield of anhydrous-sugars or accelerate decomposition and dehydration reactions to increase the yield of char, depending on the amount of acid in the pre-treatment methods.

2.7 Conclusions and research gaps

Lignocellulosic is a widely available and promising feedstock for producing biofuels as fossil fuel replacements. There is an increasing research interest of converting lignocellulosic biomass into biofuels and biochemicals via various approaches. The production and application of biofuels will mitigate the climate change by reducing carbon emission caused by using fossil fuels. Innovations in biomass refining technologies will help develop a circular bioeconomy, which will benefit the sustainable development and environment protection in the long run. In-depth understandings on the reaction pathways and kinetics during biomass treatment is essential to enable technique innovations.

Fast pyrolysis is a readily available technique that can rapidly convert lignocellulosic biomass into a major liquid fraction (named as bio-oil), a small fraction of solid (named as biochar), and a fraction of gas (named as fuel gas). High yields (up to 75%) of bio-oils can be obtained by optimised fast pyrolysis, but the fuel quality of bio-oils is far from comparable to fossil fuels. Upgrading techniques are required to either catalytically enhance the quality of bio-oils obtained from catalyst-free pyrolysis or operating catalytic fast pyrolysis. Both approaches need to be further improved based on increasing our understandings into the detailed reaction pathways of biomass and its substructures.

The literature review concluded that the fast pyrolysis performance and quality of bio-oils can be strongly varied due to factors such as raw materials, temperatures, and AAEMs. Amongst these variables, AAEMs could have a critical effect on the quality of bio-oils and the selectivity of by-products due to the catalysed reactions such as decomposition reactions. Although pre-treatment methods such as acid-leaching, acid-infusion and a combined method have been shown as efficient methods to minimize effects of AAEMs and improve the quality and quantity of bio-oil in biomass pyrolysis, understandings on the effect of acid-loading on the reactions mechanisms of biomass are lacked. Unfortunately, insights into the effect of acids on the reaction mechanisms and kinetics of lignocellulosic biomass compositions (lignin, cellulose and hemicellulose), especially the detailed primary and secondary reactions, are scarce. As cellulose is the most abundant fraction in lignocellulosic biomass, studying the effect of acid-loading on its decomposition mechanisms under pyrolysis conditions is vital to fully enable high-efficient conversion of biomass by fast pyrolysis. However, only

a few researchers reported that the acid-catalysed pyrolysis led to a dehydration reaction in the formation of dehydrated products such as 5-HMF and levoglucosan. To date, there is no systematic study on the intermediates formed from acid-catalysis in biomass pyrolysis or biomass components pyrolysis under low temperatures to develop the mechanism of acid-catalysed biomass pyrolysis. Therefore, this PhD project was conducted to study acid-catalysed cellulose pyrolysis to expand understandings into the underlying acid-catalysed pyrolysis mechansims. This research has covered studies on following aspects.

1. Understanding the formation and characteristics of acid-catalysed cellulose pyrolysis primary intermediates under different reactions, temperatures and holding times by using the analytical technique to characterise the intermediates.
2. Understanding the acid-loading effects on the formation of intermediates during the cellulose pyrolysis at different temperatures and holding times, to investigate cellulose pyrolysis behaviors and kinetics.
3. Identifying the evolution of cellulose pyrolysis primary intermediates formed from acid-catalysed pyrolysis, since they have short-lift time and rapid reactants.
4. Identifying the evolution of the secondary intermediates from the acid-catalysed pyrolysis, to understand the reaction pathway furtherly.
5. Determining the stability of the secondary intermediates, to predict the final products and pyrolysis behaviors.

2.8 Research objectives

This thesis aims to systematically characterise of reaction intermediates produced from acid-catalysed cellulose pyrolysis and its model compounds under different conditions. The major objectives of this study include:

1. Qualify and quantify water-soluble intermediates yielded from acid-catalysed cellulose pyrolysis at low temperatures with different retention times and discover the temperature and acid-loading levels effect on the formation of intermediates, to propose a mechanism for acid-catalysed cellulose pyrolysis at low temperatures.

2. Identify the evolution of one of major primary component (glucose) produced from acid-catalysed cellulose pyrolysis, to identify a reaction mechanism of the secondary reaction of the acidic glucose pyrolysis.
3. Identify the evolution of another major primary component (levoglucosan) produced from acid-catalysed cellulose pyrolysis, to identify a reaction mechanism of the secondary reaction of the primary component.
4. Investigate the effect of linkage of disaccharides formed from the polymerisation of glucose and levoglucosan to understand the role of linkage of disaccharides in the fast pyrolysis and propose a new underlying mechanism of acid-catalysed cellulose pyrolysis.

Chapter 3 Methodology and experimental techniques

3.1 Introductions

This chapter covers the overall research methodology applied in this study and explains analysis instruments, experiment setup, equipment, and sample preparation.

3.2 An Overlook of the Methodology

This study selected cellulose, glucose, levoglucosan, cellobiose and trehalose as the model compounds to study their fast pyrolysis reaction mechanisms with the presence of acids. Figure 3-1 is given to illustrate the research methodology and its linkage to the research objectives.

After conducting the fast pyrolysis experiment in a drop-tube fixed-bed reactor, the obtained solid residues from the pyrolysis were fractionated into a water-soluble fraction and a water-insoluble fraction, followed by various analysis. For the water-insoluble fraction, samples were analysed by an elemental analyser, NMR (nuclear magnetic resonance spectroscopy) and FTIR (Fourier Transform Infrared Spectroscopy). For the water-soluble fraction, samples were analysed by a TOC (total organic carbon) analyser, an IC-MS (Ion Chromatography-Mass spectrum) system and a gel permeation chromatography (GPC) in HPLC-ELDS (high-performance liquid chromatography equipped with an evaporative light scattering) detector.

The whole procedures of experiments and analysis were repeated for multiple times to ensure reproducible results. Purposes and brief experimental approaches for each model compounds are briefly given as follows.

3.2.1 Acid-catalysed cellulose pyrolysis

Two different samples including acid-loaded cellulose and raw cellulose were pyrolysed in a drop-tube/fixed bed reactor at various conditions (different pyrolysis temperatures and holding times). Chars yielded form the pyrolysis were characterised by functional groups in NMR and FTIR, respectively. Elemental analysis was conducted to determine the ratio of C, H, and O in chars.

The water-soluble intermediates were dissolved in ultra-pure water and characterised and quantified by the following analysis methods: TOC, HPAEC-PAD-MS, and HPAEC-PAD. Post-hydrolysis was applied to analyse the sugar structure in the solid product and the water-soluble intermediates. Based on this analysis, the acid-catalysed cellulose mechanism is proposed and discussed in detail in chapter 4.

3.2.2 Acid-catalysed glucose and levoglucosan pyrolysis

The model compound of glucose has been studied to determine the underlying pyrolysis mechanism of the acid-catalysed glucose as an important intermediate produced in the acid-catalysed cellulose pyrolysis at low temperatures. The acid-loaded glucose was pyrolysed in a drop-tube/fixed bed reactor. After the pyrolysis, the solid product was dissolved in ultra-pure water, and then the soluble intermediates were characterized and quantified in HPAEC-PAD-MS. Meanwhile, the total carbon in solution was analysed in TOC. Therefore, the selectivity and yield of intermediates were calculated on basis of TOC and HPAEC-PAD.

The polymers in the solid products and the yielded solid product were characterised in HPLC-ELDS. The sugar structures were analysed by the methods of post-hydrolysis and quantified in HPAEC-PAD. The reaction mechanism is proposed and discussed in detail in chapters 5 and 6.

3.2.3 Acid-catalysed disaccharides pyrolysis

The pyrolysis was conducted using the procedures outlined in section 3.2.2. The water-soluble intermediates in solid products were characterised in HPACE-PAD-MS and HPLC-ELDS. Then, the identified intermediates were quantified in HPAEC-PAD. The total carbon in solution was analysis in TOC to calculate the selectivity and yield of intermediates. Moreover, the sugar structure in solid products was analysed using post-hydrolysis. The linkage of disaccharides effects is discussed in detail in Chapter 7.

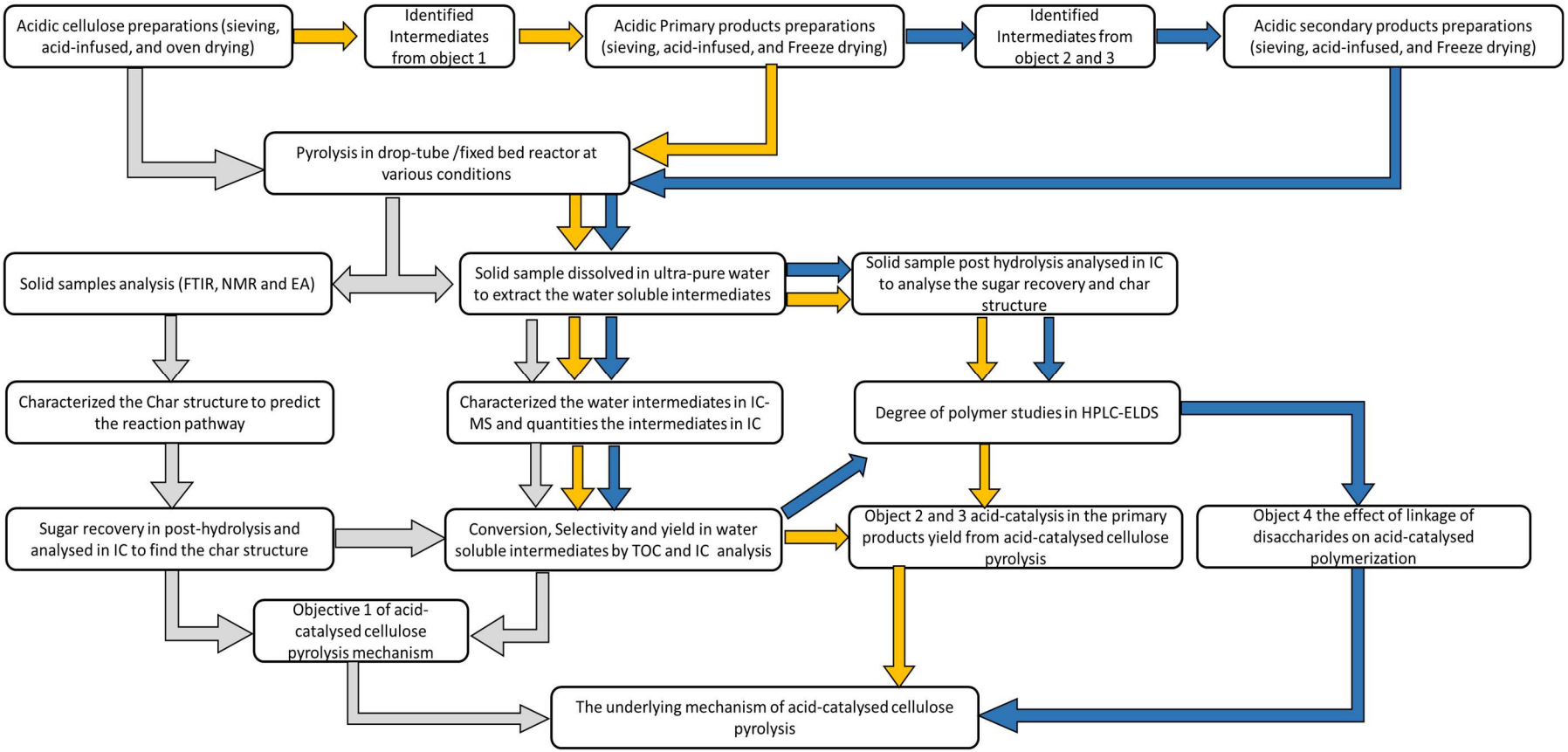

Figure 3-1 Research methodology and the linkages to the research objectives linked to section 2.8.

(Grey indicating object1, yellow indicating object 2 and 3, blue indicating object 4)

3.3 Experiment setup

3.3.1 Raw materials and Chemicals

Raw materials including cellulose (Avicel PH-101, DP: ~250), D-(+)-Cellobiose (99%), D-(+)-Glucose were purchased from Sigma-Aldrich, except Levoglucosan (1-6 anhydro-β-glucose,99%) purchased from Novachem. The sample size of cellulose was controlled as 75-106 μm by sieving. 98% sulfuric acid (AR) was purchased from ThermoFisher scientific.

The chemical standards of disaccharides used for characterised intermediates were purchased from Sigma-Aldrich including neotrehalose(99%), isomaltose (99%), kojibiose(≥98%), β-Gentiobiose (≥85%), nigerose(≥90%) and D-(+) Maltose monohydrate (≥99%). Other anhydrous disaccharides were purchased from Carbonsynth including 1,6-anhydro-4-O-α-D-glucopyranosyl-D-glucopyranose (maltosan), 1,6-anhydro-4-O-β-D-glucopyranosyl-D-glucopyranose (cellobiosan), 1,6-anhydro-3-O-α-D-glucopyranosyl-D-glucopyranose (nigerosan), 1,6-anhydro-3-O-β-D-glucopyranosyl-D-glucopyranose (laminaribiosan) and 1,6-anhydro-2-O-β-D-glucopyranosyl-D-glucopyranose (sophorosan). Disaccharide standards were purchased from Sigma-Aldrich, including 1,6-O-α-D-glucopyranosyl-D-glucose (isomaltose), 1,6-O-β-D-glucopyranosyl-β-D-glucose (gentiobiose), 1,4-O-β-D-glucopyranosyl-D-glucose (cellobiose), 1,3-O-α-D-glucopyranosyl-D-glucose (nigerose), 1,2-O-α-D-glucopyranosyl-D-glucose (kojibiose) and 1,1-O-α-D-glucopyranosyl-D-glucose (trehalose). The chemical structures of disaccharides and anhdryo-disaccharides are presented in Table 3-1 and Table 3-2.

Table 3-1Structures of disaccharides.

Common Name	IUPAC Name	Structure
Trehalose	1,1-α-D-glucopyranosyl-α-D-glucopyranoside	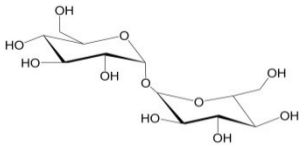
Neotrehalose	1,1-α-D-glucopyranosyl-β-D-glucopyranoside	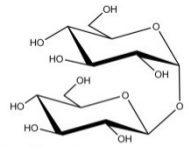
Kojibiose	1,2-O-α-D-glucopyranosyl-D-glucose	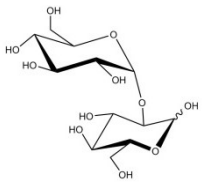
Nigerose	1,3-O-α-D-glucopyranosyl-D-glucose	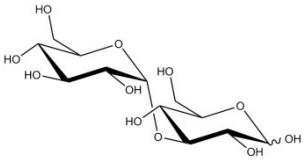
Maltose	1,4-O-α-D-glucopyranosyl-D-glucose	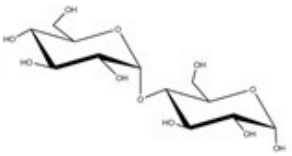
Cellobiose	1,4-O-β-D-glucopyranosyl-D-glucose	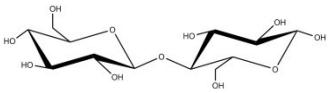
Isomaltose	1,6-O-α-D-glucopyranosyl-D-glucose	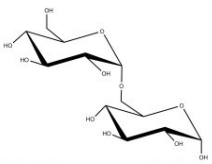
Gentiobiose	1,6-O-β-D-glucopyranosyl-β-D-glucose	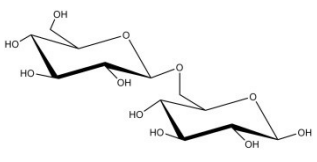

Table 3-2 Structures of anhydro-disaccharides

Common Name	IUPAC Name	Structure
Sophorosan	1,6-Anhydro-2-O-β-D-glucopyranosyl-D-glucopyranose	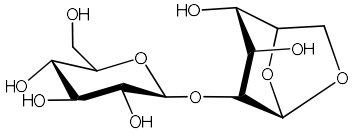
Nigerosan	1,6-Anhydro-3-O-α-D-glucopyranosyl-D-glucopyranose	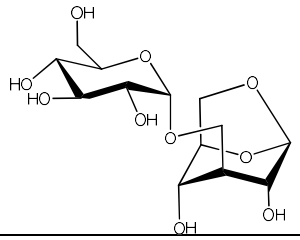
Laminaribiosan	1,6-Anhydro-3-O-β-D-glucopyranosyl-D-glucopyranose	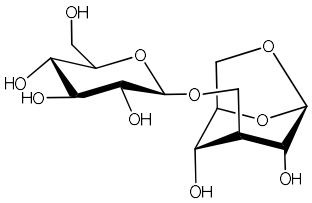
Maltosan	1,6-Anhydro-4-O-α-D-glucopyranosyl-D-glucopyranose	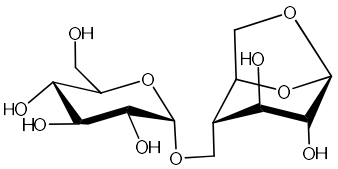
Cellobiosan	1,6-Anhydro-4-O-β-D-glucopyranosyl-D-glucopyranose	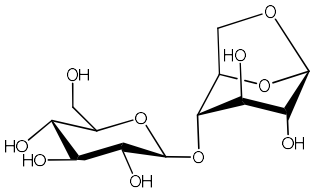

3.3.2 Preparation of different acid-loading pyrolysis samples

The cellulose (Avicel PH-101, Sigma-Aldrich) sample was sieved to the size fraction of 75-106 μm, and then the sieved cellulose (5g) was impregnated into a 25 ml sulfuric acid solution to form a slurry mixture. The slurry was stirred in an automatic shaker for 15min and then dried in an oven at 30 °C for 48 hours to remove excess water in the slurry. The yielded acid-impregnated sample was stored in a fridge at -20 °C for further pyrolysis experiments.

The acid-impregnated sugars including glucose, levoglucosan and disaccharides were prepared in similar methods as the acid-catalysed cellulose, but the formed acidic solution/slurry was dried in a Freeze dryer (Alpha 2-4 LDplus) rather than in an oven. The final solution was kept in a freezer at a temperature of −20 °C for 2 h, before drying in the freeze dryer for 48 h. The drying process was started from-50 °C for 24 hours in the primary drying process, and then the temperature was increased to -20 °C for 2 hours in the final drying process. The acidic sugars were stored in a fridge at -20 °C for further pyrolysis experiments.

3.3.3 Pyrolysis reaction system

The reactor was configured as two sections including a feeding device and a fixed-bed reactor, which are demonstrated in the section 3.3.3.1 and 3.3.3.2 respectively. The feeding device was made of stainless-steel manufactured by Swagelok. The glass reactor was made up of quartz with internal diameter ~30 mm manufactured by a local glassblower. High purity Argon (99.99%) was purchased from BOC and fed into the system to create an oxygen free environment.

3.3.3.1 The sample feeding system

Figure 3-2 demonstrates the configuration of the feed system consisting of a three-way valve, a modified sample holder (a ball valve), and a gate valve. Initially, a pre-treated sample (~0.4g) was pre-loaded into the sample holder, and then high purity argon was purged into the sample holder with the flow rate of 1.1 L/min which could remove air from the sample holder to minimise the effect from oxygen during pyrolysis experiments. After 3 min degassing, the gas was purged into the reactor by switching the three-way valve until a desired pyrolysis temperature (approximately 30 min to the static temperature). Once the pyrolysis temperature was reached, the three-valve was switched to deliver the gas into the sample holder and the gas created a ~ 30kPa pressure inside of the sample holder. Then the modified sample holder was opened to inject the sample into the reactor within a pulse feeding (one-shot) by the pressure, so the sample residence time in the reject tubing was less than ~0.1 sec. The weight loss of the sample holder was recorded to calculate the injected sample weight, and the char yield in the glass reactor.

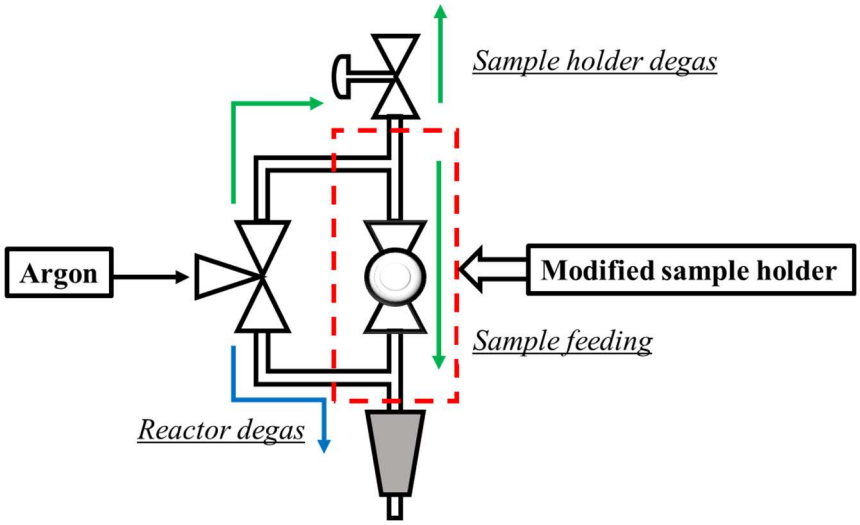

Figure 3-2 Feeding sections in the fast pyrolysis system.

3.3.3.2 The reactor system

Figure 3-3 shows the setup of the reactor system in the fast pyrolysis experiments. The isothermal zone was calibrated by injecting a k-type thermal couple into the different positions of the reactor and the reactor temperate profile was created when the furnace was set at 310 °C. Argon was continuously fed into the reactor at 1.1 L/min during the test. The reactor loading position in the furnace was recorded ensuring the sample was injected into the reactor's isothermal zone during the pyrolysis experiments.

During the pyrolysis experiments, the feeding system was pre-installed on the reactor and loaded into the furnace. Once the desired pyrolysis temperature was reached, the pre-treated sample was injected into the reactor by using the feeding system (described as above). When the residence time was reached, the reactor was lifted from the furnace and cooled with the continuous argon to the room temperature. The weight difference of the reactor before and after the experiment was recorded to calculate the yield of solid product as follow:

$$The\ yield\ of\ solid\ product = \frac{Mass_{solid\ produced}}{Mass_{sample\ loaded}} \times 100\%$$

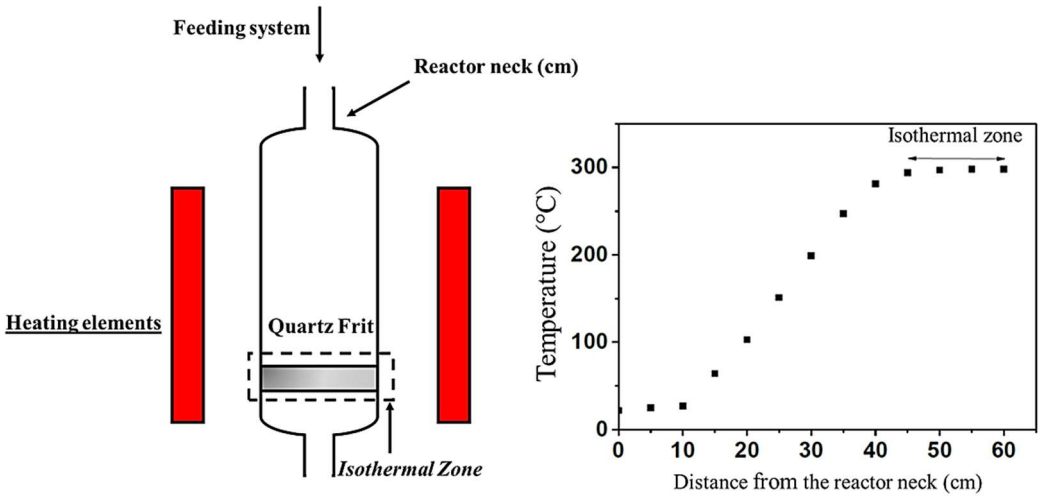

Figure 3-3 Reactor and gas temperature calibration curve in the reactor.
(Designed temperature= 300 °C, set temperature = 315°C, argon flowrate = 1.1 L/min)

3.3.3.3 Solid product analysis and extraction of water-soluble intermediates

The solid product was dissolved in ultra-pure water to extract water-soluble intermediates.

~10 mg of solid product from a pyrolysis experiment was dissolved in 10 ml ultra-pure water to form a mixture, then the mixture was stirred in an auto-shaker for 15 min at room temperature. A syringe filter (0.45 μm, PVDF) was used to separate the insoluble proportion and the water-soluble intermediates. The soluble product was analysed in the following instruments: TOC, HPAEC-PAD-MS, HPAEC-PAD, HPLC-ELDS, and post-hydrolysis. The raw solid produced from was directly analysed in FTIR, NMR, and a post-hydrolysis method.

3.3.3.4 Post hydrolysis

Post-hydrolysis is an important method to analyse mono-sugar structure in the yielded solid samples and the water-soluble intermediates. In terms of the methods proposed by National Renewable Energy Laboratory (2008)[151], ~10 mg of solid sample was firstly hydrolysed in 0.174ml sulfuric acid (72%) at 30 °C for 1 hour. During the hydrolysis process, the slurry was sent to an ultrasonic water bath for 2 min after half-hour hydrolysis. Then, the slurry was diluted to 4% sulfuric acid by adding 5ml ultra-pure water before sending to an autoclave for 1 hour. After one-hour autoclave, the solution was filtered by 0.45μm PVDF syringe filters and analysed in HPAEC-PAD. The glucose degradation was corrected by a blank test (100 ppm glucose standard) with the same method synchronously.

3.4 Instruments and analytical techniques

3.4.1 Solid product structure characterisation

The solid product was characterised in FTIR, NMR, Element analyser and KF titration, respectively. The solid sample was analysed by the basic functional group and carried out by a Perkin Elmer Spectrum 100 ATR-FTIR. ~3mg sample was loaded on the sample holder, and then a constant force of 80N was applied to the sample for analysis. The resolution of scanning was 2 cm^{-1} from 4000 cm^{-1} to 600 cm^{-1}. The baseline correction and ATR correction were processed for raw FTIR results.

In terms of the structure analysis in NMR, the sample was analysed on a Varian 400 MHz NMR spectrometer equipped with a 4 mm CP/MAS probe. To produce high-resolution ^{13}C solid NMR spectra, it employed a high-power decoupling sequence with a MAS spinning speed of ~ 7000 Hz. The rotor loaded was spun at 25 ºC with a 90º pulse, 0.04 s acquisition time and 4 s relaxation delay. An external standard of Adamantane was used for chemical shift calibration. The results were processed in the software MestRenova. The solid samples were analysed in an elemental analyser (PerkinElmer 2400 series II CHNS/O) to identify the ratio of carbon, hydrogen, and oxygen. ~2.5mg sample was packed in an aluminum vial and sent to a combustion tube in the presence of excess oxygen and combustion reagents prepacked by the instrument supplier. Then the samples were reduced to the elemental gases CO_2, and H_2O and analysed in a thermal conductivity detector in the analyser. Finally, the weight percentage of carbon and hydrogen was detected and calculated in the instrument. The weight of oxygen was calculated via the mass balance in the sample, since the organic samples consisted of C, H, and O. Before the calculation of O content, the moisture of samples was determined in KF titration (Metter V30). The solid sample was dissolved in a mixed solvent (2:1, Hydranal solvent and Hydranal formamide dry) and then titrated with a titrant (Hydranal Titrant 5).

3.4.2 Water-soluble intermediate characterisation

The major analysis methods applied in this study included TOC, HPAEC-PAD-MS, HPAEC-PAD and GPC(HPLC-EDLS).

The total carbon dissolved in the solution was analysed in TOC analyser (Shimadzu TOC-V_{CPH}). The liquid sample prepared in the previous steps (section 3.3.3.3) was delivered by a TOC auto-sampler and combusted in a combustion tube filled with catalysts (pre-packed by the supplier) at ~680 ºC. The whole process was driven by

zero grade air as a carrier gas. After the combustion, the carbon was converted to carbon dioxide, which was sent to a non-dispersive infrared detector (NDIR) for analysis. The detection limit of the system was 0.5 μg/L and the maximum detection limit is 100 mg/L.

The liquid sample was characterised by a high-performance anion-exchange chromatography (HPAEC: Dionex ICS-5000) with pulsed electrochemical detection (PAD: Au electrode and Ag/AgCl reference) equipment with Mass spectrometry (MS). There were two methods applied in this study including a gradient method and isocratic methods.

According to the gradient method, the instrument was armed with an analytical column (PA200) to identify high DP oligomers (Dp 1- Dp11) and anhydrosugar oligomers (Dp 2- Dp 17). Mobile phases of the instrument included 0.1M NaOH (line A) and 0.5M NaAc in 0.1M NaOH (line B). The details of the program were shown in Table 3-3. For the MS analysis, 0.5mM of LiCl was added in a side stream before the detector to assist in ionization of the sugars.

Table 3-3 HPAEC-PAD-MS gradient program for separation of oligomers at high DPs.

Time (min)	**Eluent (0.5ml/min)**	
	A (%) **0.5M NaAc in 0.1 M NaOH**	**B (%)** **0.1M NaOH**
0.0	4	96
30.0	45	55
35.0	45	55
35.5	4	96
45.0	4	96

Briefly[152], he sample was carried by the mobile phases and injected to the column for the separation. After separation in the column, the solution was injected into a PAD detector and MS detector for the final analysis. The results are presented in Figure 3-4.

However, the gradient method in PA200 was not suitable for analysis of low Dps<4 and isomers of disaccharides and anhydro-disaccharides. An isocratic method was developed by using a CarboPac PA20 column in HPAEC-PAD-MS. In terms of the isocratic method, 50mM NaOH was used as a mobile phase at 0.5 mL/min for 60 min.

The same solution of LiCl was used in MS to ionize the sugars. The separation details will be presented in chapter 5 and 6.

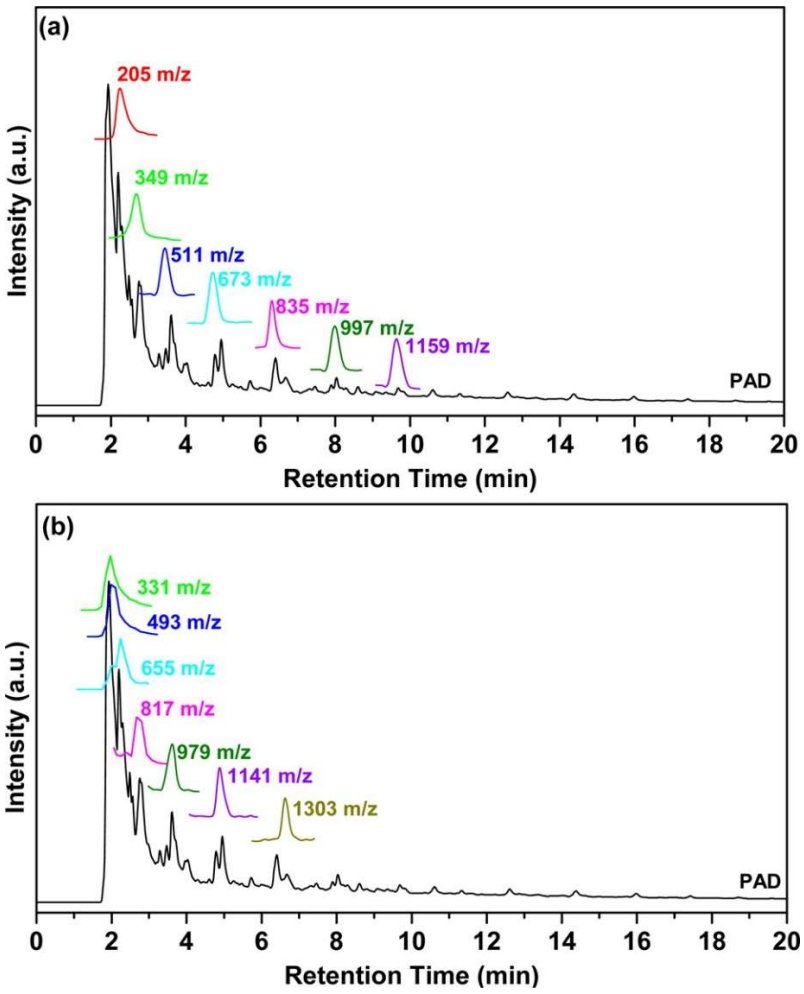

Figure 3-4 HPAEC–PAD–MS analysis of a water-soluble intermediate sample extracted from char produced from cellulose pyrolysis at 250 °C: (a) SIM scans of sugar oligomers and (b) SIM scans of anhydrosugar oligomers. Column, Dionex CarboPac PA200 analytic column; eluents, 20–225 mM sodium acetate and 100 mM NaOH over 30 min at a flow rate of 0.5 mL min–1; suppressor, Dionex AERS 500 (4 mm); suppressor current, 186 mA; MS detection mode, ESI positive; probe temperature, 450 °C; cone voltage, 75 V; and needle voltage, 3.5 kV

After the characterisation in HPAEC–PAD–MS, the water intermediates were sent to HPAEC-PAD (Dionex ICS-3000 ion chromatography) by using a CarboPac PA20 column to quantify the amount of identified sugars. The basic program of disaccharides analysis used 0.05M NaOH eluent at the flow rate of 0.5 mL/min which successfully separated the glucose disaccharides in IC. However, anhydro-

disaccharides yield from acid-catalysis levoglucosan were separated in a post-column method [153]. In order to achieve an adequate separation, ultra-pure water was used as an eluent to separate peaks of anhydro-disaccharides in the PA20 column. Before the solution was sent to the detector, 300 mM NaOH was delivered by a HPLC pump to mix with the mobile phase solution, which can emphasize the signal of the peaks and ensure the linear response in the detector. The separation gradient program is listed in Table 3-4. Therefore, anhydro-disaccharides can be quantified in this study and discussed in Chapter 6.

Table 3-4 Gradient program in the post-column method of anhydro-disaccharides separation.

Time (min)	**Eluent (0.5ml/min)**		
	A (%) 0.3M NaAc in 0.1 M NaOH	**B (%) Ultra-pure water**	**C (%) 0.3 M NaOH**
0.0	0	100	0
20	0	100	0
22.5	100	0	0
29.0	0	0	100
39	0	100	0

The liquid sample was also analyzed by gel permeation chromatography (GPC) with a column (PL aquagel-OH 20 5um 300 x 7.5 mm) to detect the formation of oligosaccharides with higher degrees of polymerization (DP of molecule weight from 21040 to 180) using a high-performance liquid chromatography (Varian 380-LC) equipped with an evaporative light scattering detector (ELSD). Deionized water was used as the mobile phase at a flow rate of 1 ml/min. The temperatures of evaporation and nebulizer were set at 80°C and 40°C in ELSD, respectively. The calibration kit of polystyrene purchased from Agilent technologies was injected into HPLC-ELSD to do a linear calibration.

3.5 Data processing

Two different data process methods were applied for the acid-catalysis cellulose pyrolysis and model compounds pyrolysis. The details are discussed in the following sections.

3.5.1 Acid-catalysis cellulose pyrolysis

Cellulose conversion was based on weight, carbon and sugar. As mentioned above, weight conversion was calculated using the difference of the reactor weight before and after the experiment. so, it can be calculated as:

$$C_{weight} = \frac{W_{cellulose} - W_{char}}{W_{cellulose}}$$

Where W_{char} (g) and $W_{cellulose}$ (g) are the weight (daf) of solid product and cellulose fed into the reactor, respectively. The sulfur content of char sample is analysed to obtain the weight (daf) of solid product.

To calculate the cellulose carbon conversion, the carbon content of solid product and cellulose were measured in an Element analyser.

$$C_{carbon} = \frac{W_{cellulose} \times C_{cellulose} - W_{char} \times C_{char}}{W_{cellulose} \times C_{cellulose}}$$

Where C_{char} (%) and $C_{cellulose}$ (%) are the carbon content (daf) of solid product and cellulose, respectively.

To determine the cellulose sugar conversion, the following method was applied in this study.

$$C_{carbon} = \frac{W_{cellulose} \times S_{cellulose} - W_{char} \times S_{char}}{W_{cellulose} \times S_{cellulose}}$$

Where S_{char} (%) and $S_{cellulose}$ (%) are the sugar content of solid product and cellulose, respectively.

Sugar content (glucose basis) was determined by Post hydrolysis and calculated as:

$$S_{wei} = \frac{W_{sugar}}{W_{sample}}$$

Where W_{sugar} (g) is the recovery of sugar products from post hydrolysis using W_{sample} (g, daf) of solid sample.

3.5.2 Acid-catalysis of model compounds (glucose, levoglucosan and disaccharides)

The below process methods were applied to the study of acid-catalysis model compounds including glucose, levoglucosan and disaccharides.

Sugar conversion during pyrolysis was determined on a carbon basis:

$$C_{carbon} = \frac{W_{sugar} \times C_{sugar} - W_{sugar,solid} \times C_{sugar}}{W_{sugar} \times C_{sugar}}$$

Where W_{sugar} (g) and $W_{sugar,\ solid}$ (g) are the weight of the glucose in the reactant and solid product after pyrolysis, respectively, and C_{sugar}(%) is the carbon content of model compounds.

The yield and selectivity of products were determined as below:

$$Y_i = \frac{W_i \times C_i}{W_{sugar} \times C_{sugar}}$$

$$S_i = \frac{W_i \times C_i}{(W_{sugar} - W_{sugar,solid}) \times C_{sugar}}$$

Where W_i (g) is the weight of qualified product i in the solid product after pyrolysis, and C_i (%) is the carbon content of product i.

3.6 Summary

Acid-impregnated cellulose and its model compounds including glucose, levoglucosan, and disaccharides have been employed to understand the underlying acid-catalysis pyrolysis mechanism of cellulose. The pyrolysis products have been quantified by HPAEC-PAD-MS systems. Moreover, the formed oligosaccharides in the pyrolysis intermediates have been characterised by GPC system. Therefore, the yields and selectivities of various compounds in the water-soluble intermediates have been calculated and discussed in this study. Based on the determined intermediates from the pyrolysis, the acid-catalysed pyrolysis reaction process can be better understood, to provide new insights into the acid-catalysed cellulose mechanism.

Chapter 4 Acid-catalysed pyrolysis of cellulose at low temperatures

4.1 Introduction

Pyrolysis is an important process for converting the abundant biomass resource into biofuels such as bio-oil and biochar at optimal pyrolysis conditions [154, 155]. For example, pyrolysis at a fast heating rate and medium temperatures (i.e., 450−550 °C) maximises bio-oil production, but favors biochar production at a slow heating rate and low temperatures (i.e., 250−350 °C) [156]. While extensive research was conducted on biomass/cellulose pyrolysis, there are still considerable scope in understanding biomass/cellulose pyrolysis reactions [157-161]. For example, β-elimination mechanism [162] is believed to be a competitive pathway leading to the formation of low molecular weight products [163-165]. Via this mechanism, organic acids may play an important role in cellulose pyrolysis [162]. Therefore, it is of critical importance to understand the role of acid during cellulose pyrolysis. It was reported that acid-catalysed cellulose pyrolysis promotes the formation of char and some dehydrated products at the expense of levoglucosan [166-168]. Especially, the pyrolysis of acid-loaded cellulose can produce significant amount of levoglucosenone [166], which is one of the value-added biochemicals with functional groups suitable for organic synthesis [169]. Acid impregnation is also considered as an effective strategy to passive the inherent inorganic species in biomass to increase the yield of pyrolytic sugars in bio-oil from biomass fast pyrolysis [26, 29, 170]. However, there are still considerable scope in understanding on the effect of acid on biomass or cellulose pyrolysis. Therefore, this study reports a set of systematic study on acid-catalysed cellulose pyrolysis at 50–325 °C.

4.2 Results and discussion

4.2.1 Cellulose conversion during acid-catalysed cellulose pyrolysis

Cellulose conversion during pyrolysis can be calculated on weight, carbon and sugar bases (with the detailed methods for calculations given in the Supplementary material). Similar conversions on the three different bases indicate that cellulose pyrolysis mainly takes place via depolymerisation reactions at the glycosidic bonds to release levoglucosan [171]. This is exactly the case for the raw cellulose pyrolysis, as shown in Figure 4-1-a. The reaction during the raw cellulose pyrolysis at temperatures <250 °C is slow but becomes rapid at temperatures >300 °C. This is because the evaporation

of levoglucosan as the pyrolysis product is slow at temperatures below its boiling point (~300 °C [162]). The results in Figure 4-1-a also suggest that some dehydration reactions also take place at temperatures >250 °C because the cellulose conversion based on sugar is slightly higher than those based on carbon and weight.

In contrast, the conversion of the acid-impregnated celluloses during pyrolysis under the same conditions follows completely different trends. As shown in in Figure 4-1-b, at an acid loading level of 0.5 mmol g^{-1}, the pyrolysis of the acid-impregnated cellulose commences at a temperature as low as 50 °C, where no pyrolysis reactions take place for the raw cellulose. The conversion of the acid-impregnated cellulose based on sugar is considerably higher than those based on weight or carbon. For example, at 180 °C, over half of the sugar structures in the acid-impregnated cellulose are converted after pyrolysis for 15 min while the carbon loss is only ~10%. At 240 °C, all sugar structures are completely converted but the carbon loss only increases to ~13%. The substantially lower carbon loss clearly indicates that sugar decomposition mainly takes place via dehydration reactions. In fact, even at 300 °C where the evaporation of levoglucosan is fast, the carbon loss only increases to ~26%. Therefore, the pyrolysis mechanism of the acid-impregnated cellulose is significantly different to that of the raw cellulose. While depolymerisation reactions play a key important role during the pyrolysis of the raw cellulose, dehydration reactions dominate during acid-catalysed cellulose pyrolysis. Such acid-catalysed dehydration reactions can start at a temperature as low as 50 °C and become intensive as the pyrolysis temperature increases. As shown in in Figure 4-1-c, the dehydration of sugar structures is also promoted at increased acid loading levels. For example, as the acid loading level increases from 0.5 to 1.0 mmol g-1, the sugar loss increases from ~27% to ~36% even at 140 °C, and all sugar structures are completely converted at 200 °C. The increased sugar destruction at high acid loading levels also slightly promotes char formation, i.e., from ~45% to ~48% when the acid loading level increases from 0.5 to 1.0 mmol g^{-1}.

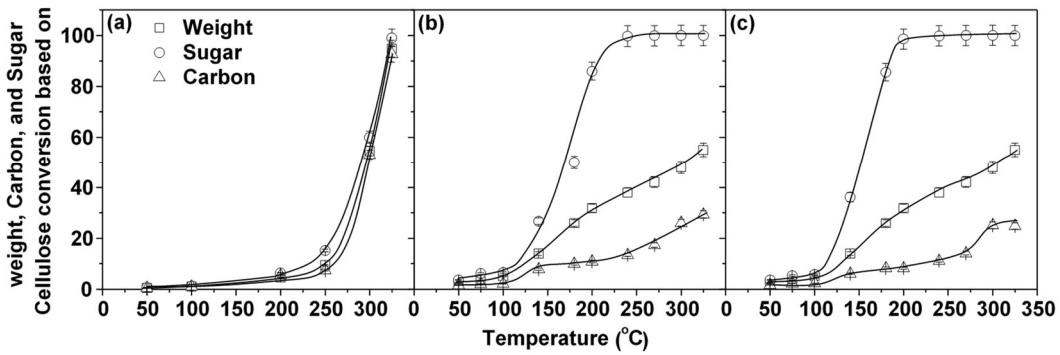

Figure 4-1 Cellulose conversions on bases of weight (daf), carbon and sugar during the pyrolysis of the raw and the acid-impregnated celluloses at different temperatures after holding for 15 min. (a) raw cellulose; (b) acid-impregnated cellulose at an acid loading level of 0.5 mmol g^{-1}; and (c) acid-impregnated cellulose at an acid loading level of 1 mmol g^{-1}.

4.2.2 Formation of water-soluble intermediates during acid-catalysed cellulose pyrolysis

The formation of reaction intermediates from biomass or cellulose pyrolysis has been widely reported in previous literatures [172, 173]. The water-soluble intermediates within the char samples produced from cellulose pyrolysis are known to contain both sugar and anhydro-sugar oligomers with a wide range of degrees of polymerisation (DP) [174, 175]. Those water-soluble intermediates are considered to be important reaction intermediates for volatile or char formation during cellulose pyrolysis [172]. For the pyrolysis of the raw and acid-impregnated celluloses in this study, Figure 4-2 presents the yields of the water-soluble intermediates at different temperatures. For the raw cellulose, the yield of the water-soluble intermediates is low at temperatures <150 °C, as the reaction intermediates are difficult to be produced at such low temperatures, since the breakage of glycosidic bonds commences at ~170 °C for amorphous cellulose and ~190 °C for crystalline cellulose [174]. As the pyrolysis temperature increases, the maximal yield of the water-soluble intermediates increases (e.g., to ~0.7% at 200 °C and ~1.7% at 250 °C, on a carbon basis). A further increase in pyrolysis temperature results in a reduction in the yield of the water-soluble intermediates. For the acid-impregnated cellulose, some water-soluble compounds are already generated even during acid impregnation. At an acid loading level of 0.5 mmol g^{-1}, the yield of the water-soluble intermediates (on a carbon basis) during pyrolysis increases

substantially from ~1.6% at room temperature to ~5.7% at 100 °C. A further increase in the pyrolysis temperature leads to a reduction in the yield of the water-soluble intermediates. At the acid loading level of 1 mmol g^{-1}, the yield of the water-soluble intermediates (on a carbon basis) increases from ~2.8% at room temperature to ~7.0% at 100 °C, but its yield follows a similar trend with increasing pyrolysis temperature.

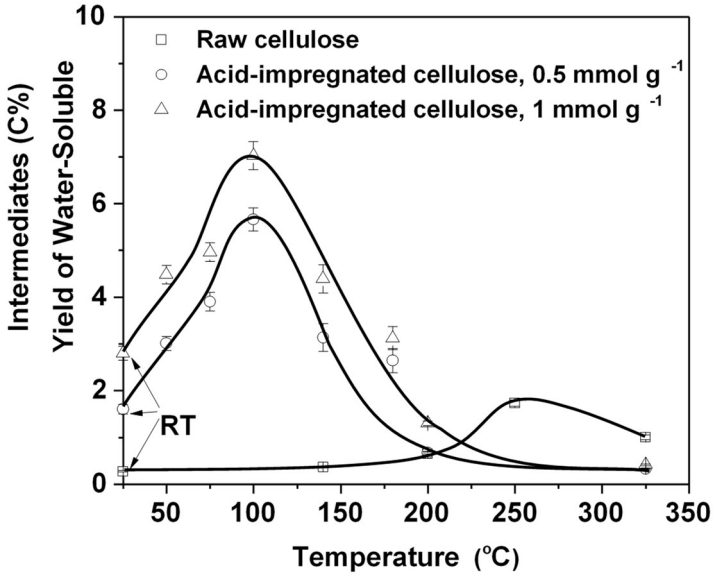

Figure 4-2 Yield of the water-soluble intermediates from the pyrolysis of the raw and the acid-impregnated celluloses at different temperatures after holding for 15 min. RT: room temperature.

The IC chromatograms of the water-soluble intermediates are presented in Figure 4-3 of the Supplementary material. For the raw cellulose, the sugar and anhydro-sugar oligomers with DP up to 8 are clearly present in the water-soluble intermediates produced from pyrolysis at temperatures >200 °C. For the acid-impregnated cellulose, it is noteworthy that glucose oligomers with DP up to 8 are already produced even during acid impregnation. At 100 °C, the glucose oligomers with DP up to 8 are still present and the formation of glucose is increased. At 140 °C, only a small amount of glucose can be found in the water-soluble intermediate and the glucose oligomers with higher DP almost completely disappear. Levoglucosan starts to appear in the water-soluble intermediates at 180 °C, which is consistent with the temperature of glycosidic bond breakage during cellulose pyrolysis [174]. The data suggest that the formation of levoglucosan via the cleavage of glycosidic bond still requires a relatively higher temperature (i.e., 180 °C) even in the presence of acid, while the acid-catalysed dehydration of sugar products can take place at a lower temperature (i.e., 140 °C).

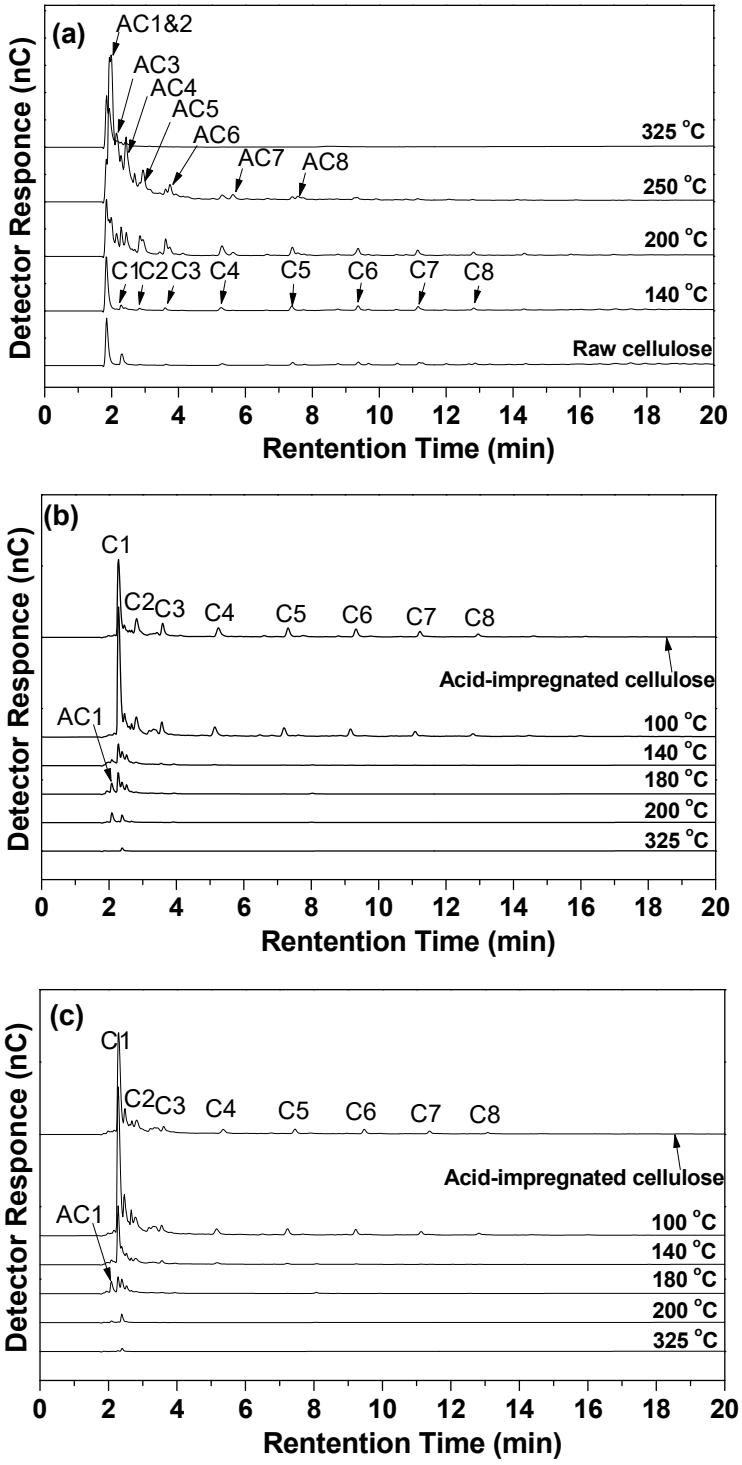

Figure 4-3 IC chromatograms of the water-soluble intermediates produced from the pyrolysis of the acid-impregnated cellulose (at an acid loading level of 0.5 mmol g^{-1}) at various temperatures for 15 min. (a) raw cellulose; (b) acid-impregnated cellulose with an acid loading level of 0.5 mmol g^{-1}; and (c) acid-impregnated cellulose with an

acid loading level of 1 mmol g^{-1}. Note: C1-C8 are sugar oligomers with DP of 1-8, and AC1-8 are anhydro-sugar oligomers with DP of 1-8.

The yields and selectivities of glucose and levoglucosan in the water-soluble intermediates produced from the pyrolysis of the raw and acid-impregnated celluloses were further determined and compared in Figure 4-4. There are distinct differences between the raw and acid-impregnated celluloses. Raw cellulose pyrolysis produces dominantly levoglucosan as reaction intermediates at temperatures >180 °C but acid-catalysed cellulose pyrolysis produces mainly glucose as reaction intermediates at temperatures <180 °C. For levoglucosan, its maximal yield from raw cellulose pyrolysis is ~0.3% (with a selectivity of ~16% on a carbon basis) obtained at 250 °C while its maximal yield for acid-impregnated cellulose pyrolysis is only ~0.03% (with a selectivity of ~1% on a carbon basis) at 180 °C. As for glucose, the maximal yield is obtained at 100 °C for the acid-impregnated cellulose, and its yield decreases rapidly at increased temperatures (>140 °C). The maximal glucose yield obtained is ~0.8 and ~1.2% at the acid loading level of 0.5 and 1 mmol g-1, respectively, corresponding to the selectivity of ~12 and ~21% on a carbon basis. Therefore, the acid present in cellulose not only promotes the hydrolysis reactions to produce glucose at low temperatures (i.e., 100 °C), but also catalyses the decomposition of sugar products at increased temperatures (>140 °C), leading to the rapid reduction of glucose in the water-soluble intermediates. In contrast, the formation of glucose is negligible during raw cellulose pyrolysis, indicating that glucose is not an important reaction intermediate during raw cellulose pyrolysis.

The results presented so far clearly show that the presence of acid in cellulose greatly influences the formation of reaction intermediates during cellulose pyrolysis. The acid in cellulose appears to weaken the hydrogen bonding networks within cellulose, leading to the formation of glucose oligomers at low temperatures (<100 °C). The evaporation of produced water (via dehydration) is slow at low temperatures, enabling the acid to catalyse the hydrolysis of glucose oligomers to glucose, which is further decomposed to other products at increased temperatures. Levoglucosan may be still produced via the cleavage of glycosidic bonds but only at a relatively high temperature (~180 °C). However, substantial sugar structures have been decomposed at temperature <180 °C (i.e., ~50% and ~85% sugar loss at 180 °C for the acid loading

level of 0.5 and 1 mmol g-1, respectively), thus the formation of levoglucosan is greatly suppressed during the pyrolysis of the acid-impregnated cellulose.

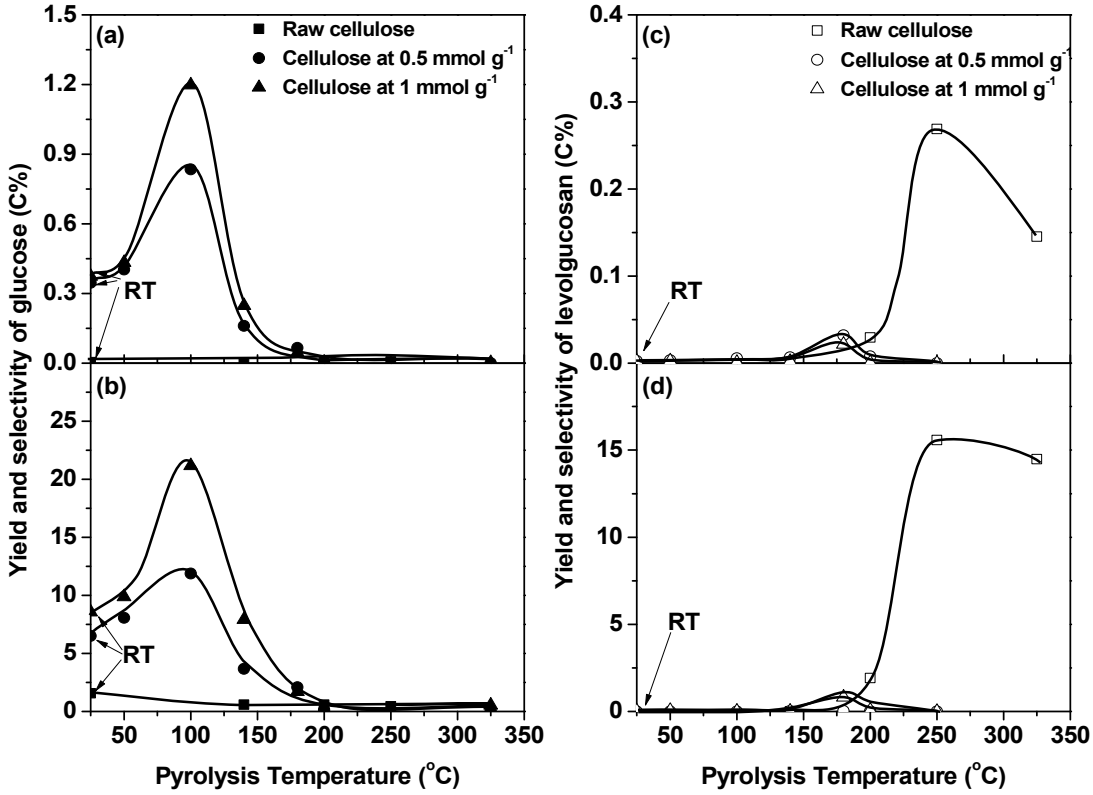

Figure 4-4 Yield and selectivity of levoglucosan (AC1) and glucose (C1) in the water-soluble intermediates produced from the pyrolysis of the raw and acid-impregnated celluloses at different temperatures for 15 min. (a) yield of glucose in the water-soluble intermediates; (b) selectivity of glucose in the water-soluble intermediates; (c) yield of levoglucosan in the water-soluble intermediates; (d) selectivity of levoglucosan in the water-soluble intermediates. RT: room temperature.

4.2.3 Characterization of char structure from acid-catalysed cellulose pyrolysis

Figure 4-5 presents the Van Krevelen diagram of the char samples obtained by the pyrolysis of the cellulose samples. The data clearly show that the pyrolysis of the raw and acid-impregnated cellulose leads to the atomic ratios of H/C and O/C of char shifting along the dehydration line. However, during raw cellulose pyrolysis, dehydration reactions only play a minor role and the depolymerisation reactions dominate to release levoglucosan as the carbon loss is substantial [20]. During the acid-catalysed cellulose pyrolysis, dehydration reactions play a dominant role and the carbon loss is small (see Figure 4-1). At an acid loading level of 0.5 mmol g^{-1}, the char at 180 °C has the atomic H/C and O/C ratios of ~1 and ~0.5, respectively, equivalent

to a molecular structure of $C_6H_6O_3$. This translates into the loss of two water molecules for each sugar monomer structure remaining in the char during pyrolysis, considering cellulose has a monomer unit of $C_6H_{10}O_5$. Similarly, the data of the char at 300 °C indicate the loss of three water molecules. Such a phenomenon can be more clearly seen at a high acid loading level of 1 mmol g^{-1}. As shown in Figure 4-5c, the dehydration reactions are much faster as the acid loading level increases, with a loss of three water molecules in each sugar monomer unit even at 200 °C.

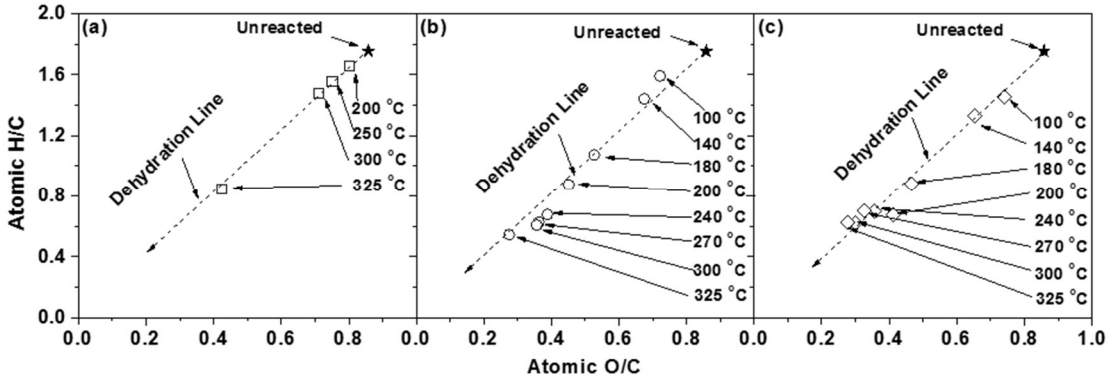

Figure 4-5 Van Krevelen diagram for the char samples produced from the pyrolysis of the raw and the acid-impregnated celluloses at different temperatures after holding for 15 min. (a) raw cellulose; (b) acid-impregnated cellulose at an acid loading level of 0.5 mmol g^{-1}; and (c) acid-impregnated cellulose at an acid loading level of 1 mmol g^{-1}.

Figure 4-6 presents the FT-IR spectra of the char samples from the pyrolysis of the raw and the acid-impregnated celluloses. It can be seen that cellulose pyrolysis without acid impregnation shows little structural changes at temperatures <250 °C (see Figure 4-6-a). The carbonyl structures (C=O) at 1800−1700 cm-1 region and C=C structures at 1680−1620 cm-1 [174, 176] are found to appear at 300 °C, apparently due to the dehydration of the hydroxyl groups in cellulose. With acid impregnation at an acid loading level of 0.5 mmol g-1, the formation of C=O and C=C structures is observed at 140 °C (see Figure 4-6-b). The reduction in the OH groups in the range of 3600−3200 cm-1 further confirms the dehydration of OH groups in cellulose. The C=O and C=C structures gradually increase with increasing pyrolysis temperature. As the acid loading level increases to 1 mmol g-1, the formation of C=O and C=C structures is observed at 100 °C (see Figure 4-6-c), and the sugar structures completely disappear at 200 °C (in consistence with the sugar loss data in Figure 4-1).

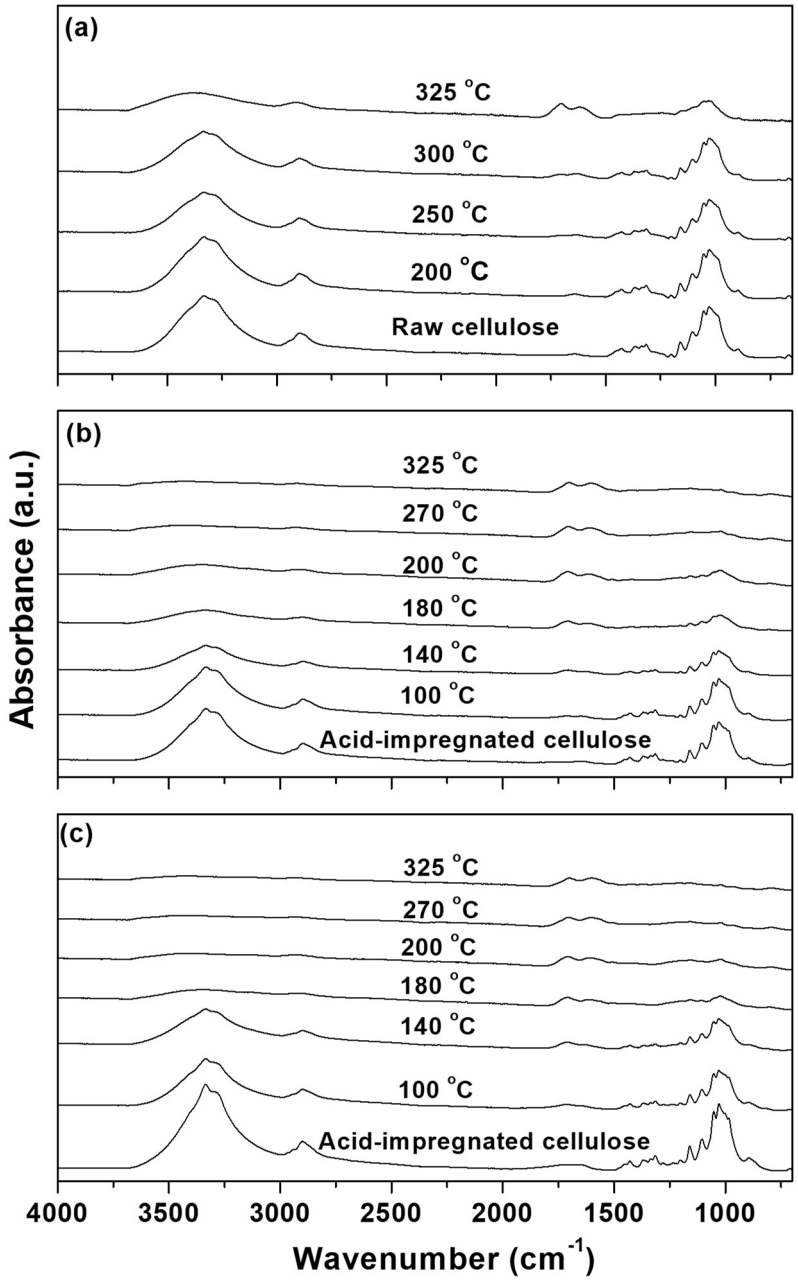

Figure 4-6 FTIR spectra of the char samples produced from the pyrolysis of the raw and the acid-impregnated celluloses at different temperatures after holding for 15 min. (a) raw cellulose; (b) acid-impregnated cellulose at an acid loading level of 0.5 mmol g^{-1}; and (c) acid-impregnated cellulose at an acid loading level of 1 mmol g^{-1}.

Several char samples collected from the acid-impregnated cellulose at an acid loading level of 0.5 mmol g-1 were also subjected to 13C NMR analysis, and the results are shown in Figure 4-7. The NMR spectra of the acid-impregnated cellulose have several sharp resonances at 65, 72, 75, 89, 105 ppm, which are assigned to the carbons in cellulose [177, 178]. At 180 °C, the aliphatic structures (at 10−60 ppm [177-179]) and the

furanic structures (at 151 ppm [178, 179]) appear, suggesting that the sugar structures are mainly converted into furanic structures via dehydration. The weak resonances at 175 and 205 ppm are assigned to carbonyl functional groups [177]. As the pyrolysis temperature increases, the sugar structures further reduce, producing more furanic and aliphatic structures. At 325 °C, the sharp resonances of sugar structures almost disappear completely, except one broad resonance at 75 ppm. The carbon structures in the char mainly contain furanic structures (at 151 and 113 ppm [179]), aromatic structures (at 127 ppm [179]), aliphatic structures (at 10 − 60 ppm [177, 178]), and carbonyl structures (at 175 and 205 ppm [177]). In sum, the NMR results indicate that the initial dehydration leads to the formation of furanic and carbonyl structures, which are further transformed into aromatic structures at high temperatures.

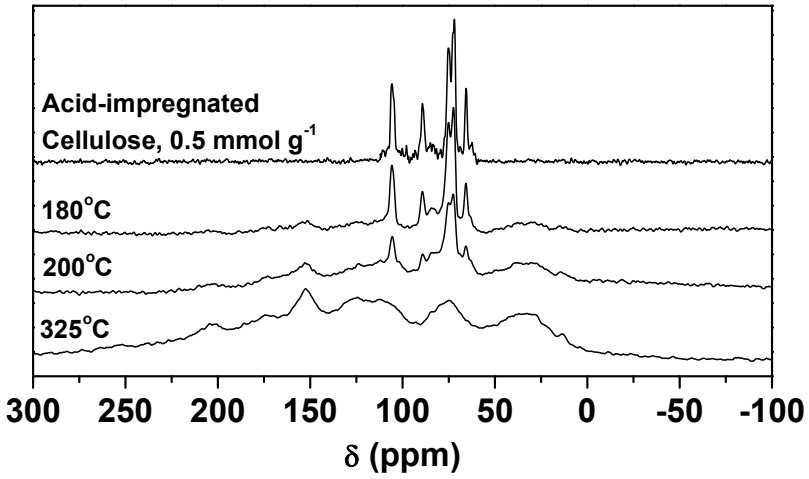

Figure 4-7 ^{13}C NMR spectra of selected char samples from the pyrolysis of the acid-impregnated cellulose (at an acid loading level of 0.5 mmol g^{-1}) at different temperatures after holding for 15 min.

4.2.4 Discussion on acid-catalysed cellulose pyrolysis mechanism

The data presented in this paper provide some new insights into the fundamental reaction mechanisms for the acid-catalysed cellulose pyrolysis. A new pyrolysis mechanism is then proposed for the acid-impregnated cellulose at low temperatures, as shown in Fig. 7. Cellulose pyrolysis without acid mainly proceeds with the depolymerisation reactions to release levoglucosan, and the dehydration reactions only play a minor role. In contrast, the acid-catalysed cellulose pyrolysis is dominantly contributed by the dehydration reactions at low temperatures (<180 °C), and the depolymerisation reactions to release levoglucosan are greatly suppressed. Several key points regarding the acid-catalysed mechanism are noted as follows.

First, the pyrolysis of the acid-impregnated cellulose can commence at a temperature (i.e., 50 °C) considerably lower than that (i.e., ~200 °C) for the raw cellulose. This is largely due to the weakened hydrogen bonding networks in cellulose during acid impregnation and/or pyrolysis processes, resulting in the formation of glucose oligomers as reaction intermediates at low temperatures (i.e., 50 °C). Such glucose oligomers have high boiling point and cannot evaporate into vapor phase hence experience further temperature-dependent decomposition reactions to low-molecular-weight compounds in the solid/liquid intermediate phase.

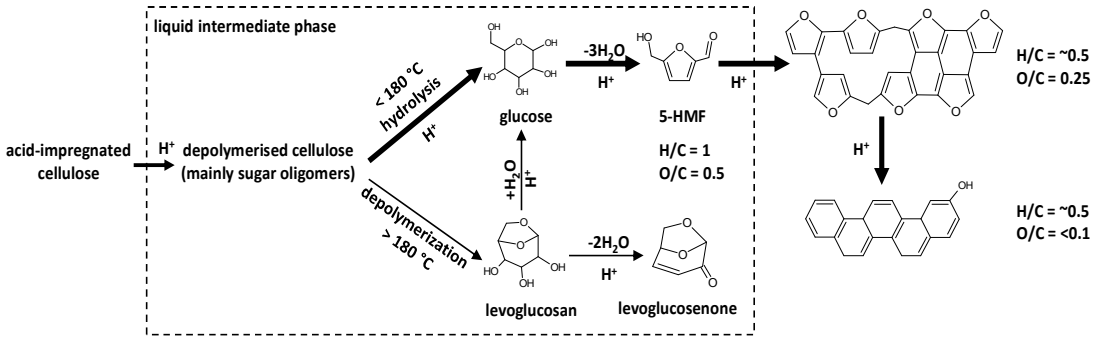

Figure 4-8 Proposed acid-catalysed cellulose pyrolysis mechanism at low temperatures.

First, the pyrolysis of the acid-impregnated cellulose can commence at a temperature (i.e., 50 °C) considerably lower than that (i.e., ~200 °C) for the raw cellulose. This is largely due to the weakened hydrogen bonding networks in cellulose during acid impregnation and/or pyrolysis processes, resulting in the formation of glucose oligomers as reaction intermediates at low temperatures (i.e., 50 °C). Such glucose oligomers have high boiling point and cannot evaporate into vapor phase hence experience further temperature-dependent decomposition reactions to low-molecular-weight compounds in the solid/liquid intermediate phase.

Second, the formation of levoglucosan is greatly suppressed in the presence of acid. Levoglucosan is produced via the cleavage of glycosidic bond and the minimal temperature for producing levoglucosan is ~170 and ~190 °C for amorphous and crystalline cellulose, respectively [174]. For the pyrolysis of acid-impregnated cellulose, this study shows that the minimal temperature required for producing levoglucosan in the water-soluble intermediates is ~180 °C, suggesting that the presence of acid has little effect on the temperature for levoglucosan formation. The low levoglucosan yield from the acid-catalysed cellulose pyrolysis may be at least due to two reasons. One is

that significant dehydration of sugar structures take place at temperatures <180 °C, greatly reducing the sugar structures available for levoglucosan formation at temperatures >180 °C. The other is that once levoglucosan is formed, it can be easily decomposed into other products (e.g., levoglucosenone) in the intermediate liquid phase, due to the catalytic effect of acid. Thus, the formation of levoglucosan is not favored in the presence of acid.

Third, in presence of acid, the hydrolysis reactions of glucose oligomers can easily take place to produce glucose as a key reaction intermediate. The hydrolysis reaction to form glucose mainly takes place at low temperatures (<100 °C), because hydrolysis reaction requires the participation of water. At low temperature, the evaporation of produced water (i.e., via dehydration) is slow, thus greatly promoting hydrolysis reactions. However, glucose is also easily decomposed at increased temperatures (>140 °C), leading to the rapid reduction in glucose yield. Therefore, glucose pyrolysis plays an important role in char formation during acid-catalysed cellulose pyrolysis. The NMR results suggest that glucose is first decomposed into furanic structures via acid-catalysed dehydration, which are further transformed into aromatic structures at high temperatures (>300 °C). Such a mechanism appears to be similar as those for char formation from glucose decomposition under hydrothermal conditions [179]. This is reasonable due to the presence of water in the liquid intermediate phase at low temperatures (<100 °C) because of the slow evaporation of water.

4.3 Conclusions

This study successfully reveals the acid-catalysed cellulose pyrolysis mechanism at low temperatures (50−325 °C). Dehydration reactions rather than depolymerisation reactions are found to play a dominate role during acid-catalysed cellulose pyrolysis. The presence of acid catalyses the formation of glucose oligomers as reaction intermediates at low temperatures (50 °C), leading to the pyrolysis of the acid-impregnated cellulose starting at 50 °C. At low temperatures (<100 °C) where the evaporation of produced water from dehydration is slow, the glucose oligomers are rapidly hydrolysed to glucose, which experiences severe dehydration reactions to form low-molecular-weight compounds at increased temperatures (>140 °C). Since the depolymerisation reactions require a higher temperature of ~180 °C, the formation of levoglucosan is greatly suppressed as the cellulose already becomes highly dehydrated at temperatures <180 °C, thus resulting in a low levoglucosan yield during acid-

catalysed cellulose pyrolysis. Consequently, the char formation is favored from the dehydrated cellulose, likely formed via furanic structures and its further transformation into aromatic structures at high temperatures (>300 °C).

Chapter 5 Polymerisation of glucose during acid-catalysed pyrolysis at low temperatures

5.1 Introduction

Fast pyrolysis converts biomass into high-energy-density renewable biofuels (i.e., bio-oil, bio-char and/or bioslurry [34, 180, 181]), which can partly replace the traditional fossil fuels (i.e., crude oil and coal) for stationary combustion applications [5, 181, 182]. However, biomass pyrolysis bio-oil suffers from some undesired properties (i.e., high water content, high acidity, high viscosity, low heating value, poor phase stability), which have hindered its further commercial applications. The poor quality of bio-oil is at least partially due to the presence of inherent alkali and alkaline earth metallic (AAEM) species present in biomass, which catalyse the fragmentation and dehydration reactions to produce low-molecular-weight products, such as formic acid and hydroxyacetaldehyde [23, 183, 184]. To improve the quality of bio-oil, various acid pretreatment methods (i.e., acid leaching [138], acid impregnation [26, 29, 145], or a combination of both) have been proposed to suppress the catalytic effect of AAEM species on biomass pyrolysis. However, the acid loading needs to be optimised since overloading of acid may lead to additional reactions catalysed by extra acid. Previous studies [28, 185] have shown that the loaded acid enhances the formation of dehydrated products (i.e., levoglucosenone) and char from cellulose pyrolysis. Therefore, it is of critical importance to understand the effect of acid loading on biomass pyrolysis.

The mechanism of biomass or cellulose pyrolysis under acidic conditions have been studied in the literature [146, 150, 185]. Recently, it was reported [186] that acid loading could significantly change the cellulose pyrolysis mechanism via enhancing the formation of reaction intermediates even at 100 °C. During acid-catalysed cellulose pyrolysis, glucose instead of levoglucosan was identified as an important intermediate at temperatures <180 °C. It is clear that acid-catalysed glucose pyrolysis plays an important role in cellulose pyrolysis under acidic conditions. However, the fundamental reaction mechanisms governing the effect of acid loading on glucose pyrolysis are largely unclear, especially the roles of polymerisation reactions under acidic conditions. It is known that polymerisation reactions take place during the pyrolysis of levoglucosan [187] or glucose under non-catalytic or acidic conditions, contributing substantially to char formation. However, previous studies on glucose pyrolysis mainly focus on the decomposition reactions to produce levoglucosan and

5-hydroxymethylfurfural at temperatures > 200 °C [188]. There has been no investigation into the polymerisation reactions of glucose during pyrolysis at temperatures < 200 °C, especially under acidic conditions. At low temperatures, the intermediates formed from the primary reactions can be identified to reveal the underlying mechanisms. Therefore, this paper reports a systematic study to understand the polymerisation of glucose during acid-catalysed pyrolysis at 60 – 150 °C.

5.2 Results and Discussion

5.2.1 Glucose conversion during acid-catalysed pyrolysis

Figure 5-1 presents the glucose conversion during the pyrolysis of the acid-impregnated glucose with an acid loading of 0.25 mmol/g at temperatures of 60 – 150 °C and holding times of 0 – 15 min. Although glucose is stable at 150 °C under acid-free conditions [189], Figure 5-1 shows that glucose conversion under acidic conditions already takes place even at 60 °C. Glucose conversion increases with holding time and reaches ~31% after 15 min holding at 60 °C. The results in Figure 5-1 further show that glucose conversion is strongly dependent on temperature. Even without holding, the glucose conversion increases rapidly from ~28% at 100 °C to ~90% at 150 °C. Therefore, the presence of acid significantly enhances glucose conversion such low temperatures.

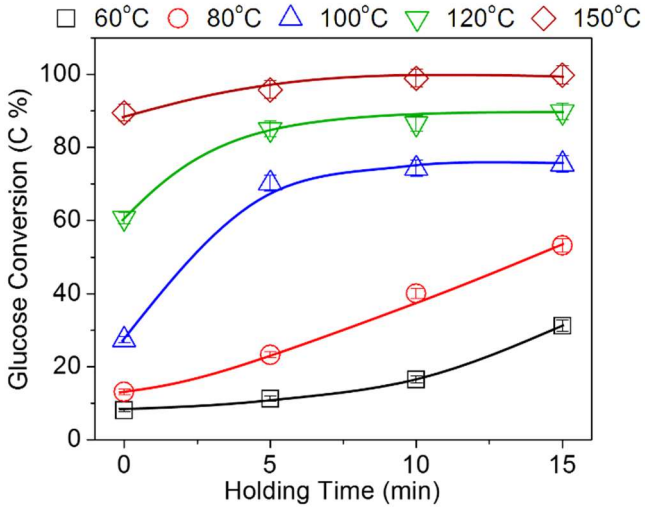

Figure 5-1 Glucose conversion as a function of holding time at 60 – 150 °C and an acid loading of 0.25 mmol/g.

However, it can be seen that the glucose conversion becomes slow as the holding time increases at high temperatures (>100 °C). This is likely due to the reduced water

content in the pyrolyzing sample, since water can assist the formation of C1-carbocation in glucose to facilitate the polymerisation reactions [190]. The moisture content of the acid-impregnated glucose sample after freeze drying is ~10%, due to the formation of glucose monohydrate [191]. The moisture content of the solid samples after pyrolysis at 120 and 150 °C were analysed and presented in Figure 5-2. It can be seen that the moisture content reduces as holding time increases, and a higher pyrolysis temperature leads to an increased reduction in the moisture content of the solid sample. For example, the moisture content of the solid sample at 150 °C reduces from ~10 to ~2% as the holding time increases from 0 to 15 min. The rapid loss of water may suppress the polymerisation reactions, thus leading to the reduced glucose conversion at high temperatures.

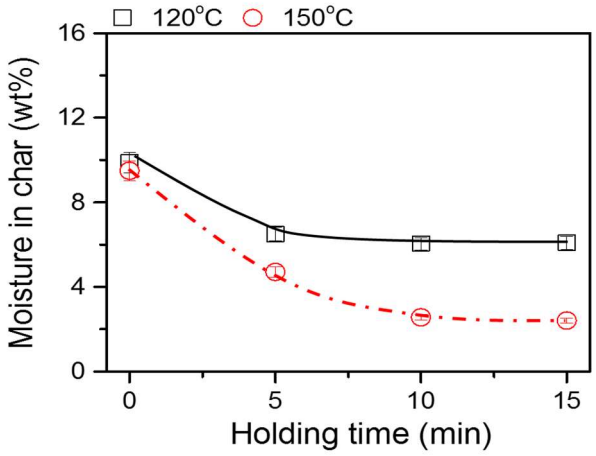

Figure 5-2 Effect of pyrolysis temperature and holding time on the moisture content of the solid sample after pyrolysis at an acid loading of 0.25 mmol/g.

5.2.2 Yields of products during acid-catalysed glucose pyrolysis

To find out the products during acid-catalysed glucose pyrolysis at low temperatures, the solid sample produced at an acid loading of 0.25 mmol/g was dissolved in deionised water and the liquid sample was analysed by HPAEC-PAD-MS. As shown in Figure 5-3, the HPAEC-PAD-MS chromatogram of a typical liquid sample at 120 °C and 15 min shows the presence of various disaccharides (349 m/z) and trisaccharides (511 m/z) in the pyrolysis products, obviously produced from polymerisation reactions of glucose. Under acidic conditions, it is known that polymerisation reactions of glucose can easily take place at various hydroxyl groups, forming disaccharides of different glycosidic bonds [192]. Figure 5-3-b shows that there

are 11 disaccharides (peaks a-k) formed during acid-catalysed pyrolysis of glucose. In this study, we have successfully identified and quantified 8 disaccharides, as listed in Table 5-1. Other 3 disaccharides were not quantified due to the unavailability of standards. Compared to disaccharides, trisaccharides are even more complicated since different α or β glycosidic bonds can form at different hydroxyl groups of the reducing end of each disaccharide. As shown in the MS chromatogram (Figure 5-3-a), more peaks of trisaccharides can be detected by MS. However, the trisaccharides were also not quantified in this study due to the complicated structure of trisaccharides and unavailability of standards. It seems that the amount of trisaccharides is less than that of disaccharides, due to the weaker MS signals for trisaccharides as shown in Figure 5-3.

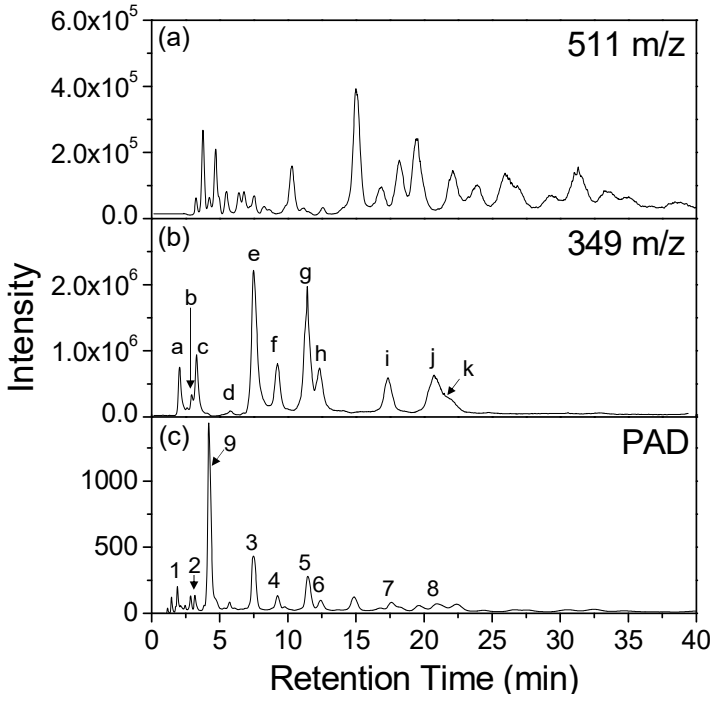

Figure 5-3 HPAEC−PAD−MS chromatogram of a water-soluble sample produced from acid-catalysed glucose pyrolysis at 120 °C and an acid loading of 0.25 mmol/g for 15 min. (a) MS chromatogram at 511 m/z; (b) MS chromatogram at 349 m/z, with 11 disaccharides (peaks a-k); and (c) PAD chromatogram with identified peaks (1. Trehalose; 2. Neotrehalose; 3. Isomaltose; 4. Kojibiose; 5. Gentiobiose; 6. Cellobiose; 7. Nigerose; 8. Maltose; 9. Glucose).

The disaccharides in the pyrolysis product during glucose pyrolysis at an acid loading of 0.25 mmol/g were further quantified and the yields of 8 disaccharides (on a carbon basis) at different temperatures and holding times are presented in Figure 5-4. Among

the 8 quantified disaccharides, the yields of gentiobiose and isomaltose are higher than others, with the highest values of ~4.9 and ~5.2 % (on a carbon basis), respectively. The yields of disaccharides as a function of holding time follow the similar trends depending on pyrolysis temperature. At low temperatures (i.e., 60 and 80 °C), the yields of disaccharides increase with holding time. For example, the yield of gentiobiose increases from ~1.9 to ~4.6 % (on a carbon basis) when the holding time increases from 0 to 15 min during pyrolysis at 80 °C. While at 100 °C, the yields of disaccharides first increase with holding time to a maximal value, followed by a decrease with further increasing holding time. When the temperature further increases to > 100 °C, the majority of disaccharides are produced during the heating-up period, and the yields of disaccharides continuously decrease with increasing holding time. For instance, the gentiobiose yield decreases from ~4.9 to ~1.4 % (on a carbon basis) at 120 °C when the holding time increases from 0 to 15 min. Therefore, the above results clearly demonstrate that disaccharides of various linkages can be produced during acid-catalysed pyrolysis of glucose at low temperatures.

Table 5-1 Structures of identified disaccharides.

Common Name	**IUPAC Name**	**Structure**
Trehalose	1,1-α-D-glucopyranosyl-α-D-glucopyranoside	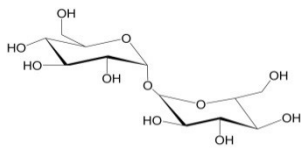
Neotrehalose	1,1-α-D-glucopyranosyl-β-D-glucopyranoside	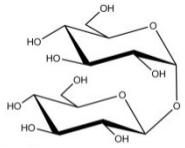
Kojibiose	1,2-O-α-D-glucopyranosyl-D-glucose	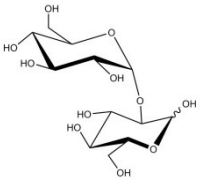
Nigerose	1,3-O-α-D-glucopyranosyl-D-glucose	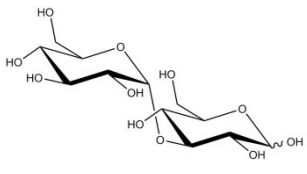

Common Name	IUPAC Name	Structure
Maltose	1,4-O-α-D-glucopyranosyl-D-glucose	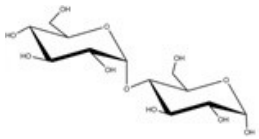
Cellobiose	1,4-O-β-D-glucopyranosyl-D-glucose	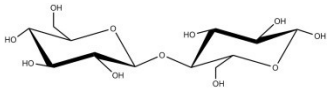
Isomaltose	1,6-O-α-D-glucopyranosyl-D-glucose	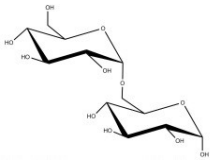
Gentiobiose	1,6-O-β-D-glucopyranosyl-β-D-glucose	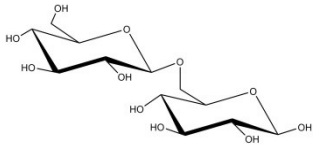

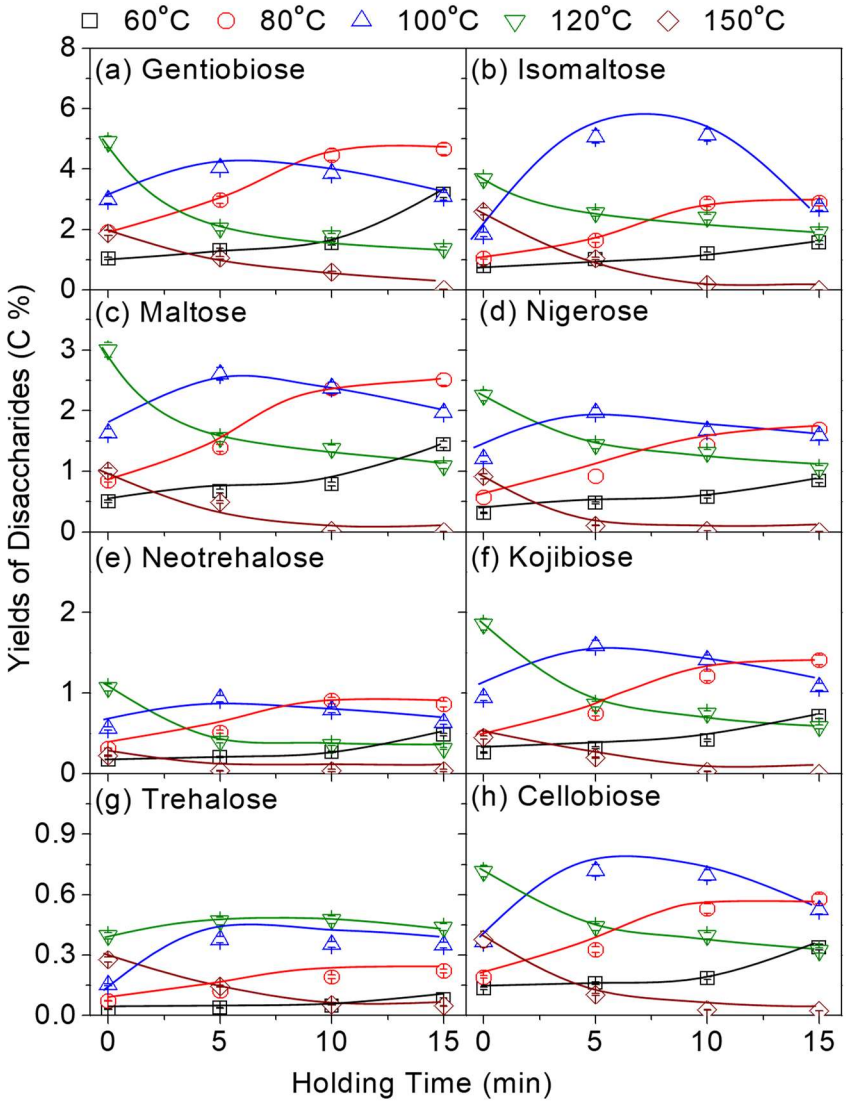

Figure 5-4 Yields of various disaccharides as a function of holding time during acid-catalysed glucose pyrolysis at 60 – 150 °C and an acid loading of 0.25 mmol/g.

5.2.3 Selectivities of products during acid-catalysed glucose pyrolysis

The selectivities of disaccharides during glucose pyrolysis at an acid loading of 0.25 mmol/g were further calculated on a carbon basis, and the selectivity of each disaccharide as a function of glucose conversion is shown in Figure 5-5. It can be seen that the selectivities of disaccharides all decrease as glucose conversion increases, indicating that the disaccharides are primary products of glucose pyrolysis under acid-catalysed conditions [193]. The initial selectivities of 8 disaccharides follow an order of gentiobiose (~15%) > isomaltose (~10%) > maltose (~6%) > nigerose (~4%) > kojibiose (~3%) > neotrehalose (~2%) > cellobiose (~1.5%) > trehalose (~0.5%). Considering the linkage of different disaccharides, it can be found that the disaccharides with 1,6-glycosidic bond (i.e., gentiobiose and isomaltose) have higher

selectivities than other disaccharides. This is understandable since the hydroxyl group on C6 is the most reactive and 1,6-glycosidic bond can reduce steric hindrance between the bulky sugar ring and an additional methylene group [194]. For the disaccharides with α-linkage, the selectivity of disaccharide follows an order of 1,6-glycosidic bond > 1,4-glycosidic bond > 1,3-glycosidic bond > 1,2-glycosidic bond > 1,1-glycosidic bond, depending on the steric hindrance between the bulky sugar rings during polymerisation reaction [189, 194].

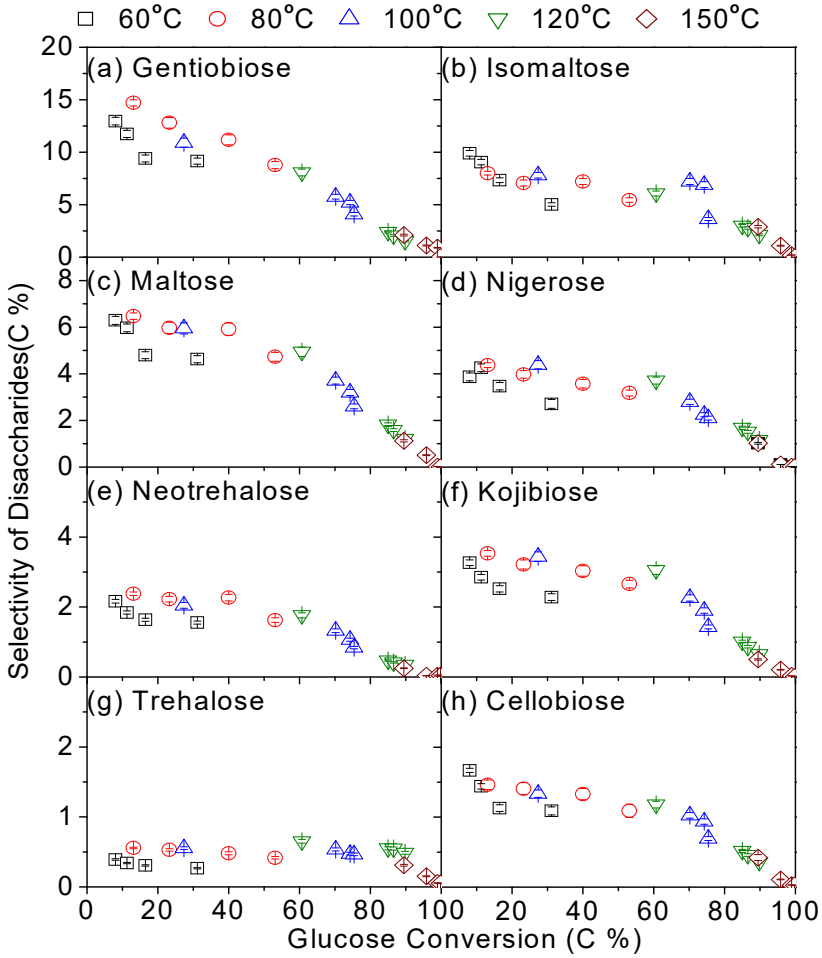

Figure 5-5 Selectivities of various disaccharides as a function of glucose conversion during acid-catalysed glucose pyrolysis at 60 – 150 °C and an acid loading of 0.25 mmol/g.

The above results have also shown that the disaccharides with α and β linkages at the same hydroxyl groups were identified in the water-soluble product from acid-catalysed glucose pyrolysis, such as gentiobiose (β-1,6 linkage) and isomaltose (α-1,6 linkage). This indicates that mutarotation reaction is also involved in acid-catalysed glucose pyrolysis. Protonation of the ring O forming the oxonium ion results in

mutarotation between the α and β-anomers [190]. The presence of acid and moisture content (i.e., ~10 wt. %) in glucose accelerates the mutarotation and polymerisation reactions during glucose pyrolysis under acidic conditions, facilitating the formation of oligosaccharides with various DPs and linkages. The formation of C1-carbocation significantly affects the reaction rate of mutarotation and polymerisation. Under the acidic conditions, the formation of C1-carbocation is enhanced and water plays an important role because of proton's high affinity to water.

Further analysis of the total selectivity of 8 quantified disaccharides shows that the quantified disaccharides only contribute to ~40% of primary product from acid-catalysed glucose pyrolysis (see Figure 5-6). Obviously, there are some other primary products during acid-catalysed glucose pyrolysis. Post hydrolysis of the solid product was performed for all conditions, and the results are also shown in Figure 5-6. It can be clearly seen that glucose recovery after post-hydrolysis is high (>92%) even at a high glucose conversion (i.e., 80%). This clearly indicates that the pyrolysis products from acid-catalysed glucose pyrolysis at low temperatures (<120 °C) are still predominantly in the form of sugars (i.e., anhydrosugars or sugar oligomers) which can be hydrolysed to glucose via post-hydrolysis. It is noteworthy that most of the identified disaccharides have α-linkage (i.e., isomaltose, maltose, nigerose, kojibiose and trehalose), and only two disaccharides have β-linkage (i.e., gentiobiose, cellobiose). Other β-linkage disaccharides with different glycosidic bonds should be produced as well, but this cannot be verified due to the unavailability of standards. Therefore, the above results demonstrate that polymerisation reactions are the main primary reactions of acid-catalysed glucose pyrolysis to produce oligosaccharides (mainly disaccharides) of various linkages as primary products. At high temperatures (i.e., 150 °C), the glucose recovery rapidly reduces to a low level (i.e., ~5%), suggesting the sugar decomposition is greatly enhanced at 150 °C.

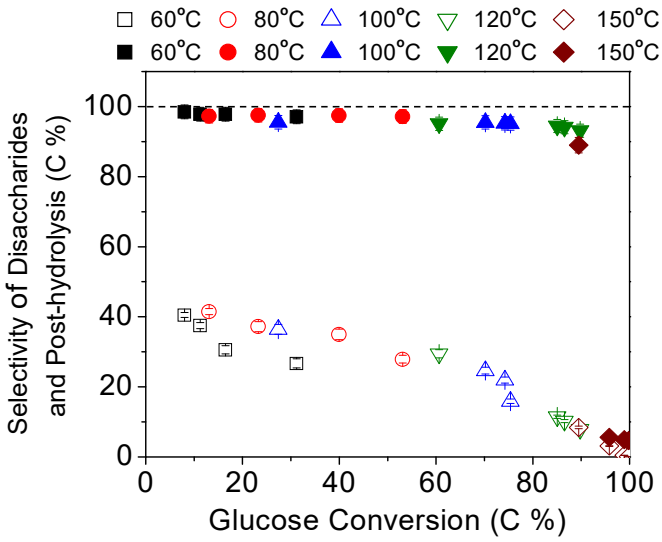

Figure 5-6 Selectivity of total quantified disaccharides as a function of glucose conversion during acid-catalysed glucose pyrolysis at 60–150 °C and an acid loading of 0.25 mmol/g. Open symbols present the selectivity of total quantified saccharides, and solid symbols present the post-hydrolysis results.

To provide evidence on the formation of high-DP oligosaccharides, the liquid samples produced at 60–120 °C and an acid loading of 0.25 mmol/g for 15 min were analysed by GPC to measure the molecular weight range of the products in the water-soluble sample. As shown in Figure 5-7, the oligosaccharides with DP >2 are clearly formed in the pyrolysis products, especially at temperatures >80 °C. The maximal DP of oligosaccharides identified in the liquid sample increases with pyrolysis temperature, from ~4 (at a retention time of 14 min) at 60 °C to ~8 (at a retention time of 13.5 min) at 80 °C, and then to ~12 and ~18 (at retention times of 13 and 12.5 min) at 100 and 120 °C, respectively. Therefore, the high-DP oligosaccharides can be easily generated during glucose pyrolysis under acidic conditions. However, the structure of such high-DP oligosaccharides is complicated, which requires more advanced analytic techniques to characterise. According to the results of disaccharides, it seems that different α or β linkages can be formed at various hydroxyl groups of oligosaccharides.

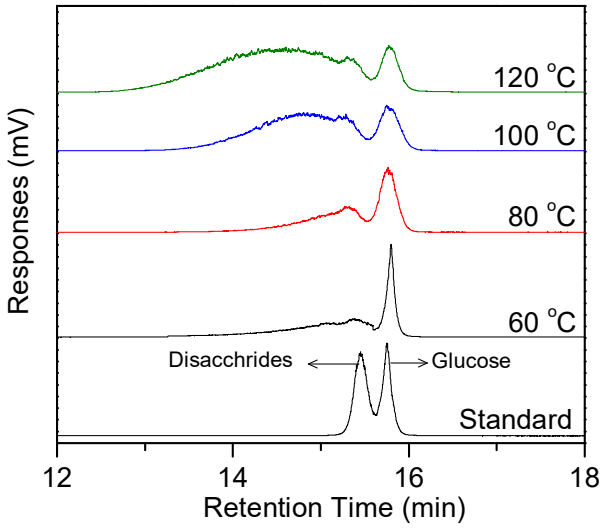

Figure 5-7 GPC analysis of the water-soluble samples from acid-catalysed glucose pyrolysis at 60 – 120 °C and an acid loading of 0.25 mmol/g for a holding time of 15 min.

5.2.4 Effect of acid loading on acid-catalysed glucose pyrolysis

To understand the effect of acid loading on glucose pyrolysis, further glucose pyrolysis experiments were performed at an acid loading of 0.5 mmol/g and 80 °C. Glucose conversion, the yields and selectivities of various diasaccharides during acid-catalysed glucose pyrolysis at different acid-loadings were compared in Figures 5-8 to 5-10, respectively. It can be seen in Figure 5-8 that glucose conversion is slightly enhanced at an increased acid loading. For example, the glucose conversion after 15 min increases from ~50 to ~62 % when the acid loading increases from 0.25 to 0.5 mmol/g. As expected, the yields of 8 identified disaccharides also increase with acid loading (see Figure 5-9). It seems that the acid loading has more significant effect on the formation of α-linkage disaccharides (i.e., isomaltose). For example, the yield of isomaltose during glucose pyrolysis at 80 °C for 15 min increases from ~3 to ~8% when the acid loading increases from 0.25 to 0.5 mmol/g, compared to a small increase (i.e., from ~4 to ~6%) for gentiobiose. This is reasonable since the α-glucose is more stable than the β-glucose under acidic conditions due to the anomeric effect [190]. The formation of α-glucose via mutarotation reaction is more preferred during acid-catalysed pyrolysis as discussed above.

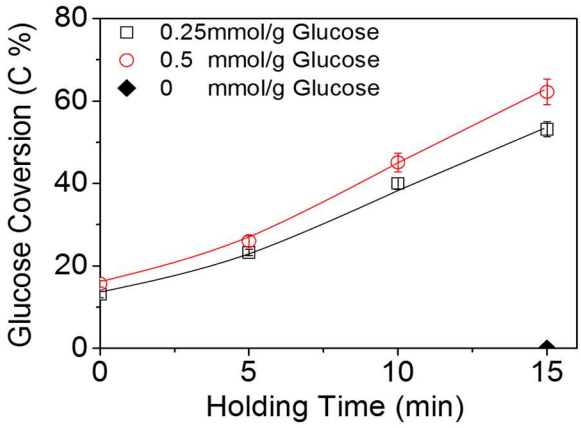

Figure 5-8 Effect of acid loading on glucose conversion during glucose pyrolysis at 80 °C.

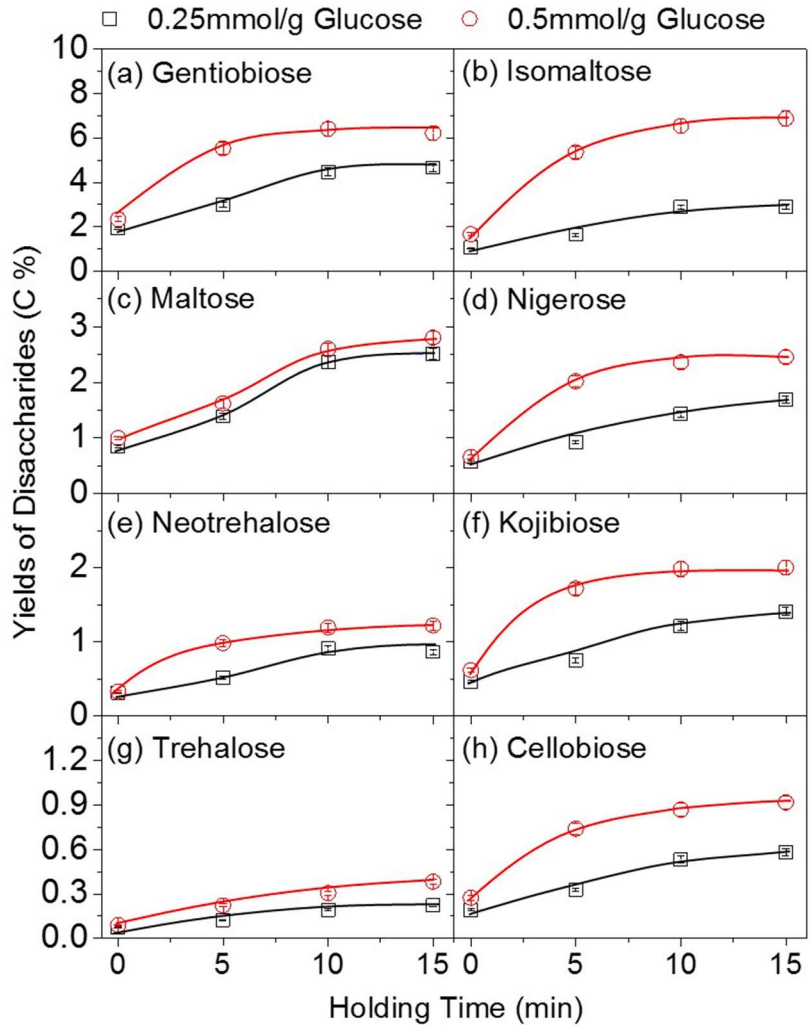

Figure 5-9 Effect of acid loading on the yields of disaccharides during glucose pyrolysis at 80 °C.

Figure 5-10 shows that an increased acid loading also increases the selectivities of disaccharides during acid-catalysed glucose pyrolysis. For example, the initial

selectivity of gentiobiose increase from ~15% (at ~12% glucose conversion) to ~27% (at ~16% glucose conversion) when the acid loading increases from 0.25 to 0.5 mmol/g. Thus, the disaccharides with 1,6-glycosidic bond (including α and β linkage) are the key primary products of acid-catalysed glucose pyrolysis, contributing to ~45% of disaccharide formation at an acid loading of 0.5 mmol/g. The above results clearly demonstrate that the acid loading can greatly affect the formation of primary products during acid-catalysed glucose pyrolysis, producing more disaccharides with 1,6-glycosidic bond (i.e., gentiobiose and isomaltose) at higher acid loading levels.

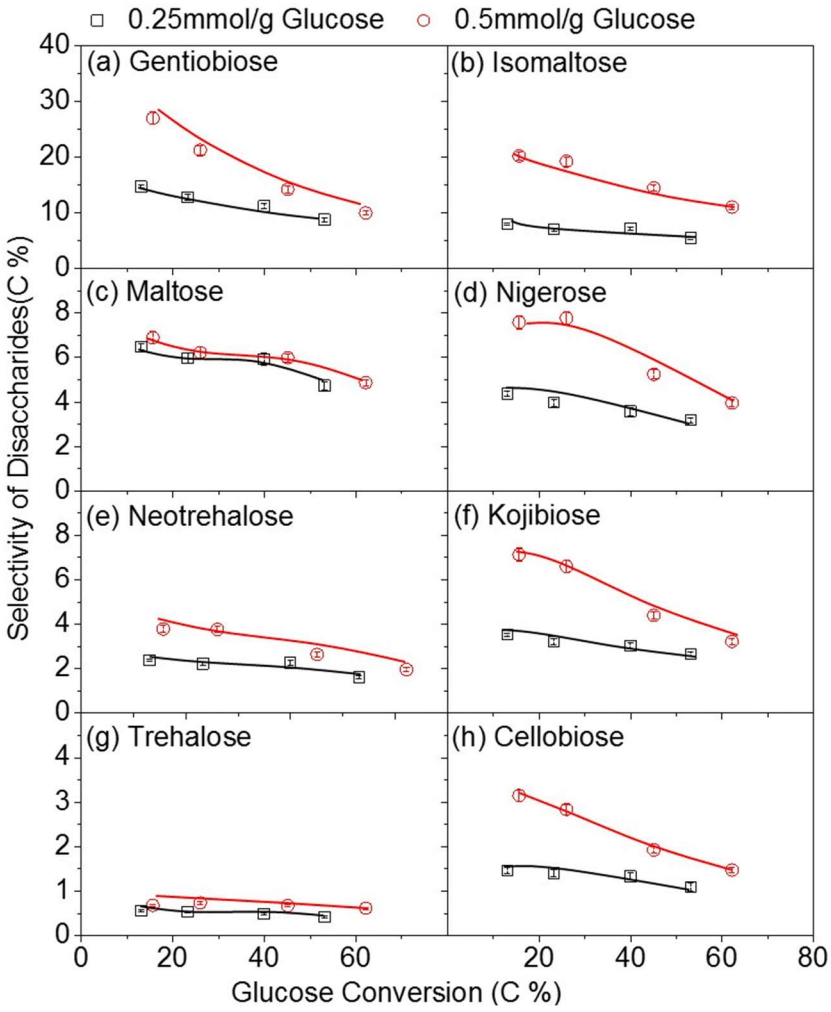

Figure 5-10 Effect of acid loading on selectivities of disaccharides during glucose pyrolysis at 80 °C.

5.2.5 Discussion on acid-catalysed glucose pyrolysis mechanism

The above results provide new insights into glucose pyrolysis mechanism under acidic conditions. According to the results in this study, acid-catalysed glucose pyrolysis

mechanism at low temperatures is proposed in Fig. 10. At the initial stage, polymerisation is the dominant primary reaction during acid-catalysed glucose pyrolysis at low temperatures, producing oligosaccharides of various linkages (especially α- and β-1,6 glycosidic bonds) as primary products. The primary products of acid-catalysed glucose pyrolysis are mainly contributed by disaccharides of various linkages (~74% on a carbon basis at an acid loading of 0.5 mmol/g), as evidenced by the HPAEC-MS results. The formation of disaccharides of various linkages has been reported from glucose hydrothermal conversion under acidic conditions [195]. It seems that water plays an important role in acid-catalysed glucose pyrolysis, since water as a reaction media can assist the formation of C1-carbocation in glucose [190]. The acid-impregnated glucose sample has a moisture content of ~10% after freeze drying, due to the formation of glucose monohydrate [191]. During pyrolysis, the water content in the pyrolyzing sample starts to reduce as glucose conversion increases, especially at temperatures >100 °C (see Fig. S1 of the Supplementary Material). As pyrolysis reactions proceed, the disaccharides are further polymerised into high-DP oligosaccharides, due to the presence of water. Our GPC results show that the DP of oligosaccharide can be as high as 18 during glucose pyrolysis at 120 °C. At high temperatures (>150 °C), the high-DP oligosaccharides start to decompose into volatiles and char, which can be seen from the significant sugar loss as shown in Figure 5-6.

Overall, our results clearly demonstrate the important role of polymerisation reactions during acid-catalysed glucose pyrolysis. Those reactions should be considered during the pyrolysis of biomass after various acid pre-treatments, i.e., acid leaching [138] and acid impregnation [26, 29, 145], to suppress the catalytic effect of AAEM species on biomass pyrolysis to produce a high-quality bio-oil. Even for biomass without acid pre-treatment, those reactions may play important roles since substantial acidic compounds are also produced during biomass pyrolysis processes.

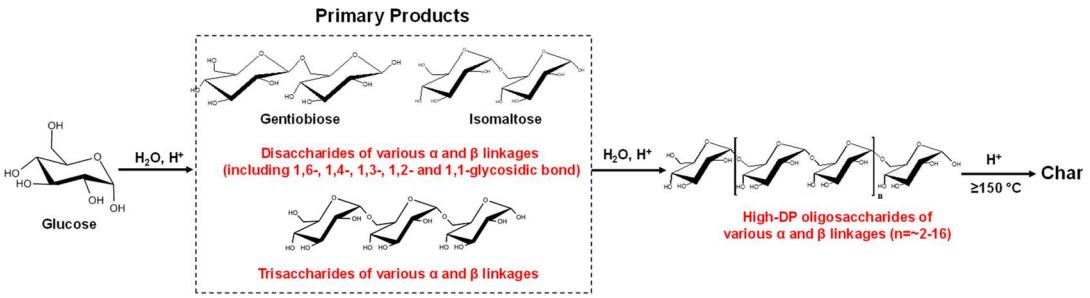

Figure 5-11 Proposed acid-catalysed glucose pyrolysis mechanism at low temperatures.

5.3 Conclusions

This study investigates the polymerisation of glucose during pyrolysis under acidic conditions, providing new insights into acid-catalysed glucose pyrolysis mechanism. Polymerisation reactions are dominant primary reactions during acid-catalysed glucose pyrolysis at low temperatures, mainly producing disaccharides of various linkages (including 1,6-, 1,4-, 1,3-, 1,2- and 1,1-glycosidic bond) as primary products. Among all the disaccharides, the formation of 1,6-glycosidic bond disaccharides (i.e., gentiobiose and isomaltose) is more favorable, likely due to the high reactivity of the hydroxyl group on C6. A higher acid loading can lead to the formation of more disaccharides as primary products. The formation of disaccharides with α and β linkages also indicates the important role of mutarotation reactions during acid-catalysed glucose pyrolysis. As pyrolysis reactions proceed, the disaccharides are further polymerised into high-DP oligosaccharides. The maximal DP of oligosaccharide increases with pyrolysis temperature, from ~4 at 60 °C to ~18 at 120 °C.

Chapter 6 Mechanistic insights into the primary reactions during acid-catalysed pyrolysis of levoglucosan at low temperatures

6.1 Introduction

Biomass fast pyrolysis can produce bio-oil as a renewable liquid fuel, which can be further upgraded/refined for producing transport fuels and value-added chemicals [34, 181, 196-199]. However, bio-oil has some undesirable properties (i.e., high water content, high acidity, low heating value, high viscosity, etc) [181], which limit the commercialization of pyrolysis technologies for producing renewable transport fuels [14].

Levoglucosan is a major product from cellulose pyrolysis, with a yield up to 70% [200, 201]. Therefore, pyrolysis is considered as a potential technology to produce sugar products from cellulose. However, the yield of sugar product from biomass pyrolysis is low, due to the inherent presence of alkali and alkaline earth metallic (AAEM) species which catalyse the fragmentation reactions of levoglucosan to produce low-molecular-weight products (i.e., formic acid and hydroxyacetaldehyde) [17, 18, 21, 23, 202]. To overcome this problem, biomass can be pretreated by acid impregnation to improve the yield of levoglucosan from biomass pyrolysis, since acid can passivate the catalytic effect of AAEM species in biomass [26, 27, 203]. Although the levoglucosan yield can be greatly improved by acid pretreatment, the optimization of acid loading is a critical factor since acid also catalyses the dehydration and polymerisation reactions of levoglucosan to produce levoglucosenone and char [28, 203]. Therefore, it is important to understand the fundamental reactions during acid-catalysed levoglucosan pyrolysis.

Previous studies have been carried out on the pyrolysis of biomass [26-28], cellulose [159, 186, 201, 204, 205], glucose [206-210] or levoglucosan [211-217] under various conditions. However, most of those studies focused on pyrolysis at high temperatures (i.e., 300 – 600 °C) to investigate the formation of volatiles, while only few studies were concerned with acid-catalysed pyrolysis at low temperatures (i.e., < 300 °C) to understand the reactions (i.e., polymerisation) in the solid phase. Our recent work [206] has highlighted the importance of polymerisation reactions during glucose pyrolysis to form disaccharides of various linkages at 60 – 150 °C. Therefore, this work continues this

series of study to understand the primary reactions during acid-catalysed levoglucosan pyrolysis at low temperatures.

6.2 Results and Discussion

6.2.1 Levoglucosan conversions and yields of products during acid-catalysed levoglucosan pyrolysis

Acid-catalysed pyrolysis of levoglucosan was undertaken at temperatures of 80 – 140 °C and holding times of 0 – 15 min. To quantify the remaining levoglucosan and various pyrolysis products, the solid product was dissolved in ultrapure water to obtain a liquid sample, which was further analysed by HPAEC-PAD-MS. Typical HPAEC-PAD chromatograms using two different methods are shown in Figure 6-1. When using 25 mM NaOH as eluent, glucose and disaccharides with various glycosidic linkages (i.e., isomaltose, kojibiose, gentiobiose, cellobiose, nigerose and trehalose) were indentified, similar as those from glucose pyrolysis under acidic conditions [206]. However, this method was unable to separate anhydro-dissacharides from levoglucosan. Using the ultrapure water as eluent, five anhydro-disaccharides (i.e., maltosan, cellobiosan, sophorosan, nigerosan, laminaribiosan) were then successfully identified in the water-soluble sample from acid-catalysed levoglucosan pyrolysis with standards. The formation of glucose indicates the presence of hydrolysis reaction during acid-catalysed levoglucosan pyrolysis at such low temperatures. While the formation of anhydro-disaccharides and disaccharides confirms the importance of polymerisation reactions during acid-catalysed levoglucosan pyrolysis. It is known that levoglucosan and glucose can be catalysed by acid to generate a carbonium-oxonium at the C1 position, leading to the formation of polymers at a free hydroxyl group on the monomer molecule [218, 219]. The identification of these key products demonstrates that both hydrolysis and polymerisation reactions play importance roles during acid-catalysed levoglucosan pyrolysis at such low temperatures.

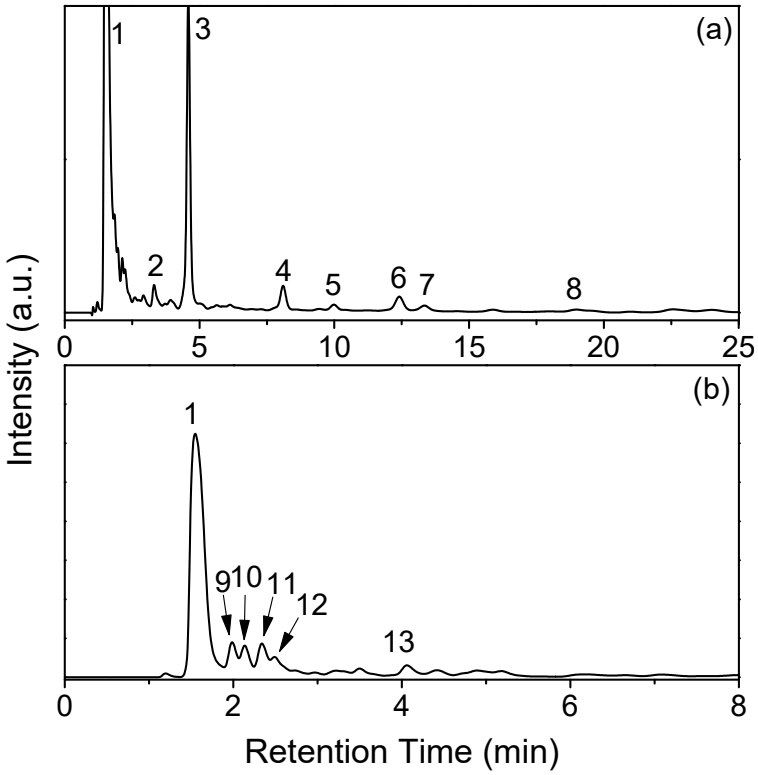

Figure 6-1 HPAEC-PAD chromatogram of a water-soluble sample from acid-catalysed levoglucosan pyrolysis at 100 °C and an acid loading of 0.25 mmol/g for 15 min. (a) use 25 mM NaOH as eluent without a post-column, and (b) use ultra-pure water as eluent with a post-colume. The identified peaks are (1) levoglucosan; (2) trehalose, (3) glucose; (4) isomaltose; (5) kojibiose; (6) gentiobiose; (7) cellobiose; (8) nigerose; (9) maltosan; (10) cellobiosan; (11) sophorosan; (12) nigerosan; (13) laminaribiosan.

The conversion rate of acid-impregnated levoglucosan also can be affected by the variable moisture content in the samples at the different pyrolysis temperatures, since water can assist in hydrolysis and the formation of C1-carboncation in glucose and levoglucosan which is beneficial to polymerisation reactions [190, 219]. For example, the moisture content of char formed at 100 °C in the holding time of 15min (~4 wt.%) is higher than the moisture of char formed at 140°C in the holding time of 15min (~2 wt.%) shown in Figure 6-2. Moreover, the acidic levoglucosan conversion is caused by hydrolysis and polymerisation in the presence of water in the samples at different pyrolysis temperatures. At pyrolysis temperatures of 80 and 100 °C, the acid-catalysed levoglucosan pyrolysis tends to form hydrolysis products (e.g., glucose and disaccharides containing two glucopyranose units) [206]. Once the pyrolysis

temperatures increase above 120 °C, hydrolysis is weakened by the loss of moisture content in samples, but polymerisation formed by levoglucosan is still enhanced by the acid catalyst, especially at the temperature of 120 °C of an optimum condition for acid-catalysed levoglucosan polymerisation [213]. Therefore, the moisture content has a signification on hydrolysis and products selectivity in polymerisation during acid-catalysed levoglucosan pyrolysis at the low temperatures.

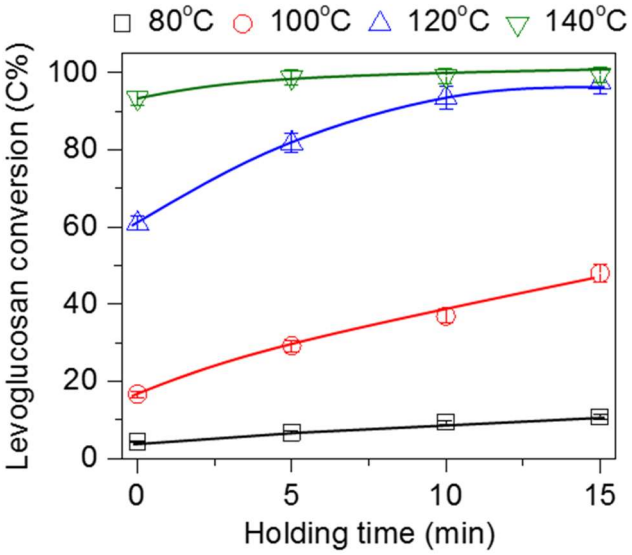

Figure 6-2 Levoglucosan conversion on a carbon basis as a function of holding time at 80–140°C and an acid loading of 0.25 mmol/g.

Figure 6-2 presents the levoglucosan conversion (on a carbon basis) under various conditions. It can be seen that levoglucosan pyrolysis can occur at a low temperature of 80 °C under acidic conditions, much lower than that of 190 °C for levoglucosan pyrolysis under non-catalytic conditions [220]. However, levoglucosan pyrolysis reactions are slow at 80 °C, with a levoglucosan conversion of 11% at a holding time of 15 min. The levoglucosan conversion increases rapidly with pyrolysis temperature. For example, the levoglucosan conversion at a holding time of 15 min increases from 11 to 97% when pyrolysis temperature increases from 80 to 140 °C. The results indicate that acid loading considerably enhances levoglucosan pyrolysis even at such low temperatures.

Figure 6-3 presents the yield (on a carbon basis) of major products, including glucose, anhydro-disaccharides (maltosan, cellobiosan, sophorosan, nigerosan, laminaribiosan) and disaccharides (isomaltose and gentiobiose), from acid-catalysed levoglucosan pyrolysis at various temperatures and holding times. At 80 °C, the initial yield (at zero holding time) of glucose is 0.9%, the highest among all identified products. Due to the

presence of moisture in the raw sample, hydrolysis of levoglucosan could easily take place to form glucose even at such a low temperature. However, the glucose yield decreases with holding time, indicating that glucose is prone to decomposition, mainly via polymerisation reactions [206]. Anhydro-disaccharides of different linkages are also formed at 80 °C, and the yields of these products are initially low but increase with holding time. For example, the yield of maltosan increases from 0.4 to 1.2% when the holding time increases from 0 to 15 min. The yields of disaccharides are even lower, and also increase with holding time. For example, the yield of isomaltose increases from 0.1 to 0.2% as the holding time increases from 0 to 15 min. As the pyrolysis temperature increases from 80 to 100 °C, although remaining the highest among all identified products, the initial glucose yield slightly reduces to 0.7%. In contrast, the initial yields of anhydro-disaccharides and disaccharides of different linkages all increases. Furthermore, as the holding time increases, the yields of maltosan, cellobiosan and laminaribiosan increase, while those of nigerosan, sophorosan, isomaltose and gentiobiose first increase then decrease.

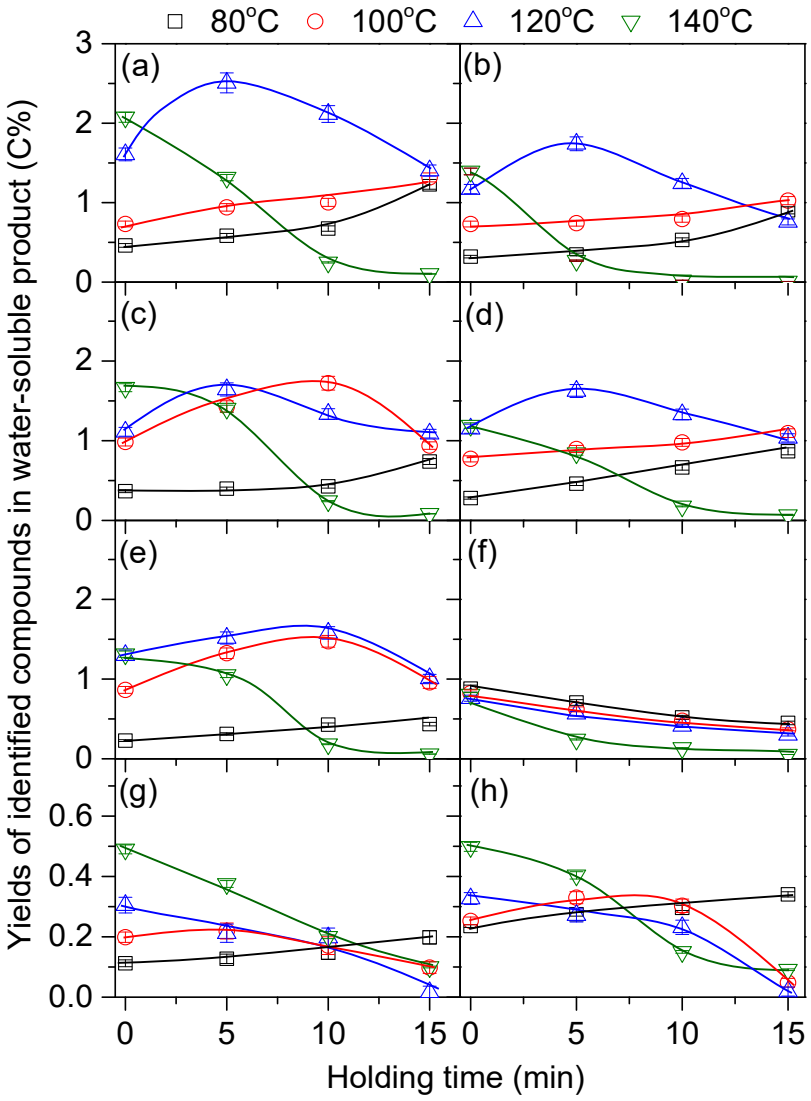

Figure 6-3 Yields of various sugar compounds on a carbon basis as a function of holding time during acid-catalysed levoglucosan pyrolysis at 80 – 140 °C and an acid loading of 0.25 mmol/g. (a) maltosan; (b) cellobiosan; (c) nigerosan; (d) laminaribiosan; (e) sophorosan; (f) glucose; (g) isomaltose and (h) gentiobiose.

As the pyrolysis temperature increases to 120 °C, the initial yields of anhydro-disaccharides are much higher than that of glucose, and the yields of those products first increase then decrease with increasing holding time. The maximal yields of those products are 2.5 and 1.7% for maltosan and cellobiosan at a holding time of 5 min, respectively. In contrast, the yields of glucose, isomaltose and gentiobiose all decrease with holding time. When the temperature further increases to 140 °C, the initial yields of anhydro-disaccharides continue to increase. For example, the initial yields of maltosan and cellobiosan increase to 2.1 and 1.4% at 140 °C from 0.4 and 0.3% at 80 °C, respectively. In contrast, the initial glucose yield decreases with increasing

temperature, attributing to the evaporation of moisture at elevated temperatures. It should be mentioned that the yields of those products all decrease with holding time. For example, the yields of maltosan and isomaltose decrease from 2.1 and 0.5% at zero holding time to 0.1 and 0.1% at a holding time of 15 min, respectively. This indicates that all sugar and anhydro-sugar products are prone to decomposition at 140 °C.

6.2.2 Selectivities of products during acid-catalysed levoglucosan pyrolysis

Figure 6-4 presents the selectivies (on a carbon basis) of identified products during acid-catalysed levoglucosan pyrolysis at an acid loading of 0.25 mmol/g, as a function of levoglucosan conversion. It can be seen that the selectivies of all identified products decrease as levoglucosan conversion increases at all temperatures. The results clearly indicate that all those products (i.e., glucose, anhydro-disaccharides, and disaccharides) are primary products during acid-catalysed levoglucosan pyrolysis. The initial selectivies of typical products follow a decreasing order of glucose (~20.0%) > cellobiosan (~6.1%) > maltosan (~6.0%) > laminaribiosan (~5.9%) > nigerosan (~5.8%) > sophorosan (~5.2%) > gentibobiose (~4.1%) > isomaltose (~2.0%). The initial selectivity of glucose being highest among all identified pyrolysis products clearly demonstrates that hydrolysis is a major primary reaction during acid-catalysed levoglucosan pyrolysis, especially at temperatures below 100 °C when the evaporation of moisture is slow. The rapid decrease of glucose selectivity at early conversions

(below 10%) also indicates that glucose is easily converted to other products (i.e., via polymerisation reactions [206]).

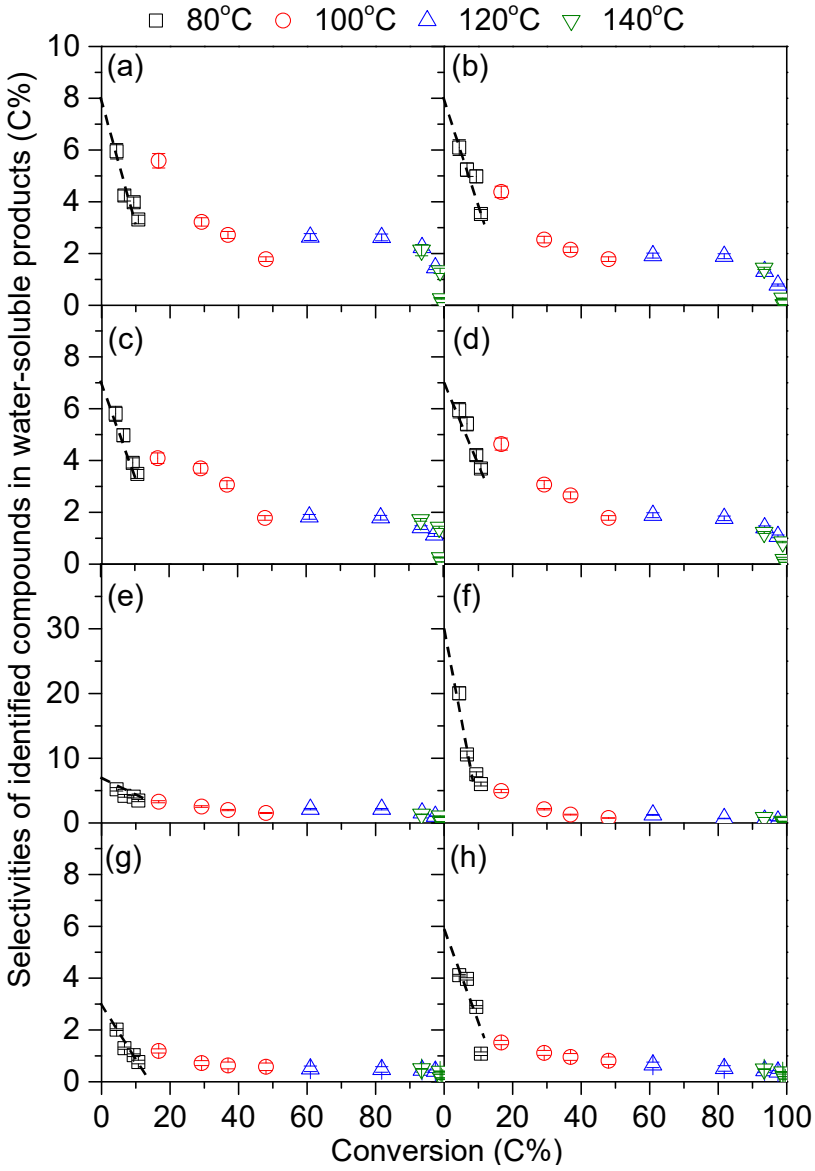

Figure 6-4 Selectivities of various sugar compounds on a carbon basis as a function of levoglucosan conversion during acid-catalysed levoglucosan pyrolysis at 80 – 140 °C and an acid loading of 0.25 mmol/g. (a) maltosan; (b) cellobiosan; (c) nigerosan; (d) laminaribiosan; (e) sophorosan; (f) glucose; (g) isomaltose and (h) gentiobiose.

Figure 6-3 also shows that polymerisation reactions of levoglucosan are also important primary reactions during acid-catalysed pyrolysis to form anydro-disaccharides of different linkages. Among the anydro-disaccharides identified, the selectivities of anhydro-disaccharides with 1,4-glycosidic linkage (i.e., maltosan and cellobiosan) are higher than those of 1,3- and 1,2-glycosidic linkages (i.e., nigerosan, laminaribiosan and sophorosan). This is understandable because the hydroxyl group on C4 is more reactive than others thus reducing steric hindrance on levoglucosan [220, 221]. The existence of anhydro-disaccharides with both α and β linkages at the same hydroxyl group indicates that mutarotation reactions are involved during acid-catalysed levoglucosan pyrolysis. Similar mutarotation reactions are also reported in acid-catalysed glucose pyrolysis [206]. This is attributed to the protonation of the ring O to form the oxonium ion as a result of the presence of acid and water in the acid-loaded sample [190]. In addition, disaccharides are also primary products from acid-catalysed levoglucosan pyrolysis, but the selectivities of these products are lower. This suggests that disaccharides of different linkages (including 1,6-, 1,4-, 1,3-, 1,2- and 1,1-glycosidic bond) can be directly produced from levoglucosan via polymerisation reactions, but mainly in the form of 1,6-glycosidic linkage (i.e., isomaltose and gentiobiose). This is consistent with the previously-reported higher selectivities of isomaltose and gentiobiose during glucose acid-catalysed pyrolysis [206].

The above results clearly show that hydrolysis and polymerisation reactions are important primary reactions during acid-catalysed levoglucosan pyrolysis at 80 – 140 °C. Figure 6-4 presents the total selectivity (on a carbon basis) of identified products as a function of conversion. It can be seen that the total initial selectivity of identified products is ~60%, demonstrating the presence of other primary products. Also shown in Figure 6-5 are the total sugar recoveries after post-hydrolysis of the solid products. It is interesting to see that almost all the pyrolysis products are still in forms of sugar products (such as anhydro-sugars or sugar oligosaccharides) that can be hydrolysed to glucose via post-hydrolysis, even at high levoglucosan conversions of ~80%. Therefore, there must be other anhydro-disaccharides and/or disaccharides of different linkages produced as primary products. These have been further confirmed by the HPAEC-PAD chromatogram (see *Figure 6-1*), which has already shown the presence of other disaccharides such as kojibiose, cellobiose and nigerose in the solid product from acid-catalysed levoglucosan pyrolysis. The post-hydrolysis results also

show that non-sugar products are produced at 140 °C, indicating the formation of char under such conditions.

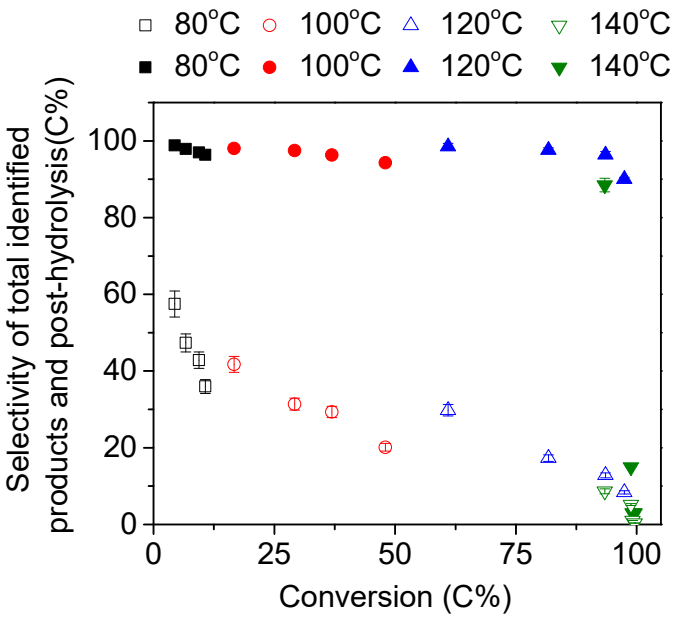

Figure 6-5 Selectivity of total quantified sugars on a carbon basis as a function of levoglucosan conversion during acid-catalysed glucose pyrolysis at 80 – 140 °C and an acid loading of 0.25 mmol/g. Open symbols present the selectivity of total quantified sugars, and solid symbols present the post-hydrolysis results.

Figure 6-5 also shows that the selectivities of primary products all decrease rapidly as conversion increases so that those primary products are prone to further decomposition to form other secondary products. The post-hydrolysis results indicate those primary products are further polymerised into high-DP anhydro-sugar or sugar products. To prove this point, the liquid samples produced at 80 – 120 °C and 15 min were also analysed by GPC to measure the molecular weight of the products in the liquid sample. As shown in Figure 6-6, the GPC results clearly show the formation of high-DP sugar oligosaccharides at temperatures > 100 °C. The maximal DPs of sugar oligosaccharides in the liquid sample were further estimated based on standards, i.e., from ~3 at 80 °C (at the retention time of 14.5 min) to ~10 at 120 °C (at a retention time of 13.5 min). Therefore, the high-DP anhydro-sugar or sugar oligosaccharides can be easily formed during acid-catalysed levoglucosan pyrolysis under the conditions. Considering the formation of anhydro-disaccharides and disaccharides of various linkages from levoglucosan polymerisation in this study, it can then be concluded that various anhydro-sugar and sugar oligosaccharides of different α or β

linkages can be formed during acid-catalysed levoglucosan pyrolysis at such low temperatures.

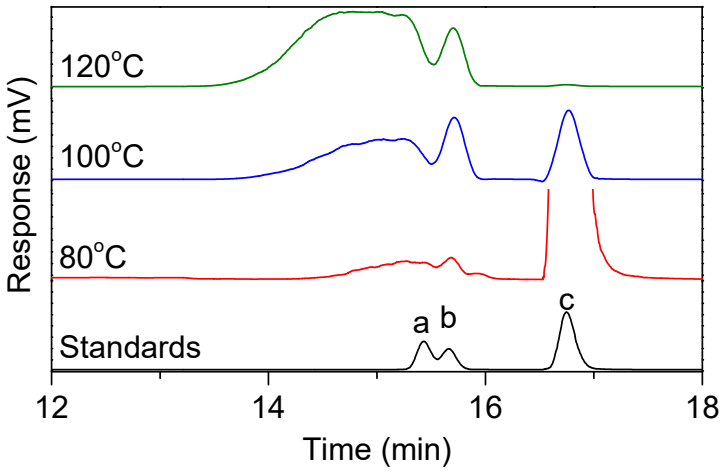

Figure 6-6 GPC analysis of the water-soluble samples from acid-catalysed levoglucosan pyrolysis at 80 – 120 °C and an acid loading of 0.25 mmol/g for a holding time of 15 min. (a) cellobiose, (b) glucose, (c) levoglucosan.

6.2.3 Effect of acid loading on acid-catalysed levoglucosan pyrolysis

To investigate the effect of acid loading on levoglucosan pyrolysis, levoglucosan pyrolysis experiments were performed at a higher acid loading level of 0.5 mmol/g. Levoglucosan conversion during acid-catalysed pyrolysis at 100 °C for two acid loading levels of 0.25 and 0.5 mmol/g are compared in Figure 6-7. An increase in the acid loading level largely enhances the levoglucosan conversion. For example, the levoglucosan conversion increases from ~19 to ~30% at zero holding time, and from ~40 to ~65% at a holding time of 15 min, when the acid loading level increases from 0.25 to 0.5 mmol/g.

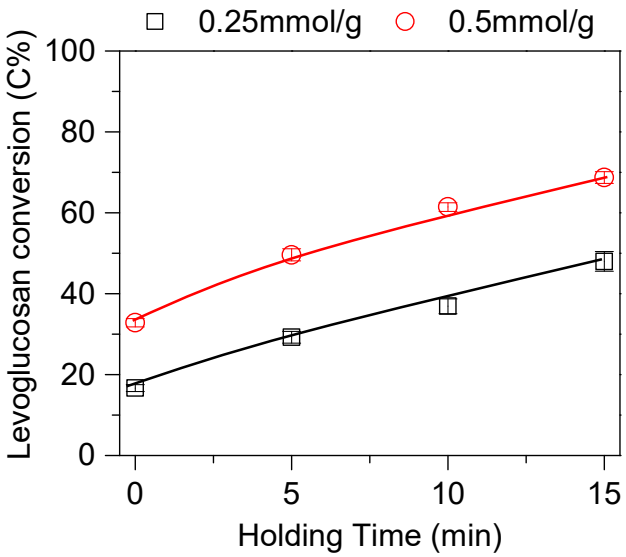

Figure 6-7 Effect of acid loading level on levoglucosan conversion on a carbon basis during acid-catalysed pyrolysis at 100 °C.

The yields and selectivities of key primary products during acid-catalysed levoglucosan pyrolysis at 100 °C for two acid loading levels were also determined, and the results are presented in Figure 6-8 and *Figure 6-9*, respectively. As the acid loading level increases from 0.25 to 0.5 mmol/g, the yields of anhydro-disaccharides only increase slightly, but the yields of glucose and disaccharides increases substantially. For example, the initial glucose and isomaltose yields increase from 0.8 to 2.4%, while little change can be found for the initial yields of anhydro-saccharides. Since the levoglucosan conversion increases with the acid loading level, this leads to reductions in the selectivities of anhydro-disaccharides. In contrast, there are only slight increases in the selectivities of glucose and disaccharides. It should be noted that although the glucose yield increases substantially with acid loading level, there is only insignificant increase in glucose selectivity. It can be therefore concluded that an increase in acid loading level leads to the suppression of polymerisation reactions to produce anhydro-saccharides, but enhances the hydrolysis and polymerisation reactions to produce glucose and disaccharides, especially isomaltose and gentiobiose, during acid-catalysed levoglucosan pyrolysis under the conditions in this study.

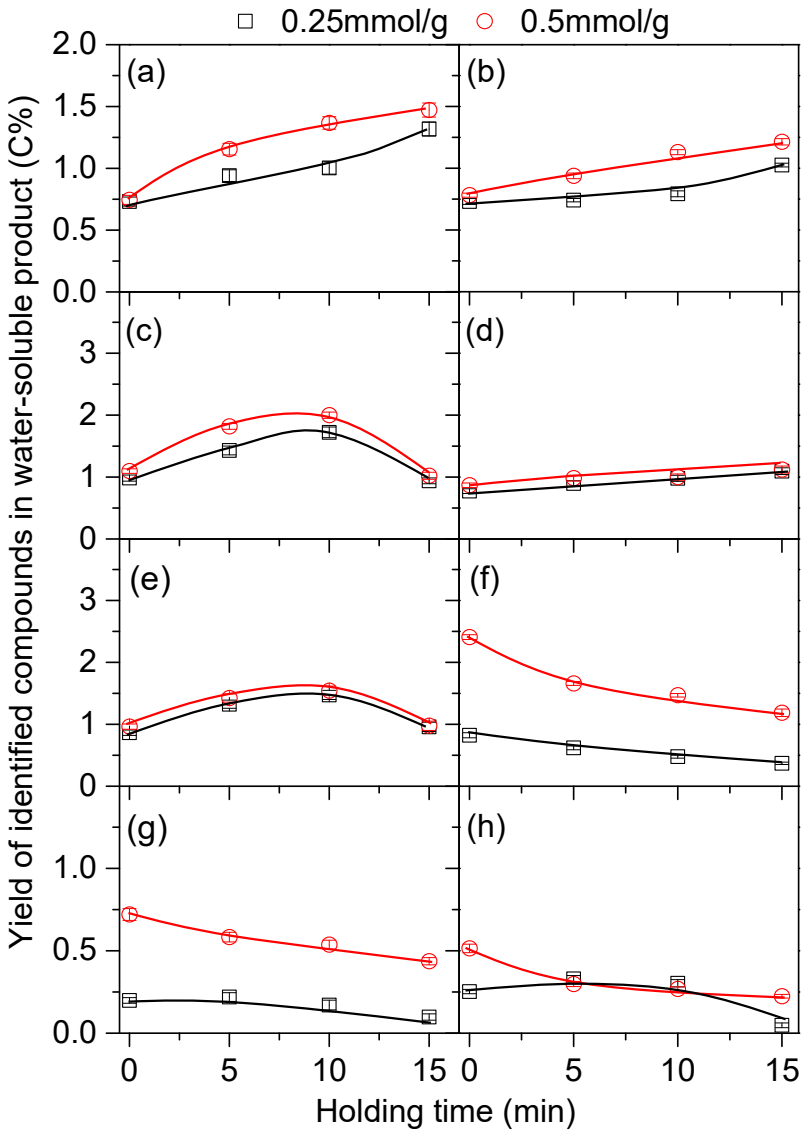

Figure 6-8 Effect of acid loading level on the yields of anhydro-disaccharides on a carbon basis during levoglucosan pyrolysis at 100 °C. (a) maltosan; (b) cellobiosan; (c) nigerosan; (d) laminaribiosan; (e) sophorosan; (f) glucose; (g) isomaltose and (h) gentiobiose.

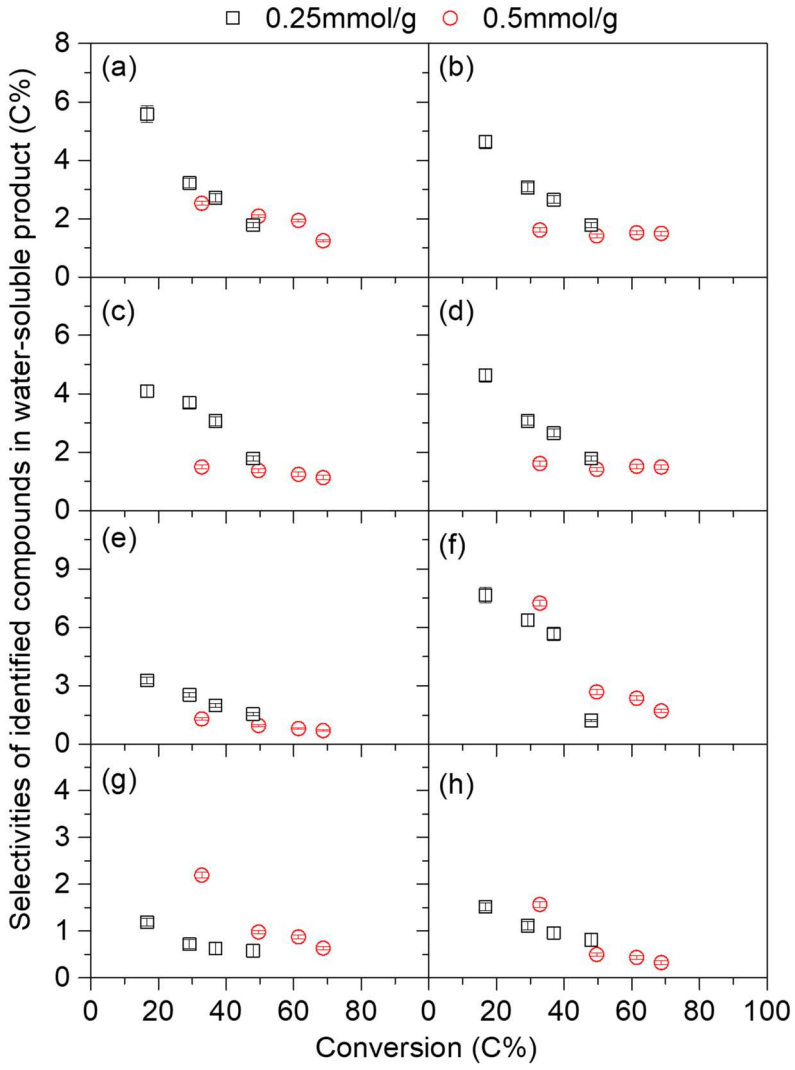

Figure 6-9 Effect of acid loading level on the selectivites of anhydro-disaccharides on a carbon basis during levoglucosan pyrolysis at 100 °C. (a) maltosan; (b) cellobiosan; (c) nigerosan; (d) laminaribiosan; (e) sophorosan; (f) glucose; (g) isomaltose and (h) gentiobiose.

6.2.4 Further discussion on the primary reactions during acid-catalysed levoglucosan pyrolysis

The above results provide new insights into the primary reactions during acid-catalysed pyrolysis of levoglucosan at low temperatures (80 – 140 °C). Further efforts were then taken (according to the delpot technique [193]) to calculate the contributions of various primary reactions during acid-catalysed levoglucosan pyrolysis. As summarized in Fig. 10, there are three important primary reactions during acid-catalysed levoglucosan pyrolysis at such low temperatures.

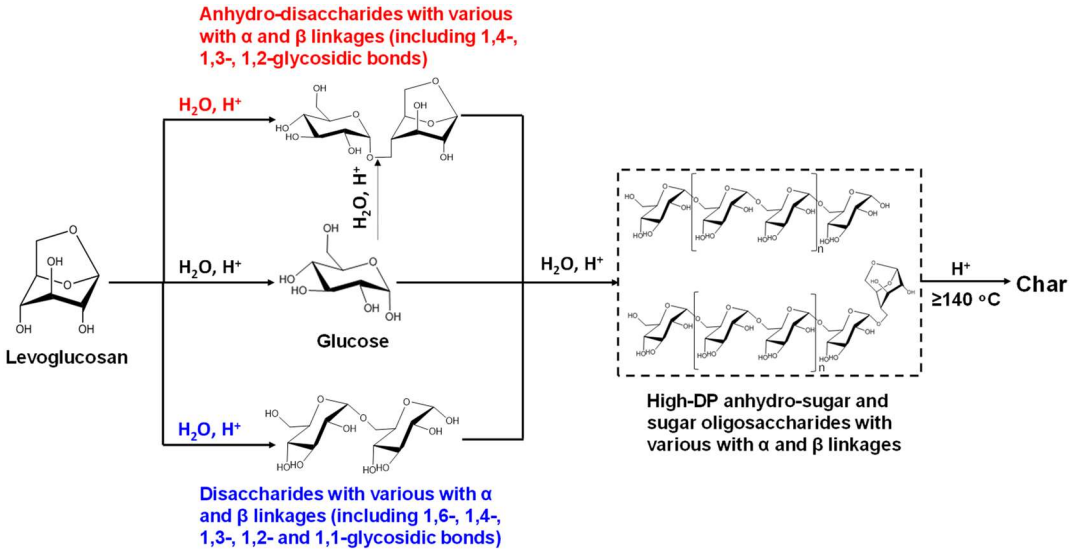

Figure 6-10 Primary reactions during acid-catalysed levoglucosan pyrolysis mechanism at low temperatures.

First, hydrolysis of levoglucosan to produce glucose is an important primary reaction, contributing to ~30% of the primary reactions. This is expected because both acid and water are present in the acid-loaded sample, leading to the formation of glucose via hydrolysis reactions even at 80 °C. The moisture contents of chars at 100 and 140 °C were also measured, and the results are presented in *Figure 6-11*. The initial moisture content of the sample is ~5%, and it reduces slowly as the holding time increases at 100 °C. However, the moisture content reduces rapidly at 120 °C, because part of water can be consumed during hydrolysis. Therefore, the hydrolysis reactions can be affected by the moisture content during acid-catalysed levoglucosan pyrolysis under the experimental conditions.

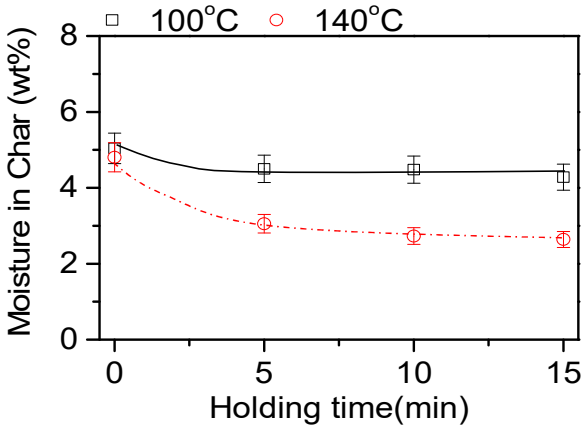

Figure 6-11 Moisture content in the char samples pyrolysed under at 100 and 140 °C.

Second, polymerisation reactions of levoglucosan to produce anhydro-disaccharides of different linkages are also important primary reactions. For example, polymerisation reactions to form the identified anhydro-disaccharides contribute to ~37% of primary reactions. It should be noted that anhydro-disaccharides can only be formed with 1,4-, 1,3-, and 1,2-glycosidic linkages, due to the presence of levoglucosan at the reducing end. It was reported that both acid and water play a critical role in the formation of C1-carbocation in levoglucosan to facilitate the polymerisation reactions to form anhydro-disaccharides [190, 221, 222]. Meanwhile, mutarotation reactions also play important roles to form anhydro-disaccharides with α and β linkages [190].

Third, polymerisation reactions of levoglucosan to produce disaccharides of various linkages (including 1,6-, 1,4-, 1,3-, 1,2- and 1,1-glycosidic bond) are minor primary reactions. For example, polymerisation reactions to form isomaltose and gentiobiose contribute to ~9% of primary reactions. It is noteworthy that such direct formation of disaccharides from levoglucosan as primary products has never been reported in the open literature. Our results show that the formation of disaccharides is enhanced as acid loading level increases. In total, the above three reactions contribute to at least 76% of primary reactions during acid-catalysed levoglucosan pyrolysis at a low temperature range of 80 – 140 °C. Unfortunately, not all the anhydro-disaccharides and disaccharides of various linkages were quantified in this study due to the unavailability of standards.

Once those primary products (i.e., glucose, anhydro-disaccharides, and disaccharides) are formed during acid-catalysed pyrolysis, those products can easily produce high-DP anhydro-sugar and sugar oligosaccharides, due to the high reactivity of the hydroxyl group on C6 [220]. The GPC results in this study (see Figure 6-5) clearly show that anhydro-sugar and sugar oligosaccharides with DP as high as ~10 can be formed in the product during acid-catalysed levoglucosan pyrolysis at 120 °C. Those high-DP anhydro-sugar and sugar oligosaccharides are stable at temperatures <120 °C. Once the pyrolysis temperature increases to 140 °C, the high-DP anhydro-sugar and sugar oligosaccharides are easily converted into volatiles and char, as indicated by the significant sugar loss in the post-hydrolysis results at 140 °C.

The above results provide direct evidence to show that hydrolysis and polymerisation reactions are important primary reactions during acid-catalysed levoglucosan

pyrolysis at a low temperature range of 80 – 140 °C. These reactions should be considered during the pyrolysis of acid-pretreated biomass sample. Even without acid pretreatment, those reactions are likely to take place due to the formation of organic acids during biomass pyrolysis.

6.3 Conclusions

This study provides new insights into the primary pyrolysis mechanism of acid-impregnated levoglucosan at low temperatures. Hydrolysis reaction to produce glucose is found to be a major primary reaction contributing to ~30% of primary reactions during acid-catalysed levoglucosan pyrolysis. Polymerisation reactions also play important roles during acid-catalysed levoglucosan pyrolysis, producing anhydro-disaccharides of various α and β linkages (including 1,4-, 1,3-, and 1,2-glycosidic bond) as major primary products, as well as disaccharides of various α and β linkages (including 1,6-, 1,4-, 1,3-, 1,2- and 1,1-glycosidic bond) as minor primary products. Our results demonstrate that polymerisation reactions to produce anhydro-disaccharides and disaccharides contribute to at least ~37 and ~9% of primary reactions during acid-catalysed levoglucosan pyrolysis, respectively. At an increased acid loading level, the hydrolysis reaction to produce glucose and the polymerisation reactions to produce disaccharides are enhanced, but the polymerisation reactions to produce anhydro-disaccharides are suppressed. Those primary products are further polymerised into high-DP anhydro-sugar and sugar oligosaccharides (i.e., with DP as high as ~10 at 120 °C) as levoglucosan conversion increase, and finally converted into char at increased temperatures.

Chapter 7 Effect of glycosidic linkage on acid-catalysed pyrolysis of disaccharide

7.1 Introduction

Bio-energy is derived from biomass to generate electricity or produce liquid fuels that can be a potential alternative energy resource in the future energy market since it has two notable advantages: zero greenhouse gas emissions [6-8, 11], and convenient storage and transport [223-225].

In the utilisation of biomass, fast pyrolysis is an effective method to convert the biomass into different high-energy renewable biofuels (i.e., bio-oil, biochar, and bio-slurry)[5]. However, the natural existence of alkali and alkaline earth metallic (AAEM) species in biomass has a negative impact on the pyrolysis process, as they can catalyse the decomposing and dehydration reactions to produce undesired products such as organic acid and hydroxyacetaldehyde[17, 18, 20, 21, 23]. The unwanted products significantly alter the characters of bio-oil quality (i.e., high water content, high acidity, high viscosity, low heating temperatures, and weak phase stability); subsequently, the poor performance hinders the commercial value and promotion of bio-oil in the market. Some methods including acid-leaching, acid-infusion and a combined approach have been reported to improve the production of bio-oil and sugars in fast pyrolysis since AAEMs presented in biomass are removed or passivated during the acid treatment processes [27, 32, 144, 147]. However, these proposed methods of acid treatment also have a negative effect on the product distribution because of the catalysed decomposition and dehydration reactions if the optimum acid loading cannot be reached in the processes of treatment or pre-treatment. For example, the yield of levoglucosone, 1,4:3,6-dihydro-α-d-glucopyranose and char were increased in the presence of acid-catalysed cellulose pyrolysis[30, 31, 148, 150]. Recently, it has been reported that glucose is a primary intermediate rather than levoglucosan at pyrolysis temperature< 180 ºC because of the dominant acid hydrolysis reactions [186]. Besides, glucose could be polymerised to form different linkages disaccharides (1,6-glycosidic bond, 1,4-glycosidic bond, 1,3-glycosidic bond, 1,2-glycosidic bond, and 1,1-glycosidic bond) and oligosaccharides contributing to the formation of char and volatiles[206]. However, the impacts of different linkages of intermediates formed in the acid-catalysed glucose pyrolysis were not investigated in the further acid-catalysed pyrolysis process. Therefore, this study focuses on the comparison of two disaccharides including 1,1-β-

glycosidic bond (unstable structure in the disaccharides) and 1,4-β-glycosidic bond (stable structure in the disaccharides) in acid-catalysed pyrolysis to reveal the effects of linkages on the distribution of the products at low temperatures via identifying the intermediates formed during the initial reactions. Furthermore, it can be beneficial to understand the underlying mechanism of acid-catalysis pyrolysis.

7.2 Results and discussion

7.2.1 Conversion during acid-catalysed pyrolysis

Figure 7-1 presents the conversion of acid-catalysed trehalose and cellobiose (0.25mmol/g) at the pyrolysis temperatures range of 40 to 225 ºC holding at 15 min. The reactivity of both disaccharides is apparently affected by the raised pyrolysis temperature and the acid pre-treatment. The conversion is increased simultaneously with the rising pyrolysis temperatures. For example, the reaction of acid-catalysed trehalose could be found at the low pyrolysis temperatures, even at 40 ºC (~7%, carbon basis), which means the catalytic effect of acid has a major contribution during the low temperature pyrolysis. The effect of acid pre-treatment is identified by comparison with the raw trehalose pyrolysis. Based on the experiment results, there is no detectable conversion on raw trehalose from 40 to 150 ºC; however, the conversion of trehalose is reached to ~85% at 100 ºC and then ~94% at 120 ºC under the acid catalytic effect. The acid-catalysed trehalose is completely converted at the pyrolysis temperature of 140 ºC. The high conversion can be detected at the presence of sulfuric acid and moisture even at low pyrolysis temperatures. Due to a weak glycosidic bond in pre-treated trehalose, the high conversion under low temperatures (≤100 ºC) can be caused by hydrolysis reactions at the presence of moisture content and acid to form other sugar products such as glucose and disaccharides [189, 206].

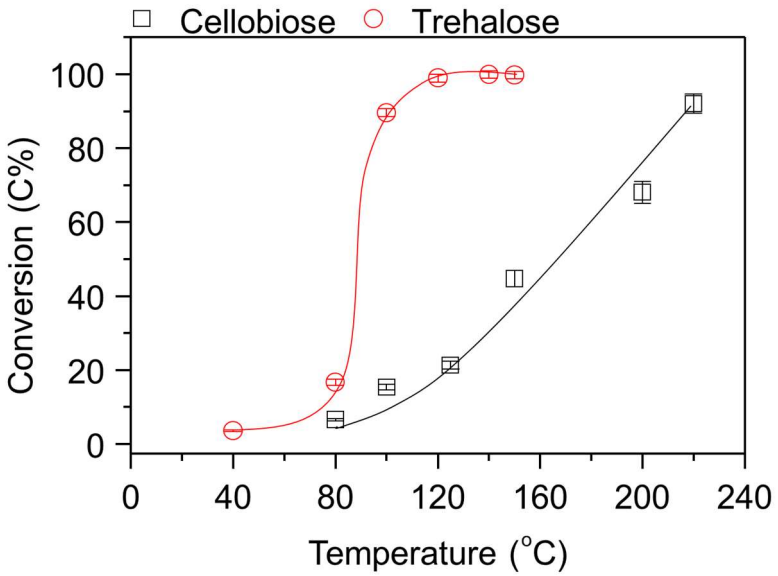

Figure 7-1 Cellobiose and trehalose conversion as a function of pyrolysis temperatures at an acid loading of 0.25mmol/g.

The acid-impregnated cellobiose (0.25mmol/g) was investigated in this study to distinguish the effect of glycosidic bonds. The results of cellobiose conversion under the acid condition are present in Figure 7-1. It shows that the conversion is increased from ~6.5% at 80 ºC to ~93% at 225ºC with rising pyrolysis temperatures. In comparison with acid trehalose pyrolysis, cellobiose conversion is gradually increased from the low pyrolysis temperature 80 ºC to the high pyrolysis temperature 225 ºC.

Acid-catalysed cellobiose is more stable than acid-catalysed trehalose when the pyrolysis temperature is less than 100 ºC. For example, there is no detectable conversion on acid-catalysed cellobiose at 40 ºC, but the acid-catalysed trehalose has ~7% conversion at the same pyrolysis condition. Moreover, when the pyrolysis temperature is increased to 120 ºC, the conversions of both disaccharides are ~94% of acidic trehalose and ~21% of acid-catalysed cellobiose respectively. So far, the results of conversion on both disaccharides can provide evidence of which 1,4-β-glycolic bond of a disaccharide is more stable than 1,1-α-glycolic bond of disaccharide under acid-catalysed pyrolysis. It provides a clear evidence of the stability of various linkage disaccharides in the our study of acid-catalysed glucose pyrolysis[206].

7.2.2 The yield of sugar products during trehalose and cellobiose acid-catalysed pyrolysis

The water-soluble products formed from the acid-catalysed trehalose and cellobiose pyrolysis were analysed by the methodology of HPAEC-PAD-MS and quantified by using sugar standards [152]. According to the our study and the developed sugar library [206], this study has successfully detected seven disaccharides (gentibiose, maltose, neotrehalose, cellobiose, isomaltose, kejibiose, and nigerose), glucose and other anhydro-products (levoglucosan, mannaosan, AGF and organic acids).

Figure 7-2 and Figure 7-3 show the major products produced in the water-soluble solution during acidic trehalose and cellobiose pyrolysis at acid loading of 0.25 mmol/g. Generally, the yields of sugar products (disaccharides and glucose) present an incremental trend from the pyrolysis temperature of 40 to 100 ºC. The yields are dropped suddenly once the pyrolysis temperature is increased to > 100 ºC. Figure 7-2 clearly presents that acid-catalysed trehalose yields more sugar products than acid-catalysed cellobiose during pyrolysis process. The products of disaccharides from acid-catalysed cellobiose are isomaltose and trehalose, and isomaltose has the highest yield among the disaccharides generated from acid-catalysed cellobiose. For example, isomaltose reaches the highest yield of ~0.75% at 100 ºC and then drops to ~0.012% at 225 ºC. In comparison with the detected disaccharides from acid-catalysed cellobiose pyrolysis, there are several disaccharides detected from acid-catalysed trehalose pyrolysis, including gentioboise, neotrehalose, and maltose. For example, the most abundant product of gentiobiose in acid-catalysed trehalose pyrolysis increases from ~1.56% to ~5.62% (40 to 100 ºC), then it drops to ~0.3%.

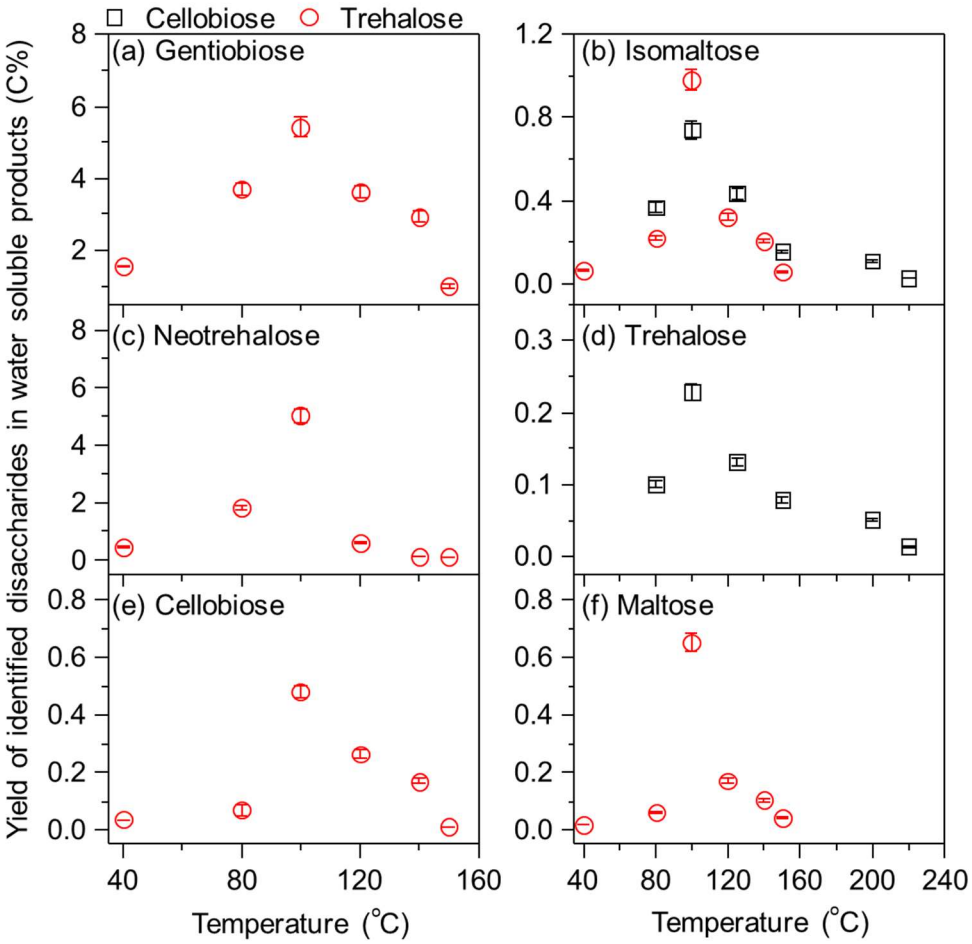

Figure 7-2 Yields of sugars as a function of pyrolysis temperatures with holding 15min during acid-catalysed trehalose and cellobiose pyrolysis at 40-150 ºC and an acid loading of 0.25 mmol/g.

The total yield of 1, 6-glycosidic bond disaccharides (gentiobiose and isomaltose) have a higher yield than other identified sugars in trehalose and cellobiose during acid-catalysis pyrolysis. For example, gentiobiose occupies ~5.62% in acid-catalysed trehalose and isomaltose occupies ~ 0.75% in acid-catalysed cellobiose at the pyrolysis temperature of 100 ºC. This is followed by the other identified disaccharides in acid-catalysed trehalose: neotrehalose ~5%, glucose ~2%, and 1, 4-glycosidic bond disaccharides (cellobiose ~4.8% and maltose ~0.65%). It is worth mentioning that the produced disaccharides are mainly produced at the pyrolysis temperature lower than 120 ºC in both acid-catalysed disaccharides' pyrolysis.

Among the identified water-soluble products presented in Figure 7-3, the results show two different trends on the produced products based on the pyrolysis temperatures and product structures. Glucose is identified as a major product from both acid-catalysed

disaccharides' pyrolysis, which can reach the maximum yield at the pyrolysis temperature 100 ºC and then quickly drops at the pyrolysis temperature ≥100 ºC. For instance, glucose generated from acid-catalysed trehalose pyrolysis is raised from ~0.5% to ~2% (40 to 100 ºC), and then the yield of glucose is rapidly decreased to 0.28% at the pyrolysis temperature of 150 ºC. Moreover, glucose produced from acid-catalysed cellobiose pyrolysis is ~2.5% at 100 ºC and drops to 0.02% at 225 ºC. It is worth noting that the maximum yield of sugars can be reached at the pyrolysis temperature of 100 ºC since moisture is present at the low temperatures (<=100ºC) which could have advantages on hydrolysis during acid-catalysis pyrolysis[27, 206]. Other products such as organic acid, mannosan and AGF can be detected in acid-catalysed cellobiose rather than acid-catalysed trehalose at the high pyrolysis temperatures.

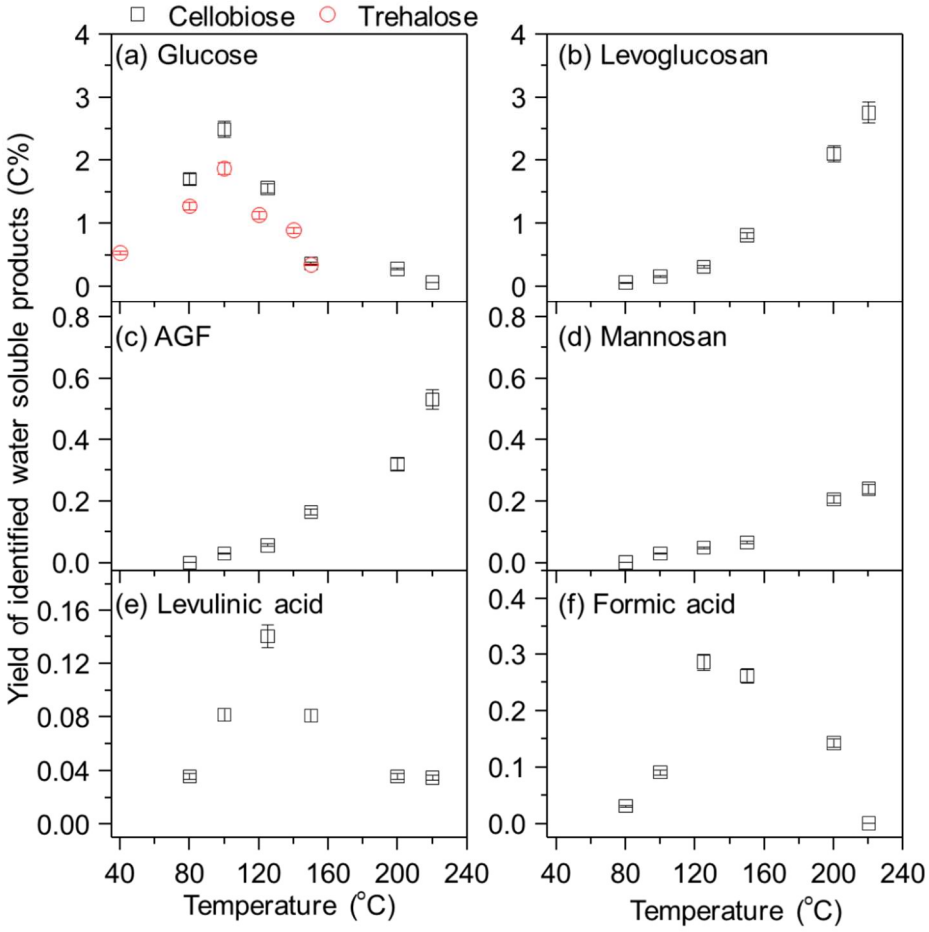

Figure 7-3 Yield of identified water-soluble products as a function of pyrolysis temperature during acid-catalysed 0.25mmol/g trehalose and cellobiose pyrolysis at 40-225 °C.

The detected dehydrated products such as levoglucosan, anhydro-manopyranose (Mannosan), and anhydro-glucofuranose (AGF) become dominant products and present an increasing trend in the yield of water-soluble products when the pyrolysis temperature is raised to ≥125 ºC in acid-catalysed cellobiose pyrolysis. Levoglucosan is the major anhydro-product produced in the pyrolysis process, showing a rapid increasing trend at the pyrolysis temperature > 125 ºC. It is worth noting that the highest yield of levoglucosan is reached ~2.85% at 225 ºC, followed by ~1% mannosan and ~0.1% AGF, which means the high temperature is prone to producing anhydro-products. Two organic acids are detected in this study, including formic acid and levulinic acid. Both acids have the highest yield at 125 ºC (e.g., ~0.3% formic acid and ~0.09% levulinic acid) then they rapidly decrease at high pyrolysis temperature.

As above, the yielded products profile can be divided into two major sections: sugar products and dehydrated products, based on the pyrolysis temperatures and the structure of disaccharides. When the pyrolysis temperature is ≤ 125 ºC, the significant products produced from the pyrolysis are glucose, gentiobiose, isomaltose, and trehalose produced in the acid catalysis pyrolysis, especially in acid-catalysed trehalose pyrolysis. However, the dehydrated products such as levoglucosan, mannosan, and AGF gradually become dominant products at ≥ 125 ºC produced in acid-catalysed cellobiose pyrolysis. The results could prove that the high yield of identified sugars can be promoted at the presence of moisture and low temperature acid pyrolysis. However, the stable cellobiose is prone to produce dehydrated products mainly at high pyrolysis temperatures because of containing the linkage of 1,4-β-glycolic bond.

7.2.3 Selectivities of sugar products during trehalose acid-catalysed pyrolysis

The selectivity of identified water-soluble products from acid-catalysed trehalose and cellobiose pyrolysis was calculated as carbon basis and present in Figure 7-4 and Figure 7-5 as the function of pyrolysis temperatures. Figure 7-4 initially presents the selectivity of identified sugars produced from acid-catalysed trehalose pyrolysis which occur in order of high selectivity: gentibiose (~43%) > neotrehalose > (~12.5%) > isomaltose (~1.8%) > cellobiose (~0.98%) > maltose (~0.51%), and the order of identified disaccharides from acid-catalysed cellobiose pyrolysis is isomaltose (~2%) > trehalose (~1.7%). The selectivity of the disaccharides with 1, 6-glycosidic bond (i.e., gentibiose and isomaltose) is higher than other disaccharides in line with the previous

study on acid-catalysed glucose pyrolysis[206], because the hydroxyl group on C6 is most reactive and more stable. Meanwhile, the high selectivity of glucose is identified in both acid-catalysed disaccharides pyrolysis studies since hydrolysis is a predominant reaction when trehalose pyrolysis is conducted at low temperatures (< 100 ºC). It can be noticed that the selectivity of neotrehalose formed in the acid-catalysed trehalose pyrolysis is higher than 1, 4-glycosidic bond disaccharides (i.e., cellobiose and maltose) which does not follow in the order of the disaccharides' stability 1, 6-glycosidic bond > 1, 4-glycosidic bond > 1, 3-glycosidic bond > 1, 2-glycosidic bond > 1, 1-glycosidic bond. A comparison of the internal structure of trehalose and neotrehalose clearly shows that the only difference is on the linkage orientation rather than the glycosidic bond position. For instance, trehalose contains two α-glucose, and neotrehalose has one α-glucose unit and one β-glucose unit. Therefore, it could prove that there are low energy barriers converting trehalose to neotrehalose without dissociating the glycosidic bond.

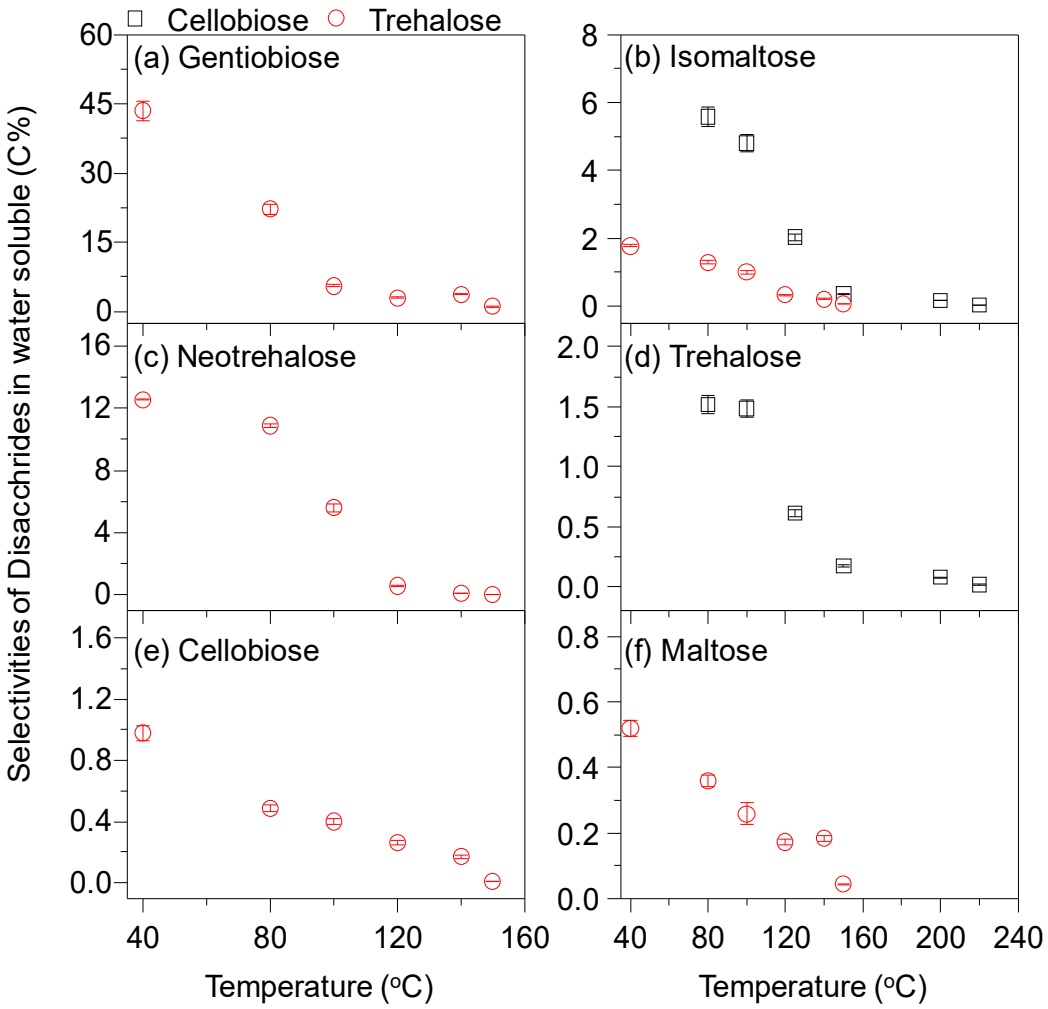

Figure 7-4 Selectivities of quantified disaccharides as a function of temperatures during acid-catalysed trehalose pyrolysis at 40-225 ºC with an acid loading of 0.25mmol/g.

The existence of α and β linkages in disaccharides proves that mutarotation reaction is enclosed in the acid-catalysed pyrolysis, such as gentiobiose (β-1, 6 linkage) and isomaltose (α-1, 6 linkage), since the presence of moisture and acid can assist in protonation of the ring O forming the oxonium ion to convert the α and β-anomers[190]. The formation rate of C1-carbocation can be accelerated under acid-catalysis pyrolysis by the moisture content, which can produce various DPs and linkages of oligosaccharides during the acid pyrolysis.

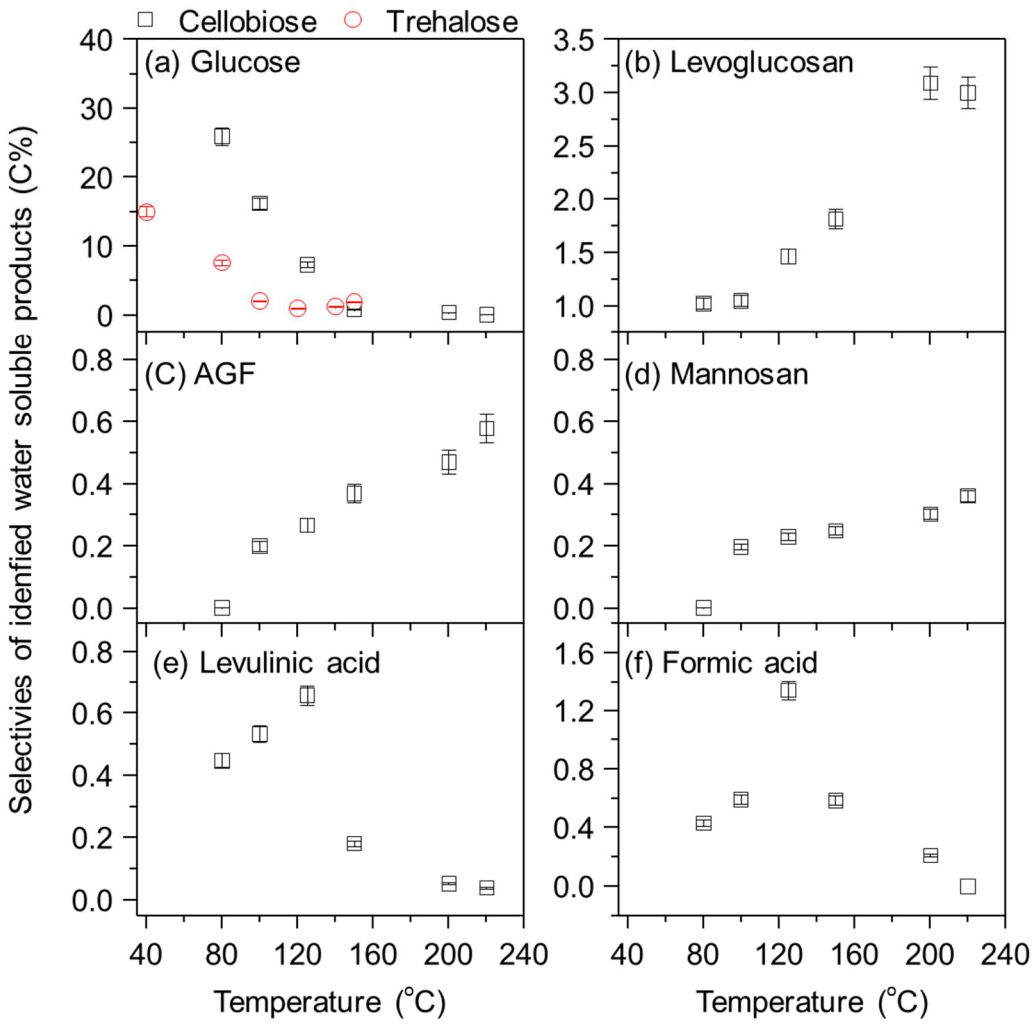

Figure 7-5 Selectivities of quantified products as a function of pyrolysis temperatures during acid-catalysed trehalose pyrolysis at 40-225 °C with an acid loading of 0.25mmol/g.

The selectivity of quantified other products in this study are calculated and presented in Figure 7-5. The glucose generated in both disaccharides' pyrolysis has high selectivity and presents a decreasing trend along with the increased pyrolysis temperatures. For example, the highest selectivity of glucose is ~17% at 40 ºC and ~27% at 80 ºC produced from acid-catalysed trehalose and acid-catalysed cellobiose respectively. In contrast, the dehydrated products (e.g., levoglucosan, mannosan, AGF) produced from the acid-catalysed cellobiose pyrolysis present an opposite trend with glucose, which are increased with the pyrolysis temperatures. For instance, levoglucosan is increased from ~1% at 80 ºC to ~3.2% at 225 ºC. It is worth noting that mutarotation is also a dominant reaction beside the dehydration in the acid-

catalysed pyrolysis process at high temperatures, demonstrated by the dehydrated isomers formed, including AGF, levoglucosan, and mannosan [226]. The acid enhances the mutarotation to form not only various disaccharides at low temperatures pyrolysis, but also the isomers of dehydrated sugars at high temperatures pyrolysis.

To understand the residues in the structure of produced solid residues, the post-hydrolysis was processed with solid samples produced from trehalose and cellobiose in the acid-catalysis pyrolysis. The results of post-hydrolysis and total selectivity in both disaccharides are present in Figure 7-6. Based on the results of total selectivity, the quantified disaccharides and glucose have a contribution of ~75% under the pyrolysis temperature of 40 ºC in acid-catalysed trehalose pyrolysis. Disaccharides and glucose are major primary products in the acid-catalysed pyrolysis, but there are still other products that cannot be quantified in the formed products. Therefore, the post-hydrolysis was conducted to identify the possible structures in the unquantified residues. ~98% glucose recovery is identified in the post-hydrolysis at the pyrolysis temperature 40 ºC, which demonstrates the unquantified residues still contain an intact D (+) glucose structure such as other low contributed disaccharides and dehydrated sugars. The high glucose recovery can still be reached at ~90% in the formed solid sample at 120 ºC, but the glucose recovery drops to ~65% at the pyrolysis temperature of 140 ºC. Then, only ~5% glucose can be recovered at the pyrolysis temperature of 150 ºC, indicating the decomposed products are formed from the acid-catalysed trehalose pyrolysis temperature of 140 ºC.

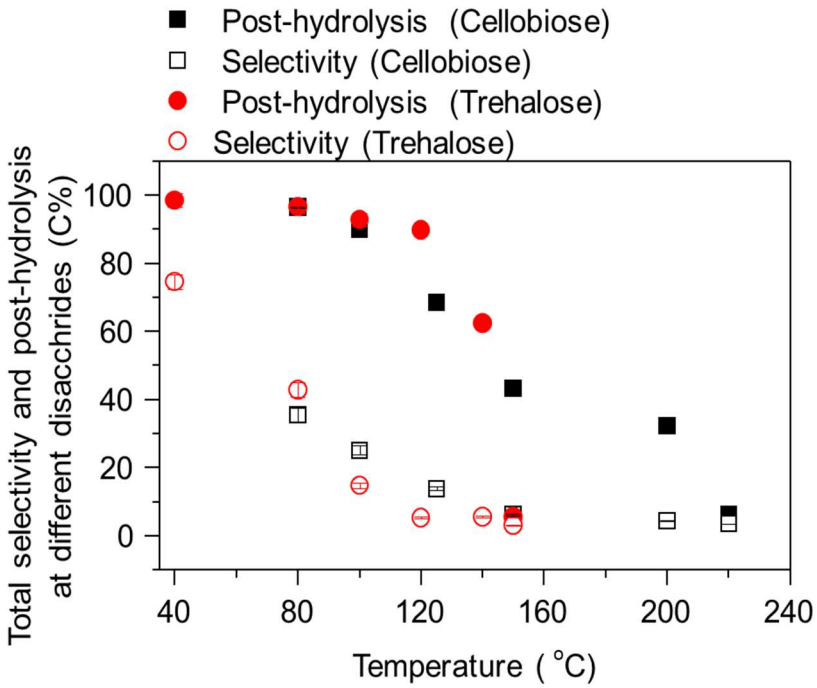

Figure 7-6 Total selectivity of quantified water-soluble products during acid-catalysed pyrolysis at 40-255 ºC.

The high recovery of glucose and low selectivity of disaccharides demonstrate that oligosaccharides are formed at the acid-catalysed trehalose pyrolysis (≥80ºC). The samples formed at various pyrolysis temperatures were analysed by GPC to measure the molecular weight range, and the results are presented in Figure 7-7. Initially, the oligomers with DP=2 are clearly shown at the pyrolysis temperature 40 ºC, which is consistent with the high selectivity (~75%) of disaccharides at 40 ºC. Once the pyrolysis temperature is increased from 40 to 140 ºC, the DP of oligosaccharide grows quickly, especially at temperature 125 ºC. For example, the maximal DP of oligomer is increased from DP ~ 4 at temperature 100 ºC (retention time 14.5 min) to DP ~10 at temperature 125 ºC (retention time 13.2 min), then the DP reaches the maximum identified DP ~ 15 at temperature 140 ºC (retention time 12.8 min) in this study. According to the results of GPC, it is evident that polymerisation is a major reaction during the acid-catalysed trehalose pyrolysis. However, the current analysis is insufficient to identify the structure of high-DP since the existing α or β linkages oligosaccharides can be easily generated under the acid condition based on the results of disaccharides containing various α or β linkages.

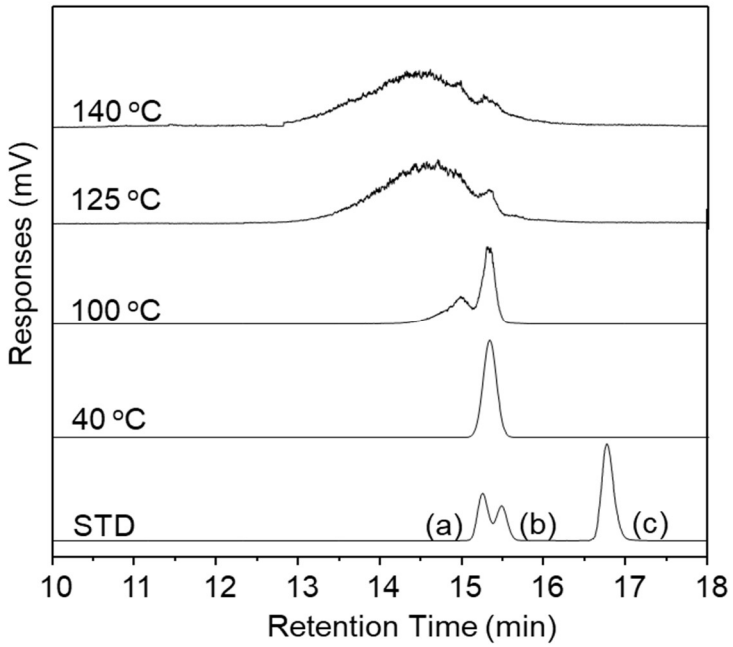

Figure 7-7 GPC analysis of water-soluble samples from acid-catalysed trehalose pyrolysis at 40 - 140 °C with an acid loading 0.25 mmol/g. (a) disaccharides, (b) glucose, (c) levoglucosan.

The results of acid-catalysed cellobiose pyrolysis, total selectivity, and post hydrolysis present a clear decreasing trend accompanied by an increased cellobiose conversion. The result of post hydrolysis, indicating the component of monosaccharide in solid residues, shows a decreased glucose recovery from ~96% to ~12% as the cellobiose conversion increases from ~ 6.5% to 93%. At the conversion of 6.5%, the main products in solid samples contain mono-saccharide structure, although the total selectivity of identified sugar products is only quantified as ~33% (disaccharides and glucose). Understandably, the low DP oligo-saccharides could be easily formed in acid-catalysed pyrolysis condition [206], but they cannot be present in this study because of the complicated structure and the limited sensitivity of HPLC-ELDS if the low concentration is present. Even at the cellobiose conversion of ~15%, the concentration of oligo-saccharides still cannot be detected in HPLC-ELDS, but the glucose recovery could reach ~92%. It could indicate that the oligomersation could be a slow reaction rate from 1,4-β-glycolic bond disaccharide by comparing this with the results from acid-catalysed trehalose pyrolysis. Therefore, 1,1-α-glycolic bond disaccharide is a structure that makes it easier to process polymerisation than 1,4-β-glycolic bond disaccharide because of the weakened glycolic bond during the acid catalysis pyrolysis.

When the pyrolysis temperature is raised (≥125 ºC), dehydration or decomposition reactions are the primary dominant reactions in both disaccharides' acid-pyrolysis. For instance, the glucose recovery from post-hydrolysis is ~68% at the cellobiose conversion of ~21% (125 ºC), because polymerisation reaction is suppressed due to the rapid loss of moisture which can assist in the formation of C1-carbocation as a reaction media [190]. The low glucose recovery in solid samples also proves the dehydration and decomposition gradually show as dominant reactions during the acid-catalysed cellobiose pyrolysis process.

7.3 Discussion on acid-catalysed pyrolysis mechanism of the two structures of disaccharides

This study aims to understand the acid-catalysed pyrolysis mechanism of different glycolic bonds in disaccharide by comparing the pyrolysis behaviors of trehalose (1,1-α-glycolic bond) and cellobiose (1,4-β-glycolic bond), which have been found in the pyrolysis of acid-catalysed glucose. The new insights of pyrolysis behaviors in two different structures of disaccharides have been proposed in Figure 7-8. In the comparison of the results from acid-catalysed trehalose and cellobiose pyrolysis, the apparent pyrolysis behaviors can be concluded as:

1. Cellobiose is more stable than trehalose under acid-catalysed pyrolysis at low temperatures in line with previous studies on the reversion reaction of glucose [189, 194], which is present as the identified lower conversion in cellobiose during the acid-catalysed pyrolysis under the same temperature profile. Moreover, the highest conversion of cellobiose occurs at the pyrolysis temperature 225 °C in comparison with trehalose which occurs at the pyrolysis temperature 120 °C.
2. Hydrolysis, polymerisation, and mutarotation are significant reactions at the acid-catalysed pyrolysis caused by the presence of moisture and acid at low temperature pyrolysis. Polymerisation and mutarotation are promoted by the formation of C1 carbocation and the oxonium ion on O-ring to convert the α and β-anomers. Acid-catalysed-Trehalose is prone to yield high DP (DP 15 at 140 °C) at current conditions, but high DP polymers are not major products in the acid-catalysed-cellobiose pyrolysis due to the factor that the 1,4-β-glycolic bond has a stable structure at low temperatures≤ 80 ºC. When the pyrolysis temperature is raised, the formed glucose tends to experience dehydration and mutarotation rather than polymerisation, which can be proved by the

increasing yield of dehydration products such as levoglucosan, mananosan, and AGF.

3. The formation of char at the high temperature could be contributed by two different routes in the various disaccharides. The char could be formed by the decomposed oligosaccharides formed by the unstable trehalose at high temperatures (≥140) indicated by the reduced glucose recovery (in Figure 7-6). However, cellobiose is more stable than trehalose, so the char could be formed by two routes in acid-catalysed cellobiose pyrolysis enclosing the decomposed oligo-saccharides, which has a lesser contribution, and the decomposed cellobiose via 5-HMF pathway implied by the gradual glucose loss along with the slowly increased cellobiose conversion (Figure *7-6*) during the acid-catalysed-catalysed pyrolysis process[186], which has a major contribution on the char formation .

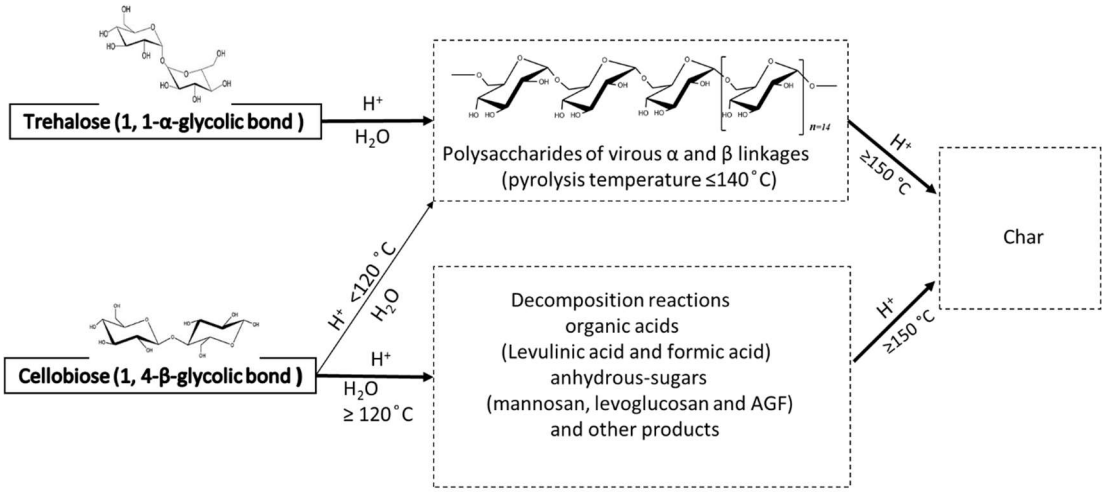

Figure 7-8 Proposed pyrolysis mechanism of acid-catalysed pyrolysis of disaccharides.

7.4 Conclusion

The acid-catalysed pyrolysis behaviors of trehalose and cellobiose were systemically investigated to understand the effect of glycolic bonds on the pyrolysis mechanism. The unstable 1,1-α-glycolic bond of trehalose mainly experiences polymerisation reaction to form oligosaccharides at low temperatures and the highest DP 15 is formed at 140 °C. Meanwhile, mutarotation has a high contribution to α and β isomers and complicated DP structures. Then, the oligosaccharides could be decomposed into char and volatiles during the high-temperature pyrolysis. Acid-catalysed cellobiose has a similar pyrolysis process (polymerisation and mutarotation) to form glucose,

disaccharides and low oligosaccharides at a low pyrolysis temperature <100 °C, though the main reactions are dehydration and decomposition which occur at high temperatures ≥ 150°C. Mutarotation results in different dehydration products, including levoglucosan, mannosan, and AGF. In conclusion, the above results show that polymerisation could be a major route in the formation of char at low temperatures (≤150 °C) pyrolysis process, especially when there exists an unstable of 1,1-α glycolic bond disaccharides. Conversely, the char formed at high temperatures could be contributed by the decomposition reaction pathway mainly occurring at high temperatures (≥150 °C), when the stable structure of 1,4-β-glycolic bond exists.

Chapter 8 Conclusions and Recommendations

This chapter concludes the main achievements of Chapters 3 to 7 in Section 8.1 to 8.4, respectively. Based on current achievements, recommendations for future studies are given in Section 8.5.

8.1 Acid-catalysed cellulose pyrolysis at low temperatures

- The pyrolysis of acid-impregnated cellulose was studied at 50 – 325 °C to provide an insight into the pyrolysis mechanism via water soluble intermediates analysis in HPAEC-PAD chromatogram. The analysis of water-soluble intermediates indicates the formation of glucose oligomers as reaction intermediates.
- Dehydration reactions played an important role in the acid-catalysed cellulose pyrolysis at the high temperatures pyrolysis, resulting in the yield of low molecular weight compounds from glucose decomposition. The high dehydration further suppressed the depolymerisation reactions leading to a low levoglucosan yield during the acid-catalysed pyrolysis of cellulose.
- Glucose was the dominant product rather than levoglucosan of the acid catalysis process under the low pyrolysis temperatures (< 100°C) in the presence of acid in the pyrolysis process. This study shows that the minimal temperature required for producing levoglucosan in the water-soluble intermediates is ~180 °C, suggesting that the presence of acid has little effect on the temperature for levoglucosan formation.
- The analysis of FTIR and NMR has identified the major structures of char formed in the acid-catalysed pyrolysis to be aromatic structures when the pyrolysis temperatures are higher than 300 °C.

8.2 Polymerisation of glucose during acid-catalysed pyrolysis at low temperatures

- Acid-catalysed glucose pyrolysis was identified and studied at low temperatures of 60-150 °C. Under the current studies, polymerisations were major reactions during the acid-catalysed pyrolysis which produce oligosaccharides of various linkage and degrees of polymerisation (DP) during the pyrolysis process.

- The various linkages of disaccharides were identified in HPAEC-PAD-MS which verify that mutarotation reactions play an important role in acid catalysed glucose pyrolysis. Moreover, the major linkages were composed of α and β including 1,6-, 1,4-, 1,3-, 1,2- and 1,1-glycodidic bond. 1,6-glycosidic bond (i.e., gentiobiose and isomaltose) are more favorably formed with high initial selectivities among the identified disaccharides. Meanwhile, a higher acid loading can produce more disaccharides as primary products.
- The α-linkages products were formed in the following order of decreasing quantity: 1,6-glycosidic bond > 1,4-glycosidic bond > 1,3-glycosidic bond > 1,2-glycosidic bond > 1,1-glycosidic bond. A high acid loading led to producing the 1,6-glycosidic bond disaccharides.
- The results of DP analysis in HPLC-ELDS show that the high pyrolysis temperatures can favorably form a high DP oligosaccharide such as the detected maximum DP ~ 4 at 60 °C to ~18 to 120 °C.

8.3 Acid-catalysed levoglucosan pyrolysis at low temperatures

- Levoglucosan, as a major intermediate, was investigated under acid-catalysed pyrolysis at 80-140 °C. Polymerisations played an important role in the acid-catalysed pyrolysis, and various linkage disaccharides and anhydro-disaccharides were qualified and quantified in this study.
- At the low temperatures, hydrolysis was found to be an important reaction and the α and β of disaccharides including 1,6-, 1,4-, 1,3-, 1,2- and 1,1-glycosidic bond were identified, signaling that the yield of glucose was rapidly polymerised at the presence of the acid pyrolysis process.
- Furthermore, the existing α and β structures proved that mutarotation reactions were important during the polymerisation process. the α and β linkages of anhydro-disaccharides of 1,4-, 1,3-, 1,2- glycosidic bond were identified and were major products based on the high selectivities in the products.
- The high acid loading was studied and compared with the low acid loading. Results show that the high acid loading can enhance the hydrolysis reactions to produce more glucose to catalyse the polymerisation reactions, but the producing disaccharides are suppressed. Those primary products are further polymerised into high-DP anhydro-sugar and sugar oligosaccharides (i.e., with

DP as high as ~10 at 120 °C) as levoglucosan conversion increase, and finally converted into char at increased temperatures.

8.4 Acid-catalysed disaccharide pyrolysis at low temperatures

- Two major disaccharides of cellobiose and trehalose has been investigated to understand the effect of glycolic bonds on the pyrolysis mechanism. Cellobiose is more stable than trehalose under acid-catalysed pyrolysis at low temperatures, in line with previous studies on the reversion reaction of glucose, which is present as the identified lower conversional cellobiose during the acid-catalysed pyrolysis under the same temperature profile. Moreover, the highest conversion of cellobiose occurs at 225 °C in comparison with trehalose which occurs at 120 °C.
- Polymerisation and mutarotation are significant reactions at the acid-catalysed disaccharides pyrolysis caused by the presence of moisture and acid. The highest DP 15 was formed during acid-catalysed trehalose pyrolysed at 140 °C, and the formed of structures of α and β-anomers were found in this study and.
- The formation of char could be achieved by two different routes in the studied disaccharides. The char could be formed by the decomposition of oligosaccharides formed by the unstable trehalose at high temperatures (≥140). However, cellobiose is more stable than trehalose, so the char is formed by two routes in acidic cellobiose pyrolysis enclosing the decomposed oligosaccharides and the decomposed cellobiose via 5-HMF pathway.

8.5 Further recommendations on acid-catalysed pyrolysis of biomass

Although the study has achieved all the objectives stated in Chapter 2, other gaps should be further explored. The following recommendations should be considered for further research activities.

- Firstly, the formation process from oligosaccharide to char was still not clearly identified in this study due to the current applied techniques. In-situ analysis methods such as FTIR, NMR, or Pyrolysis-Gas Chromatography-Mass spectrometry is recommended to clarify the char formation process. Meanwhile, the future works also can intensively study the secondary reaction if the pyrolysis time is extended and other product phases (gas, liquid and solid) are occurred.

- Secondly, oligosaccharides have a significant effect on the char formation process, but the complex structure is still not identified to prove what structure could contribute to forming the char during the acid-catalysis pyrolysis.
- Thirdly, levoglucosan and glucose were studied, and anhydro-oligosaccharides and oligosaccharides are the most numerous primary products. Disaccharides consisting of various glycolic bonds have high selectivities in the primary products. Therefore, it is necessary to study the pyrolysis behaviors of disaccharides which could have a significant effect on the final pyrolysis product selectivities.
- Fourthly, it is necessary to continue the acid-catalysis study on the model compounds of hemicellulose (which occupies 30% of the dry weight of biomass) which has a low decomposition temperature to form organic acids such as acetic acid[227, 228]. Decomposed products could influence the cellulose pyrolysis behaviours during the pyrolysis process.
- Last but not least, the fast pyrolysis of biomass which is composed of cellulose, hemicellulose and lignin, is more complexed than model compounds since the thermal stability are different and following with the order hemicellulose < cellulose < lignin during the fast pyrolysis. The products from other constituents should have heavily effects on the whole pyrolysis process. Therefore, it is worth to develop a systemic research plan on the acid-fused biomass pyrolysis to fully understand the biomass pyrolysis mechanism which can be beneficial to optimize the quality and quantity of the pyrolysis products.

References

1. Preston, B. L.; Jones, R. N., *Climate change impacts on Australia and the benefits of early action to reduce global greenhouse gas emissions*. Commonwealth Scientific and Industrial Research Organisation: Aspendale, Vic., 2005.
2. Haines, A., Climate Change 2001: The Scientific Basis. Contribution of Working Group 1 to the Third Assessment report of the Intergovernmental Panel on Climate Change.: JT Houghton, Y Ding, DJ Griggs, M Noguer, PJ van der Winden, X Dai. Cambridge: Cambridge University Press, 2001, pp. 881, £34.95 (HB) ISBN: 0-21-01495-6; £90.00 (HB) ISBN: 0-521-80767-0. *International Journal of Epidemiology* **2003,** 32, (2), 321-321.
3. World Wind Energy Association: Renewables 2018 Global Status Report: Now available! In New Delhi, 2018.
4. Czernik, S.; Bridgwater, A. V., Overview of Applications of Biomass Fast Pyrolysis Oil. *Energy & Fuels* **2004,** 18, (2), 590-598.
5. Bridgwater, A. V., Review of fast pyrolysis of biomass and product upgrading. *Biomass and Bioenergy* **2012,** 38, 68-94.
6. Fan, J.; Kalnes, T. N.; Alward, M.; Klinger, J.; Sadehvandi, A.; Shonnard, D. R., Life cycle assessment of electricity generation using fast pyrolysis bio-oil. *Renewable Energy* **2011,** 36, (2), 632-641.
7. Han, J.; Elgowainy, A.; Dunn, J. B.; Wang, M. Q., Life cycle analysis of fuel production from fast pyrolysis of biomass. *Bioresource Technology* **2013,** 133, 421-428.
8. Iribarren, D.; Peters, J. F.; Dufour, J., Life cycle assessment of transportation fuels from biomass pyrolysis. *Fuel* **2012,** 97, 812-821.
9. Roberts, K. G.; Gloy, B. A.; Joseph, S.; Scott, N. R.; Lehmann, J., Life Cycle Assessment of Biochar Systems: Estimating the Energetic, Economic, and Climate Change Potential. *Environmental Science & Technology* **2010,** 44, (2), 827-833.
10. Vienescu, D. N.; Wang, J.; Le Gresley, A.; Nixon, J. D., A life cycle assessment of options for producing synthetic fuel via pyrolysis. *Bioresource Technology* **2018,** 249, 626-634.
11. Yu, Y.; Wu, H., Bioslurry as a Fuel. 2. Life-Cycle Energy and Carbon Footprints of Bioslurry Fuels from Mallee Biomass in Western Australia. *Energy & Fuels* **2010,** 24, (10), 5660-5668.
12. Bertero, M.; de la Puente, G.; Sedran, U., Effect of Pyrolysis Temperature and Thermal Conditioning on the Coke-Forming Potential of Bio-oils. *Energy & Fuels* **2011,** 25, (3), 1267-1275.
13. Diebold, J., *A review of the chemical and physical mechanisms of the storage stability of fast pyrolysis bio-oils*. 2002; p 243-292.
14. Oasmaa, A.; Czernik, S., Fuel Oil Quality of Biomass Pyrolysis OilsState of the Art for the End Users. *Energy & Fuels* **1999,** 13, (4), 914-921.
15. Oasmaa, A.; Fonts, I.; Pelaez-Samaniego, M. R.; Garcia-Perez, M. E.; Garcia-Perez, M., Pyrolysis Oil Multiphase Behavior and Phase Stability: A Review. *Energy & Fuels* **2016,** 30, (8), 6179-6200.
16. Oasmaa, A.; Sipilä, K.; Solantausta, Y.; Kuoppala, E., Quality Improvement of Pyrolysis Liquid: Effect of Light Volatiles on the Stability of Pyrolysis Liquids. *Energy & Fuels* **2005,** 19, (6), 2556-2561.
17. Collard, F.-X.; Blin, J.; Bensakhria, A.; Valette, J., Influence of impregnated metal on the pyrolysis conversion of biomass constituents. *Journal of Analytical and Applied Pyrolysis* **2012,** 95, 213-226.

18. Eom, I.-Y.; Kim, J.-Y.; Kim, T.-S.; Lee, S.-M.; Choi, D.; Choi, I.-G.; Choi, J.-W., Effect of essential inorganic metals on primary thermal degradation of lignocellulosic biomass. *Bioresource Technology* **2012,** 104, 687-694.
19. Haddad, K.; Jeguirim, M.; Jellali, S.; Guizani, C.; Delmotte, L.; Bennici, S.; Limousy, L., Combined NMR structural characterization and thermogravimetric analyses for the assessment of the AAEM effect during lignocellulosic biomass pyrolysis. *Energy (Oxford, U. K.)* **2017,** 134, 10-23.
20. Liu, D.; Yu, Y.; Hayashi, J.-i.; Moghtaderi, B.; Wu, H., Contribution of dehydration and depolymerization reactions during the fast pyrolysis of various salt-loaded celluloses at low temperatures. *Fuel* **2014,** 136, 62-68.
21. Liu, D.; Yu, Y.; Long, Y.; Wu, H., Effect of MgCl2 loading on the evolution of reaction intermediates during cellulose fast pyrolysis at 325°C. *Proceedings of the Combustion Institute* **2015,** 35, (2), 2381-2388.
22. Mourant, D.; Wang, Z.; He, M.; Wang, X. S.; Garcia-Perez, M.; Ling, K.; Li, C.-Z., Mallee wood fast pyrolysis: effects of alkali and alkaline earth metallic species on the yield and composition of bio-oil. *Fuel* **2011,** 90, (9), 2915-2922.
23. Yu, Y.; Liu, D.; Wu, H., Formation and Characteristics of Reaction Intermediates from the Fast Pyrolysis of NaCl- and MgCl2-Loaded Celluloses. *Energy & Fuels* **2014,** 28, (1), 245-253.
24. Zhu, C.; Paulsen, A.; Dauenhauer, P. In *Natural inorganic catalysts in eellulose pyrolysis*, 2015; American Chemical Society: 2015; pp CATL-276.
25. Julien, S.; Chornet, E.; Overend, R. P., Influence of acid pretreatment (H2SO4, HCl, HNO3) on reaction selectivity in the vacuum pyrolysis of cellulose. *Journal of Analytical and Applied Pyrolysis* **1993,** 27, (1), 25-43.
26. Kuzhiyil, N.; Dalluge, D.; Bai, X.; Kim, K. H.; Brown, R. C., Pyrolytic Sugars from Cellulosic Biomass. *ChemSusChem* **2012,** 5, (11), 2228-2236.
27. Shafizadeh, F.; Stevenson, T. T., Saccharification of douglas-fir wood by a combination of prehydrolysis and pyrolysis. *Journal of Applied Polymer Science* **1982,** 27, (12), 4577-4585.
28. Wang, Z.; Zhou, S.; Pecha, B.; Westerhof, R. J. M.; Garcia-Perez, M., Effect of Pyrolysis Temperature and Sulfuric Acid During the Fast Pyrolysis of Cellulose and Douglas Fir in an Atmospheric Pressure Wire Mesh Reactor. *Energy & Fuels* **2014,** 28, (8), 5167-5177.
29. Zhou, S.; Mourant, D.; Lievens, C.; Wang, Y.; Li, C.-Z.; Garcia-Perez, M., Effect of sulfuric acid concentration on the yield and properties of the bio-oils obtained from the auger and fast pyrolysis of Douglas Fir. *Fuel* **2013,** 104, 536-546.
30. Dobele, G.; Rossinskaja, G.; Telysheva, G.; Meier, D.; Faix, O., Cellulose dehydration and depolymerization reactions during pyrolysis in the presence of phosphoric acid. *Journal of Analytical and Applied Pyrolysis* **1999,** 49, (1), 307-317.
31. Tan, H.; Wang, S.-r., Experimental study of the effect of acid-washing pretreatment on biomass pyrolysis. *Journal of Fuel Chemistry and Technology* **2009,** 37, (6), 668-672.
32. Wang, S.; Liao, Y.; Liu, Q.; Luo, Z.; Cen, K., Experimental study of the influence of acid wash on cellulose pyrolysis. *Frontiers of Chemical Engineering in China* **2007,** 1, (1), 35-39.
33. Schultes, R. E., Handbook of Charcoal Making: The Traditional and Industrial Methods (Book Review). In 1986; Vol. 40, pp 395-395.
34. Bridgwater, A. V.; Meier, D.; Radlein, D., An overview of fast pyrolysis of biomass. *Organic Geochemistry* **1999,** 30, (12), 1479-1493.

35. Fan, L.; Zhang, Y.; Liu, S.; Zhou, N.; Chen, P.; Cheng, Y.; Addy, M.; Lu, Q.; Omar, M. M.; Liu, Y.; Wang, Y.; Dai, L.; Anderson, E.; Peng, P.; Lei, H.; Ruan, R., Bio-oil from fast pyrolysis of lignin: Effects of process and upgrading parameters. *Bioresource Technology* **2017,** 241, 1118-1126.
36. Shen, J.; Wang, X.-S.; Garcia-Perez, M.; Mourant, D.; Rhodes, M. J.; Li, C.-Z., Effects of particle size on the fast pyrolysis of oil mallee woody biomass. *Fuel* **2009,** 88, (10), 1810-1817.
37. Wang, B.; Xu, F.; Zong, P.; Zhang, J.; Tian, Y.; Qiao, Y., Effects of heating rate on fast pyrolysis behavior and product distribution of Jerusalem artichoke stalk by using TG-FTIR and Py-GC/MS. *Renewable Energy* **2019,** 132, 486-496.
38. Zhou, S.; Garcia-Perez, M.; Pecha, B.; Kersten, S. R. A.; McDonald, A. G.; Westerhof, R. J. M., Effect of the Fast Pyrolysis Temperature on the Primary and Secondary Products of Lignin. *Energy & Fuels* **2013,** 27, (10), 5867-5877.
39. ORGANIZATION, F. A. A., Global Forest Resources Assessment 2010. *Global Forest Resources Assessment* **2010**.
40. Pan, Y.; Birdsey, R. A.; Phillips, O. L.; Jackson, R. B., The Structure, Distribution, and Biomass of the World's Forests. *Annual Review of Ecology, Evolution, and Systematics* **2013,** 44, (1), 593-622.
41. Lauri, P.; Havlík, P.; Kindermann, G.; Forsell, N.; Böttcher, H.; Obersteiner, M., Woody biomass energy potential in 2050. *Energy Policy* **2014,** 66, 19-31.
42. Wang, S. a., *Pyrolysis of biomass / Shurong Wang, Zhongyang Luo*. Berlin : De Gruyter: 2017.
43. Heredia, A.; Jiménez, A.; Guillén, R., Composition of plant cell walls. *Zeitschrift für Lebensmittel-Untersuchung und Forschung* **1995,** 200, (1), 24-31.
44. Rytioja, J.; Hildén, K.; Yuzon, J.; Hatakka, A.; Vries, R. P.; Mäkelä, M., *Plant-Polysaccharide-Degrading Enzymes from Basidiomycetes*. 2014; Vol. 78, p 614-649.
45. Sjoestroem, *Wood Chemistry. Fundamentals and Applications*. 1993.
46. Kolpak, F. J.; Blackwell, J., Determination of the Structure of Cellulose II. *Macromolecules* **1976,** 9, (2), 273-278.
47. van Lith, S. C.; Alonso-Ramírez, V.; Jensen, P. A.; Frandsen, F. J.; Glarborg, P., Release to the Gas Phase of Inorganic Elements during Wood Combustion. Part 1: Development and Evaluation of Quantification Methods. *Energy & Fuels* **2006,** 20, (3), 964-978.
48. Liaw, S. B.; Wu, H., Leaching Characteristics of Organic and Inorganic Matter from Biomass by Water: Differences between Batch and Semi-continuous Operations. *Industrial & Engineering Chemistry Research* **2013,** 52, (11), 4280-4289.
49. Franceschi, V. R.; Horner, H. T., Calcium oxalate crystals in plants. *The Botanical Review* **1980,** 46, (4), 361-427.
50. Wu, H.; Yip, K.; Kong, Z.; Li, C.-Z.; Liu, D.; Yu, Y.; Gao, X., Removal and Recycling of Inherent Inorganic Nutrient Species in Mallee Biomass and Derived Biochars by Water Leaching. *Industrial & Engineering Chemistry Research* **2011,** 50, (21), 12143-12151.
51. Shen, D.; Xiao, R.; Gu, S.; Zhang, H., The overview of thermal decomposition of cellulose in lignocellulosic biomass. In *Cellulose-Biomass Conversion*, IntechOpen: 2013.
52. Lee, J. H.; Brown, R. M.; Kuga, S.; Shoda, S.; Kobayashi, S., Assembly of synthetic cellulose I. *Proceedings of the National Academy of Sciences* **1994,** 91, (16), 7425-7429.
53. Xi, J.; Du, W.; Zhong, L., *Probing the Interaction Between Cellulose and Cellulase with a Nanomechanical Sensor*. 2013.

54. Liu, D.; Yu, Y.; Wu, H., Evolution of Water-Soluble and Water-Insoluble Portions in the Solid Products from Fast Pyrolysis of Amorphous Cellulose. *Industrial & Engineering Chemistry Research* **2013,** 52, (36), 12785-12793.
55. Ciolacu, D.; Popa, V. I., The correlation between the reactivity and the supramolecular structure of allomorphs of cellulose. *Rev Roum Chim* **2007,** 52, (4), 361-366.
56. Ciolacu, D.; Popa, V. I., On the thermal degradation of cellulose allomorphs. *Cellulose chemistry and technology* **2006,** 40, (6), 445.
57. Ciolacu, D.; Popa, V., *Structural changes of cellulose determined by dissolution in aqueous alkali solution*. 2005; Vol. 39, p 179-188.
58. Ciolacu, D.; Popa, V. I., *Cellulose allomorphs: Structure, accessibility and reactivity*. 2013; p 1-69.
59. Kontturi, E.; Tammelin, T.; Österberg, M., Cellulose—model films and the fundamental approach. *Chemical Society Reviews* **2006,** 35, (12), 1287-1304.
60. PÉrez, S.; Samain, D., Structure and Engineering of Celluloses. In *Advances in Carbohydrate Chemistry and Biochemistry*, Horton, D., Ed. Academic Press: 2010; Vol. 64, pp 25-116.
61. Sarko, A.; Southwick, J.; Hayashi, J., Packing Analysis of Carbohydrates and Polysaccharides. 7. Crystal Structure of Cellulose IIII and Its Relationship to Other Cellulose Polymorphs. *Macromolecules* **1976,** 9, (5), 857-863.
62. Weimer, P. J.; French, A. D.; Calamari, T. A., Differential Fermentation of Cellulose Allomorphs by Ruminal Cellulolytic Bacteria. *Applied and Environmental Microbiology* **1991,** 57, (11), 3101-3106.
63. Sjostrom, E., *Wood chemistry : fundamentals and applications / Eero Sjostrom*. New York : Academic Press: New York, 1981.
64. van den Brink, J.; de Vries, R. P., Fungal enzyme sets for plant polysaccharide degradation. *Applied Microbiology and Biotechnology* **2011,** 91, (6), 1477.
65. Harris, P. J. a. S., B. A., Chemistry and Molecular Organization of Plant Cell Walls. In *Biomass Recalcitrance*, Blackwell Publishing Ltd, : Oxford, United Kingdom., 2009; pp 61-93.
66. Holtzapple, M. T., HEMICELLULOSES. In *Encyclopedia of Food Sciences and Nutrition (Second Edition)*, Caballero, B., Ed. Academic Press: Oxford, 2003; pp 3060-3071.
67. Alen, R., *Structure and Chemical Composition of Wood*. 2000.
68. Novaes, E.; Kirst, M.; Chiang, V.; Winter-Sederoff, H.; Sederoff, R., Lignin and Biomass: A Negative Correlation for Wood Formation and Lignin Content in Trees. *Plant Physiology* **2010,** 154, (2), 555-561.
69. Boerjan, W.; Ralph, J.; Baucher, M., Lignin biosynthesis. *Annual review of plant biology* **2003,** 54, (1), 519-546.
70. Carder, A., Forest giants of the world, past and present. **1994**.
71. Haghdan, S.; Renneckar, S.; Smith, G. D., 1 - Sources of Lignin. In *Lignin in Polymer Composites*, Faruk, O.; Sain, M., Eds. William Andrew Publishing: 2016; pp 1-11.
72. Butler, E.; Devlin, G.; Meier, D.; McDonnell, K., Characterisation of spruce, salix, miscanthus and wheat straw for pyrolysis applications. *Bioresource Technology* **2013,** 131, 202-209.
73. Möller, R.; Toonen, M.; Beilen, J.; Salentijn, E.; Clayton, D., Crop platforms for cell wall biorefining: lignocellulose feedstocks. **2007**.

74. Sannigrahi, P.; Ragauskas, A. J.; Tuskan, G. A., Poplar as a feedstock for biofuels: A review of compositional characteristics. *Biofuels, Bioproducts and Biorefining* **2010,** 4, (2), 209-226.
75. Emrich, W., *Handbook of Charcoal Making: the Traditional and Industrial Methods*. 1985.
76. Garcia-Nunez, J. A.; Pelaez-Samaniego, M. R.; Garcia-Perez, M. E.; Fonts, I.; Abrego, J.; Westerhof, R. J. M.; Garcia-Perez, M., Historical Developments of Pyrolysis Reactors: A Review. *Energy and Fuels* **2017,** 31, (6), 5751-5775.
77. Chiaramonti, D.; Oasmaa, A.; Solantausta, Y., Power generation using fast pyrolysis liquids from biomass. *Renewable and sustainable energy reviews* **2007,** 11, (6), 1056-1086.
78. Balat, M.; Balat, M.; Kırtay, E.; Balat, H., Main routes for the thermo-conversion of biomass into fuels and chemicals. Part 1: Pyrolysis systems. *Energy Conversion and Management* **2009,** 50, (12), 3147-3157.
79. Balat, M., An Overview of the Properties and Applications of Biomass Pyrolysis Oils. *Energy Sources, Part A: Recovery, Utilization, and Environmental Effects* **2011,** 33, (7), 674-689.
80. Qambrani, N. A.; Rahman, M. M.; Won, S.; Shim, S.; Ra, C., Biochar properties and eco-friendly applications for climate change mitigation, waste management, and wastewater treatment: A review. *Renewable and Sustainable Energy Reviews* **2017,** 79, 255-273.
81. Li, S.; Harris, S.; Anandhi, A.; Chen, G., Predicting biochar properties and functions based on feedstock and pyrolysis temperature: A review and data syntheses. *Journal of Cleaner Production* **2019,** 215, 890-902.
82. Sohi, S. P.; Krull, E.; Lopez-Capel, E.; Bol, R., Chapter 2 - A Review of Biochar and Its Use and Function in Soil. In *Advances in Agronomy*, Academic Press: 2010; Vol. 105, pp 47-82.
83. Ji, C.; Cheng, K.; Nayak, D.; Pan, G., Environmental and economic assessment of crop residue competitive utilization for biochar, briquette fuel and combined heat and power generation. *Journal of Cleaner Production* **2018,** 192, 916-923.
84. Shafizadeh, F.; Fu, Y. L., Pyrolysis of cellulose. *Carbohydrate Research* **1973,** 29, (1), 113-122.
85. Molton, P. M.; Demmitt, T. F., *Reaction mechanisms in cellulose pyrolysis: a literature review*. 1978.
86. Zhang, X.; Yang, W.; Dong, C., Levoglucosan formation mechanisms during cellulose pyrolysis. *Journal of Analytical and Applied Pyrolysis* **2013,** 104, 19-27.
87. Lipska, A. E.; Parker, W. J., Kinetics of the pyrolysis of cellulose in the temperature range 250–300°C. *Journal of Applied Polymer Science* **1966,** 10, (10), 1439-1453.
88. Chatterjee, P. K., Chain reaction mechanism of cellulose pyrolysis. *Journal of Applied Polymer Science* **1968,** 12, (8), 1859-1864.
89. Scheirs, J.; Camino, G.; Tumiatti, W., Overview of water evolution during the thermal degradation of cellulose. *European Polymer Journal* **2001,** 37, (5), 933-942.
90. Shafizadeh, F.; Lai, Y. Z., Thermal degradation of 1,6-anhydro-.beta.-D-glucopyranose. *The Journal of Organic Chemistry* **1972,** 37, (2), 278-284.
91. Chaiwat, W.; Hasegawa, I.; Tani, T.; Sunagawa, K.; Mae, K., Analysis of Cross-Linking Behavior during Pyrolysis of Cellulose for Elucidating Reaction Pathway. *Energy Fuels* **2009,** 23, (12), 5765-5772.
92. Kato, K. L.; Cameron, R. E., A review of the relationship between thermally-accelerated ageing of paper and hornification. *Cellulose* **1999,** 6, (1), 23-40.

93. Lin, Y.; Cho, J.; Tompsett, G.; Westmoreland, P.; Huber, G., Kinetics and Mechanism of Cellulose Pyrolysis. *J. Phys. Chem. C* **2009,** 113, (46), 20097-20107.
94. Abella, L.; Yamamoto, K.; Fukuda, K.; Nanbu, S.; Oikawa, N.; Morita, K.; Matsumoto, T., Ab initio calculations for the reaction paths of levoglucosan: An intermediate of cellulose pyrolysis. *Memoirs of the Faculty of Engineering, Kyushu University* **2006,** 66, (2), 147-168.
95. Liu, C.; Huang, J.; Huang, X.; Li, H.; Zhang, Z., Theoretical studies on formation mechanisms of CO and CO2 in cellulose pyrolysis. *Computational and Theoretical Chemistry* **2011,** 964, (1-3), 207-212.
96. Shafizadeh, F.; Bradbury, A. G. W., Thermal degradation of cellulose in air and nitrogen at low temperatures. *Journal of Applied Polymer Science* **1979,** 23, (5), 1431-1442.
97. Dawes, G. J. S.; Scott, E. L.; Le Nôtre, J.; Sanders, J. P. M.; Bitter, J. H., Deoxygenation of biobased molecules by decarboxylation and decarbonylation – a review on the role of heterogeneous, homogeneous and bio-catalysis. *Green Chemistry* **2015,** 17, (6), 3231-3250.
98. Piskorz, J.; Radlein, D.; Scott, D. S., On the mechanism of the rapid pyrolysis of cellulose. *Journal of Analytical and Applied Pyrolysis* **1986,** 9, (2), 121-137.
99. Shen, D. K.; Gu, S., The mechanism for thermal decomposition of cellulose and its main products. *Bioresource Technology* **2009,** 100, (24), 6496-6504.
100. Kilzer, F. J.; Broido, A., Speculations on the nature of cellulose pyrolysis. *Pyrodynamics. 2: 151-163* **1965,** 2, 151-163.
101. Agrawal, R. K., Kinetics of reactions involved in pvrolvsis of cellulose II. The modified kilzer ‐ bioid model. *Canadian Journal of Chemical Engineering* **1988,** 66, (3), 413-418.
102. Broido, A.; Nelson, M. A., Char yield on pyrolysis of cellulose. *Combustion and Flame* **1975,** 24, (C), 263-268.
103. Bradbury, A. G. W.; Sakai, Y.; Shafizadeh, F., A kinetic model for pyrolysis of cellulose. *Journal of Applied Polymer Science* **1979,** 23, (11), 3271-3280.
104. Várhegyi, G.; Szabó, P.; Mok, W. S.-L.; Antal, M. J., Kinetics of the thermal decomposition of cellulose in sealed vessels at elevated pressures. Effects of the presence of water on the reaction mechanism. *Journal of Analytical and Applied Pyrolysis* **1993,** 26, (3), 159-174.
105. Lédé, J.; Blanchard, F.; Boutin, O., Radiant flash pyrolysis of cellulose pellets: products and mechanisms involved in transient and steady state conditions. *Fuel* **2002,** 81, (10), 1269-1279.
106. Wooten, J. B.; Seeman, J. I.; Hajaligol, M. R., Observation and Characterization of Cellulose Pyrolysis Intermediates by 13C CPMAS NMR. A New Mechanistic Model. *Energy & Fuels* **2004,** 18, (1), 1-15.
107. Yu, Y.; Liu, D.; Wu, H., Characterization of Water-Soluble Intermediates from Slow Pyrolysis of Cellulose at Low Temperatures. **2012**.
108. Diebold, J. P., A unified, global model for the pyrolysis of cellulose. *Biomass and Bioenergy* **1994,** 7, (1-6), 75-85.
109. Hosoya, T.; Kawamoto, H.; Saka, S., Pyrolysis behaviors of wood and its constituent polymers at gasification temperature. *Journal of Analytical and Applied Pyrolysis* **2007,** 78, (2), 328-336.
110. Mamleev, V.; Bourbigot, S.; Le Bras, M.; Yvon, J., The facts and hypotheses relating to the phenomenological model of cellulose pyrolysis: Interdependence of the steps. *Journal of Analytical and Applied Pyrolysis* **2009,** 84, (1), 1-17.

111.Basch, A.; Lewin, M., The influence of fine structure on the pyrolysis of cellulose. I. Vacuum pyrolysis. *Journal of Polymer Science: Polymer Chemistry Edition* **1973,** 11, (12), 3071-3093.
112.Liu, D.; Yu, Y.; Wu, H., *Differences in Water-Soluble Intermediates from Slow Pyrolysis of Amorphous and Crystalline Cellulose*. 2013; Vol. 27, p 1371–1380.
113.Wang, Z.; McDonald, A. G.; Westerhof, R. J. M.; Kersten, S. R. A.; Cuba-Torres, C. M.; Ha, S.; Pecha, B.; Garcia-Perez, M., Effect of cellulose crystallinity on the formation of a liquid intermediate and on product distribution during pyrolysis. *Journal of Analytical and Applied Pyrolysis* **2013,** 100, 56-66.
114.Ateş, F.; Pütün, E.; Pütün, A. E., Fast pyrolysis of sesame stalk: yields and structural analysis of bio-oil. *Journal of Analytical and Applied Pyrolysis* **2004,** 71, (2), 779-790.
115.Onay, Ö.; Beis, S. H.; Koçkar, Ö. M., Fast pyrolysis of rape seed in a well-swept fixed-bed reactor. *Journal of Analytical and Applied Pyrolysis* **2001,** 58-59, 995-1007.
116.Pütün, A. E.; Önal, E.; Uzun, B. B.; Özbay, N., Comparison between the "slow" and "fast" pyrolysis of tobacco residue. *Industrial Crops and Products* **2007,** 26, (3), 307-314.
117.Tsai, W. T.; Lee, M. K.; Chang, Y. M., Fast pyrolysis of rice husk: Product yields and compositions. *Bioresource Technology* **2007,** 98, (1), 22-28.
118.Şensöz, S.; Demiral, İ.; Ferdi Gerçel, H., Olive bagasse (Olea europea L.) pyrolysis. *Bioresource Technology* **2006,** 97, (3), 429-436.
119.Ben Hassen-Trabelsi, A.; Kraiem, T.; Naoui, S.; Belayouni, H., Pyrolysis of waste animal fats in a fixed-bed reactor: Production and characterization of bio-oil and bio-char. *Waste Management* **2014,** 34, (1), 210-218.
120.Julien, S.; Chornet, E.; Tiwari, P. K.; Overend, R. P., Vacuum pyrolysis of cellulose: Fourier transform infrared characterization of solid residues, product distribution and correlations. *Journal of Analytical and Applied Pyrolysis* **1991,** 19, (C), 81-104.
121.Angın, D., Effect of pyrolysis temperature and heating rate on biochar obtained from pyrolysis of safflower seed press cake. *Bioresource Technology* **2013,** 128, 593-597.
122.Garg, R.; Anand, N.; Kumar, D., Pyrolysis of babool seeds (Acacia nilotica) in a fixed bed reactor and bio-oil characterization. *Renewable Energy* **2016,** 96, 167-171.
123.Paenpong, C.; Pattiya, A., Effect of pyrolysis and moving-bed granular filter temperatures on the yield and properties of bio-oil from fast pyrolysis of biomass. *Journal of Analytical and Applied Pyrolysis* **2016,** 119, 40-51.
124.Pütün, A. E.; Apaydın, E.; Pütün, E., Rice straw as a bio-oil source via pyrolysis and steam pyrolysis. *Energy* **2004,** 29, (12), 2171-2180.
125.Alvarez, J.; Lopez, G.; Amutio, M.; Bilbao, J.; Olazar, M., Bio-oil production from rice husk fast pyrolysis in a conical spouted bed reactor. *Fuel* **2014,** 128, 162-169.
126.Abdullah, N.; Gerhauser, H., Bio-oil derived from empty fruit bunches. *Fuel* **2008,** 87, (12), 2606-2613.
127.Islam, M. R.; Parveen, M.; Haniu, H., Properties of sugarcane waste-derived bio-oils obtained by fixed-bed fire-tube heating pyrolysis. *Bioresource Technology* **2010,** 101, (11), 4162-4168.
128.Volli, V.; Singh, R. K., Production of bio-oil from de-oiled cakes by thermal pyrolysis. *Fuel* **2012,** 96, 579-585.
129.Jung, S.-H.; Kang, B.-S.; Kim, J.-S., Production of bio-oil from rice straw and bamboo sawdust under various reaction conditions in a fast pyrolysis plant equipped

with a fluidized bed and a char separation system. *Journal of Analytical and Applied Pyrolysis* **2008,** 82, (2), 240-247.
130.Isahak, W. N. R. W.; Hisham, M. W. M.; Yarmo, M. A.; Yun Hin, T.-y., A review on bio-oil production from biomass by using pyrolysis method. *Renewable and Sustainable Energy Reviews* **2012,** 16, (8), 5910-5923.
131.Huang, X.; Cao, J.-P.; Shi, P.; Zhao, X.-Y.; Feng, X.-B.; Zhao, Y.-P.; Fan, X.; Wei, X.-Y.; Takarada, T., Influences of pyrolysis conditions in the production and chemical composition of the bio-oils from fast pyrolysis of sewage sludge. *Journal of Analytical and Applied Pyrolysis* **2014,** 110, 353-362.
132.Ly, H. V.; Kim, S.-S.; Woo, H. C.; Choi, J. H.; Suh, D. J.; Kim, J., Fast pyrolysis of macroalga Saccharina japonica in a bubbling fluidized-bed reactor for bio-oil production. *Energy* **2015,** 93, 1436-1446.
133.Patwardhan, P. R.; Satrio, J. A.; Brown, R. C.; Shanks, B. H., Influence of inorganic salts on the primary pyrolysis products of cellulose. *Bioresource Technology* **2010,** 101, (12), 4646-4655.
134.Müller-Hagedorn, M.; Bockhorn, H.; Krebs, L.; Müller, U., A comparative kinetic study on the pyrolysis of three different wood species. *Journal of Analytical and Applied Pyrolysis* **2003,** 68-69, 231-249.
135.Shimada, N.; Kawamoto, H.; Saka, S., Different action of alkali/alkaline earth metal chlorides on cellulose pyrolysis. *Journal of Analytical and Applied Pyrolysis* **2008,** 81, (1), 80-87.
136.Varhegyi, G.; Antal Jr, M. J.; Szekely, T.; Till, F.; Jakab, E., Simultaneous thermogravimetric-mass spectrometric studies of the thermal decomposition of biopolymers. 1. Avicel cellulose in the presence and absence of catalysts. *Energy & fuels* **1988,** 2, (3), 267-272.
137.Khelfa, A.; Finqueneisel, G.; Auber, M.; Weber, J. V., Influence of some minerals on the cellulose thermal degradation mechanisms. *Journal of Thermal Analysis and Calorimetry* **2008,** 92, (3), 795-799.
138.Shafizadeh, F.; Stevenson, T. T., Saccharification of douglas‐fir wood by a combination of prehydrolysis and pyrolysis. *Journal of Applied Polymer Science* **1982,** 27, (12), 4577-4585.
139.Liou, T.-H.; Chang, F.-W.; Lo, J.-J., Pyrolysis kinetics of acid-leached rice husk. *Industrial & engineering chemistry research* **1997,** 36, (3), 568-573.
140.Oudenhoven, S.; Westerhof, R. J. M.; Kersten, S. R., Fast pyrolysis of organic acid leached wood, straw, hay and bagasse: Improved oil and sugar yields. *Journal of analytical and applied pyrolysis* **2015,** 116, 253-262.
141.Zhou, S.; Wang, Z.; Liaw, S. S.; Li, C. Z.; Garcia-Perez, M., Effect of sulfuric acid on the pyrolysis of Douglas fir and hybrid poplar wood: Py-GC/MS and TG studies. *Journal of Analytical and Applied Pyrolysis* **2013,** 104, 117-130.
142.Brown, R. C.; Radlein, D.; Piskorz, J., Pretreatment processes to increase pyrolytic yield of levoglucosan from herbaceous feedstocks. In *ACS Symposium Series*, 2001; Vol. 784, pp 123-132.
143.Stals, M.; Thijssen, E.; Vangronsveld, J.; Carleer, R.; Schreurs, S.; Yperman, J., Flash pyrolysis of heavy metal contaminated biomass from phytoremediation: influence of temperature, entrained flow and wood/leaves blended pyrolysis on the behaviour of heavy metals. *Journal of Analytical and Applied Pyrolysis* **2010,** 87, (1), 1-7.
144.Sun, L.; Qiu, K., Vacuum pyrolysis and hydrometallurgical process for the recovery of valuable metals from spent lithium-ion batteries. *Journal of hazardous materials* **2011,** 194, 378-384.

145.Dalluge, D. L.; Daugaard, T.; Johnston, P.; Kuzhiyil, N.; Wright, M. M.; Brown, R. C., Continuous production of sugars from pyrolysis of acid-infused lignocellulosic biomass. *Green Chemistry* **2014,** 16, (9), 4144-4155.
146.Broido, A.; Evett, M.; Hodges, C. C., Yield of 1,6-anhydro-3,4-dideoxy-β-d-glycero-hex-3-enopyranos-2-ulose (levoglucosenone) on the acid-catalyzed pyrolysis of cellulose and 1,6-anhydro-β-d-glucopyranose (levoglucosan). *Carbohydrate Research* **1975,** 44, (2), 267-274.
147.Wang, Z.; Zhou, S.; Pecha, B.; Westerhof, R. J. M.; Garcia-Perez, M., Effect of pyrolysis temperature and sulfuric acid during the fast pyrolysis of cellulose and douglas fir in an atmospheric pressure wire mesh reactor. *Energy and Fuels* **2014,** 28, (8), 5167-5177.
148.Fan, Y.; Zhang, D.; Zheng, A.; Zhao, Z.; Li, H.; Yang, T., Selective production of anhydrosugars and furfural from fast pyrolysis of corncobs using sulfuric acid as an inhibitor and catalyst. *Chemical Engineering Journal* **2019,** 358, 743-751.
149.Pecha, B.; Arauzo, P.; Garcia-Perez, M., Impact of combined acid washing and acid impregnation on the pyrolysis of Douglas fir wood. *Journal of Analytical and Applied Pyrolysis* **2015,** 114, 127-137.
150.Shafizadeh, F.; Furneaux, R. H.; Stevenson, T. T.; Cochran, T. G., Acid-catalyzed pyrolytic synthesis and decomposition of 1,4:3,6-dianhydro-α-d-glucopyranose. *Carbohydrate Research* **1978,** 61, (1), 519-528.
151.Sluiter, A.; Hames, B.; Ruiz, R.; Scarlata, C.; Sluiter, J.; Templeton, D.; Crocker, D., *Determination of structural carbohydrates and lignin in biomass, in: Laboratory Analytical Procedure (LAP)*. 2008.
152.Yu, Y.; Song, B.; Long, Y.; Wu, H., Mass Spectrometry Analysis of Sugar and Anhydrosugar Oligomers from Biomass Thermochemical Processing. *Energy & Fuels* **2016,** 30, (10), 8787-8789.
153.Liaw, S. B.; Yu, Y.; Wu, H., Association of inorganic species release with sugar recovery during wood hydrothermal processing. *Fuel* **2016,** 166, 581-584.
154.Mohan, D.; Pittman Jr., C. U.; Steele, P. H., Pyrolysis of Wood/Biomass for Bio-oil: A Critical Review. *Energy Fuels* **2006,** 20, 848-889.
155.Várhegyi, G.; Chen, H.; Godoy, S., Thermal Decomposition of Wheat, Oat, Barley, and Brassica carinata Straws. A Kinetic Study. *Energy & Fuels* **2009,** 23, (2), 646-652.
156.Bridgwater, A. V.; Meier, D.; Radlein, D., An overview of fast pyrolysis of biomass. *Org. Geochem.* **1999,** 30, 1479-1493.
157.Golova, O. P., Chemical Effects of Heat on Cellulose. *Russian Chem. Rev.* **1975,** 44, 687-697.
158.Ponder, G. R.; Richards, G. N.; Stevenson, T. T., Influence of linkage position and orientation in pyrolysis of polysaccharides: a study of several glucans. *J. Anal. Appl. Pyrolysis* **1992,** 22, 217-229.
159.Chaiwat, W.; Hasegawa, I.; Tani, T.; Sunagawa, K.; Mae, K., Analysis of Cross-Linking Behavior during Pyrolysis of Cellulose for Elucidating Reaction Pathway. *Energy & Fuels* **2009,** 23, (12), 5765-5772.
160.Mettler, M. S.; Vlachos, D. G.; Dauenhauer, P. J., Top ten fundamental challenges of biomass pyrolysis for biofuels. *Energy Environ. Sci.* **2012,** 5, 7797-7809.
161.Yamaguchi, Y.; Fushimi, C.; Tasaka, K.; Furusawa, T.; Tsutsumi, A., Kinetic Study on the Pyrolysis of Cellulose Using the Novel Continuous Cross-Flow Moving Bed Type Differential Reactor. *Energy & Fuels* **2006,** 20, (6), 2681-2685.

162.Mamleev, V.; Bourbigot, S.; Le Bras, M.; Yvon, J., The facts and hypotheses relating to the phenomenological model of cellulose pyrolysis. Interdependence of the steps. *J. Anal. Appl. Pyrolysis* **2009,** 84, (1), 1-17.
163.Antal, M. J., Jr.; Varhegyi, G., Cellulose Pyrolysis Kinetics: The Current State of Knowledge. *Ind. Eng. Chem. Res.* **1995,** 34, (3), 703-717.
164.Banyasz, J. L.; Li, S.; Lyons-Hart, J. L.; Shafer, K. H., Cellulose pyrolysis: the kinetics of hydroxyacetaldehyde evolution. *J. Anal. Appl. Pyrolysis* **2001,** 57, (2), 223-248.
165.Piskorz, J.; Radlein, D.; Scott, D. S., On the mechanism of the rapid pyrolysis of cellulose. *J. Anal. Appl. Pyrolysis* **1986,** 9, (2), 121-137.
166.Shaik, S. M.; Sharratt, P. N.; Tan, R. B. H., Influence of selected mineral acids and alkalis on cellulose pyrolysis pathways and anhydrosaccharide formation. *J. Anal. Appl. Pyrolysis* **2013,** 104, (0), 234-242.
167.Dobele, G.; Rossinskaja, G.; Telysheva, G.; Meier, D.; Faix, O., Cellulose dehydration and depolymerization reactions during pyrolysis in the presence of phosphoric acid. *J. Anal. Appl. Pyrolysis* **1999,** 49, (1–2), 307-317.
168.Wang, Z.; Zhou, S.; Pecha, B.; Westerhof, R. J. M.; Garcia-Perez, M., Effect of Pyrolysis Temperature and Sulfuric Acid During the Fast Pyrolysis of Cellulose and Douglas Fir in an Atmospheric Pressure Wire Mesh Reactor. *Energy Fuels* **2014,** 28, (8), 5167-5177.
169.Miftakhov, M. S.; Valeev, F. A.; Gaisina, I. N., Levoglucosenone: the properties, reactions, and use in fine organic synthesis. *Russian Chem. Rev.* **1994,** 63, (10), 869-882.
170.Dalluge, D. L.; Daugaard, T.; Johnston, P.; Kuzhiyil, N.; Wright, M. M.; Brown, R. C., Continuous production of sugars from pyrolysis of acid-infused lignocellulosic biomass. *Green Chem.* **2014,** 16, (9), 4144-4155.
171.Liu, D.; Yu, Y.; Long, Y.; Wu, H., Effect of MgCl2 loading on the evolution of reaction intermediates during cellulose fast pyrolysis at 325 °C. *P. Combust. Inst.* **2015,** 35, (2), 2381-2388.
172.Lédé, J., Cellulose pyrolysis kinetics: An historical review on the existence and role of intermediate active cellulose. *J. Anal. Appl. Pyrolysis* **2012,** 94, 17-32.
173.Dufour, A.; Castro-Díaz, M.; Marchal, P.; Brosse, N.; Olcese, R.; Bouroukba, M.; Snape, C., In Situ Analysis of Biomass Pyrolysis by High Temperature Rheology in Relations with ^{1}H NMR. *Energy Fuels* **2012,** 26, 6432-6441.
174.Liu, D.; Yu, Y.; Wu, H., Differences in Water-Soluble Intermediates from Slow Pyrolysis of Amorphous and Crystalline Cellulose. *Energy Fuels* **2013,** 27, (3), 1371-1380.
175.Yu, Y.; Liu, D.; Wu, H., Formation and Characteristics of Reaction Intermediates from the Fast Pyrolysis of NaCl- and MgCl2-Loaded Celluloses. *Energy Fuels* **2014,** 28, (1), 245-253.
176.Julien, S.; Chornet, E.; Tiwari, P. K.; Overend, R. P., Vacuum pyrolysis of cellulose: Fourier transform infrared characterization of solid residues, product distribution and correlations. *J. Anal. Appl. Pyrolysis* **1991,** 19, 81-104.
177.Pastorova, I.; Botto, R. E.; Arisz, P. W.; Boon, J. J., Cellulose char structure: a combined analytical Py-GC-MS, FTIR, and NMR study. *Carbohydr. Res.* **1994,** 262, (1), 27-47.
178.Wooten, J. B.; Seeman, J. I.; Hajaligol, M. R., Observation and characterization of cellulose pyrolysis intermediates by 13C CPMAS NMR. A new mechanistic model. *Energy Fuels* **2004,** 18, (1), 1-15.

179.Falco, C.; Perez Caballero, F.; Babonneau, F.; Gervais, C.; Laurent, G.; Titirici, M.-M.; Baccile, N., Hydrothermal Carbon from Biomass: Structural Differences between Hydrothermal and Pyrolyzed Carbons via 13C Solid State NMR. *Langmuir* **2011,** 27, (23), 14460-14471.
180.Wu, H.; Yu, Y.; Yip, K., Bioslurry as a Fuel. 1. Viability of a Bioslurry-Based Bioenergy Supply Chain for Mallee Biomass in Western Australia. *Energy Fuels* **2010,** 24, (10), 5652-5659.
181.Mohan, D.; Pittman, C. U.; Steele, P. H., Pyrolysis of Wood/Biomass for Bio-oil: A Critical Review. *Energy & Fuels* **2006,** 20, (3), 848-889.
182.Huber, G. W.; Iborra, S.; Corma, A., Synthesis of Transportation Fuels from Biomass: Chemistry, Catalysts, and Engineering. *Chemical Reviews* **2006,** 106, (9), 4044-4098.
183.Liu, D.; Yu, Y.; Long, Y.; Wu, H., Effect of MgCl2 loading on the evolution of reaction intermediates during cellulose fast pyrolysis at 325 °C. *Proceedings of the Combustion Institute* **2015,** 35, (2), 2381-2388.
184.Patwardhan, P. R.; Satrio, J. A.; Brown, R. C.; Shanks, B. H., Influence of inorganic salts on the primary pyrolysis products of cellulose. *Bioresour. Technol.* **2010,** 101, (12), 4646-4655.
185.Dobele, G.; Rossinskaja, G.; Telysheva, G.; Meier, D.; Faix, O., Cellulose dehydration and depolymerization reactions during pyrolysis in the presence of phosphoric acid. *Journal of Analytical and Applied Pyrolysis* **1999,** 49, (1–2), 307-317.
186.Long, Y.; Yu, Y.; Chua, Y. W.; Wu, H., Acid-catalysed cellulose pyrolysis at low temperatures. *Fuel* **2017,** 193, 460-466.
187.Bai, X.; Johnston, P.; Brown, R. C., An experimental study of the competing processes of evaporation and polymerization of levoglucosan in cellulose pyrolysis. *Journal of Analytical and Applied Pyrolysis* **2013,** 99, (Supplement C), 130-136.
188.Sanders, E. B.; Goldsmith, A. I.; Seeman, J. I., A model that distinguishes the pyrolysis of d-glucose, d-fructose, and sucrose from that of cellulose. Application to the understanding of cigarette smoke formation. *Journal of Analytical and Applied Pyrolysis* **2003,** 66, (1–2), 29-50.
189.Pilath, H. M.; Nimlos, M. R.; Mittal, A.; Himmel, M. E.; Johnson, D. K., Glucose Reversion Reaction Kinetics. *Journal of Agricultural and Food Chemistry* **2010,** 58, (10), 6131-6140.
190.Liu, D.; Nimlos, M. R.; Johnson, D. K.; Himmel, M. E.; Qian, X., Free Energy Landscape for Glucose Condensation Reactions. *The Journal of Physical Chemistry A* **2010,** 114, (49), 12936-12944.
191.Momany, F. A.; Appell, M.; Strati, G.; Willett, J. L., B3LYP/6-311++G** study of monohydrates of α- and β-d-glucopyranose: hydrogen bonding, stress energies, and effect of hydration on internal coordinates. *Carbohydrate Research* **2004,** 339, (3), 553-567.
192.Durand, H. W.; Dull, M. F.; Tipson, R. S., Polymerization of α-D-Glucose in the Solid State, in the Presence of Metaboric Acid1. *Journal of the American Chemical Society* **1958,** 80, (14), 3691-3697.
193.Bhore, N. A.; Klein, M. T.; Bischoff, K. B., The delplot technique: a new method for reaction pathway analysis. *Industrial & Engineering Chemistry Research* **1990,** 29, (2), 313-316.
194.Thompson, A.; Anno, K.; Wolfrom, M. L.; Inatome, M., Acid Reversion Products from D-Glucose. *Journal of the American Chemical Society* **1954,** 76, (5), 1309-1311.

195.Pilath, H. M.; Nimlos, M. R.; Mittal, A.; Himmel, M. E.; Johnson, D. K., Glucose Reversion Reaction Kinetics. *J. Agric. Food. Chem.* **2010,** 58, (10), 6131-6140.
196.Iisa, K.; French, R. J.; Orton, K. A.; Dutta, A.; Schaidle, J. A., Production of low-oxygen bio-oil via ex situ catalytic fast pyrolysis and hydrotreating. *Fuel* **2017,** 207, 413-422.
197.Pinheiro Pires, A. P.; Arauzo, J.; Fonts, I.; Domine, M. E.; Fernández Arroyo, A.; Garcia-Perez, M. E.; Montoya, J.; Chejne, F.; Pfromm, P.; Garcia-Perez, M., Challenges and Opportunities for Bio-oil Refining: A Review. *Energy & Fuels* **2019,** 33, (6), 4683-4720.
198.Benés, M.; Bilbao, R.; Santos, J. M.; Alves Melo, J.; Wisniewski, A.; Fonts, I., Hydrodeoxygenation of Lignocellulosic Fast Pyrolysis Bio-Oil: Characterization of the Products and Effect of the Catalyst Loading Ratio. *Energy & Fuels* **2019,** 33, (5), 4272-4286.
199.Pujro, R.; Panero, M.; Bertero, M.; Sedran, U.; Falco, M., Hydrogen Transfer between Hydrocarbons and Oxygenated Compounds in Coprocessing Bio-Oils in Fluid Catalytic Cracking. *Energy & Fuels* **2019,** 33, (7), 6473-6482.
200.Yu, Y.; Chua, Y. W.; Wu, H., Characterization of Pyrolytic Sugars in Bio-Oil Produced from Biomass Fast Pyrolysis. *Energy & Fuels* **2016,** 30, (5), 4145-4149.
201.Shafizadeh, F.; Furneaux, R. H.; Cochran, T. G.; Scholl, J. P.; Sakai, Y., Production of levoglucosan and glucose from pyrolysis of cellulosic materials. *Journal of Applied Polymer Science* **1979,** 23, (12), 3525-3539.
202.Leng, E.; Wang, Y.; Gong, X.; Zhang, B.; Zhang, Y.; Xu, M., Effect of KCl and CaCl2 loading on the formation of reaction intermediates during cellulose fast pyrolysis. *Proceedings of the Combustion Institute* **2017,** 36, (2), 2263-2270.
203.David, G. F.; Perez, V. H.; Rodriguez Justo, O.; Garcia-Perez, M., Effect of acid additives on sugarcane bagasse pyrolysis: Production of high yields of sugars. *Bioresource Technology* **2017,** 223, 74-83.
204.Bennadji, H.; Khachatryan, L.; Lomnicki, S. M., Kinetic Modeling of Cellulose Fractional Pyrolysis. *Energy & Fuels* **2018,** 32, (3), 3436-3446.
205.Si, T.; Huang, K.; Lin, Y.; Gu, M., ReaxFF Study on the Effect of CaO on Cellulose Pyrolysis. *Energy & Fuels* **2019,** 33, (11), 11067-11077.
206.Long, Y.; Yu, Y.; Song, B.; Wu, H., Polymerization of glucose during acid-catalyzed pyrolysis at low temperatures. *Fuel* **2018,** 230, 83-88.
207.Fang, Y.; Li, J.; Chen, Y.; Lu, Q.; Yang, H.; Wang, X.; Chen, H., Experiment and Modeling Study of Glucose Pyrolysis: Formation of 3-Hydroxy-γ-butyrolactone and 3-(2H)-Furanone. *Energy & Fuels* **2018,** 32, (9), 9519-9529.
208.Ansari, K. B.; Arora, J. S.; Chew, J. W.; Dauenhauer, P. J.; Mushrif, S. H., Effect of Temperature and Transport on the Yield and Composition of Pyrolysis-Derived Bio-Oil from Glucose. *Energy & Fuels* **2018,** 32, (5), 6008-6021.
209.Yue, L.; Rao, L.; Wang, L.; An, L.; Hou, C.; Ma, C.; DaCosta, H.; Hu, X., Efficient CO2 Adsorption on Nitrogen-Doped Porous Carbons Derived from d-Glucose. *Energy & Fuels* **2018,** 32, (6), 6955-6963.
210.Sun, K.; Xu, Q.; Shao, Y.; Zhang, L.; Liu, Q.; Zhang, S.; Wang, Y.; Hu, X., Cross-Polymerization between the Typical Sugars and Phenolic Monomers in Bio-Oil: A Model Compounds Study. *Energy & Fuels* **2019,** 33, (8), 7480-7490.
211.Abe, H.; Prins, W., Addition polymerization of anhydrosugar derivatives. II. The molecular weight distribution of polyanhydroglucose addition polymers. *Die Makromolekulare Chemie* **1960,** 42, (1), 216-229.

212.Bai, X.; Johnston, P.; Brown, R. C., An experimental study of the competing processes of evaporation and polymerization of levoglucosan in cellulose pyrolysis. *Journal of Analytical and Applied Pyrolysis* **2013,** 99, 130-136.
213.da Silva Carvalho, J.; Prins, W.; Schuerch, C., Addition Polymerization of Anhydrosugar Derivatives. I. A Polyanhydroglucose1. *Journal of the American Chemical Society* **1959,** 81, (15), 4054-4058.
214.Kawamoto, H.; Murayama, M.; Saka, S., Pyrolysis behavior of levoglucosan as an intermediate in cellulose pyrolysis: polymerization into polysaccharide as a key reaction to carbonized product formation. *Journal of Wood Science* **2003,** 49, (5), 469-473.
215.Thompson, A.; Wolfrom, M. L., The Composition of Pyrodextrins. *Journal of the American Chemical Society* **1958,** 80, (24), 6618-6620.
216.Wolfrom, M. L.; Thompson, A.; Ward, R. B., The Composition of Pyrodextrins. II. Thermal Polymerization of Levoglucosan1. *Journal of the American Chemical Society* **1959,** 81, (17), 4623-4625.
217.Wolfrom, M. L.; Thompson, A.; Ward, R. B.; Horton, D.; Moore, R. H., The Composition of Pyrodextrins. III. Thermal Polymerization of Levoglucosan1. *The Journal of Organic Chemistry* **1961,** 26, (11), 4617-4620.
218.Durand, H. W.; Dull, M. F.; Tipson, R. S., *Polymerization of α-D-Glucose in the Solid State, in the Presence of Metaboric Acid1*. Journal of the American Chemical Society: 1958; Vol. 80.
219.Goldstein, I. J.; Hullar, T. L., Chemical Synthesis of Polysaccharides**The preparation of this review was supported, in part, by a grant (GM 129922-01) from the National Institutes of Health, U. S. Public Health Service. In *Advances in Carbohydrate Chemistry*, Wolfrom, M. L.; Tipson, R. S., Eds. Academic Press: 1967; Vol. 21, pp 431-512.
220.Houminer, Y.; Patai, S., Thermal polymerization of levoglucosan. *Journal of Polymer Science Part A-1: Polymer Chemistry* **1969,** 7, (10), 3005-3014.
221.Wollwage, P. C.; Seib, P. A., Acid-catalyzed polymerization of 1,6-anhydro-β-D-glucopyranose. *Journal of Polymer Science Part A-1: Polymer Chemistry* **1971,** 9, (10), 2877-2892.
222.Ponder, G. R.; Richards, G. N., Polysaccharides from thermal polymerization of glucosides. *Carbohydrate Research* **1990,** 208, 93-104.
223.Brammer, J. G.; Lauer, M.; Bridgwater, A. V., Opportunities for biomass-derived "bio-oil" in European heat and power markets. *Energy Policy* **2006,** 34, (null), 2871.
224.Bridgwater, A. V., *The future for biomass pyrolysis and gasification: status, opportunities and policies for Europe. Contract No: 4.1030/S/01–009/2001*. 2002; Vol. null, p null.
225.Bridgwater, A. V., Renewable fuels and chemicals by thermal processing of biomass. *Chem. Eng. J.* **2003,** 91, (null), 87.
226.Helm, R. F.; Young, R. A.; Conner, A. H., The reversion reactions of d-glucose during the hydrolysis of cellulose with dilute sulfuric acid. *Carbohydrate Research* **1989,** 185, (2), 249-260.
227.Yang, H.; Yan, R.; Chen, H.; Lee, D. H.; Zheng, C., Characteristics of hemicellulose, cellulose and lignin pyrolysis. *Fuel* **2007,** 86, (12-13), 1781-1788.
228.Zhou, X.; Li, W.; Mabon, R.; Broadbelt, L. J., A mechanistic model of fast pyrolysis of hemicellulose. *Energy & Environmental Science* **2018,** 11, (5), 1240-1260.